1995-03

Evaluation of an interactive regional wind analysis procedure for the tropics

Jeffries, Richard Allen.

Monterey, California. Naval Postgraduate School

NAVAL POSTGRADUATE SCHOOL
Monterey, California

THESIS

EVALUATION OF AN INTERACTIVE REGIONAL WIND ANALYSIS PROCEDURE FOR THE TROPICS

by

Richard Allen Jeffries

September 1995

Advisor: R. L. Elsberry
Advisor: L. E. Carr, III

Approved for public release; distribution unlimited

REPORT DOCUMENTATION PAGE

Form Approved OMB No. 0704-0188

1. AGENCY USE ONLY *(Leave blank)*	2. REPORT DATE September 95	3. REPORT TYPE AND DATES COVERED Master's Thesis

4. **TITLE AND SUBTITLE** Evaluation of an Interactive Regional Wind Analysis Procedure for the Tropics

5. **FUNDING NUMBERS**

6. **AUTHOR(S)** Richard A. Jeffries

7. **PERFORMING ORGANIZATION NAME(S) AND ADDRESS(ES)** Naval Postgraduate School, Monterey CA 93943-5000

8. **PERFORMING ORGANIZATION REPORT NUMBER**

9. **SPONSORING/MONITORING AGENCY NAME(S) AND ADDRESS(ES)**

10. **SPONSORING/MONITORING AGENCY REPORT NUMBER**

11. **SUPPLEMENTARY NOTES** The views expressed in this thesis are those of the author and do not reflect the official policy or position of the Department of Defense or the U.S. Government.

12a. **DISTRIBUTION/AVAILABILITY STATEMENT** Approved for public release; distribution is unlimited.

12b **DISTRIBUTION CODE**

13. ABSTRACT *(maximum 200 words)*

An interactive tropical wind analysis technique is developed that combines the best features of the automated and subjective analyses over a limited region. An automated, large-scale analysis is used as a first-guess field. Composite observations over two 6-hour synoptic times and synthetic observations are added as increments to the first-guess field. Complete sets of synthetic observations are introduced to represent the upper- and lower-level structure of tropical cyclones, Tropical Upper Tropospheric Trough cells, upper-level anticyclonic cells, weak low-level cyclones, and point outflows from convective clusters. Point synthetic observations are inserted to represent satellite-observed features such as confluent asymptotes, or offset bad observations. A Multi-Quadric interpolation technique that draws closely to the wind observations effectively and efficiently provides an analysis on a 1° lat./long. grid. A sequence of 200 mb and 850 mb interactive analyses that includes Typhoon Robyn and Tropical Storm Steve is used to demonstrate changes from the first-guess and especially the vertical wind shear when synthetic observations are added.

14. **SUBJECT TERMS** Tropical Wind Analysis, Tropical Synoptic Models, Interactive Analysis.

15. **NUMBER OF PAGES** 148

16. **PRICE CODE**

17. SECURITY CLASSIFICATION OF REPORT	18. SECURITY CLASSIFICATION OF THIS PAGE	19. SECURITY CLASSIFICATION OF ABSTRACT	20. LIMITATION OF ABSTRACT
Unclassified	Unclassified	Unclassified	UL

NSN 7540-01-280-5500

Standard Form 298 (Rev. 2-89)
Prescribed by ANSI Std. 239-18 298-102

Approved for public release; distribution unlimited

EVALUATION OF AN INTERACTIVE REGIONAL WIND ANALYSIS PROCEDURE FOR THE TROPICS

Richard Allen Jeffries
Lieutenant, United States Navy
B.A., Eastern Illinois University, 1987

Submitted in partial fulfillment
of the requirements for the degree of

MASTER OF SCIENCE IN METEOROLOGY AND PHYSICAL OCEANOGRAPHY

from

NAVAL POSTGRADUATE SCHOOL

September 1995

Author: [redacted]

R. A. Jeffries

Approved by: [redacted]

Russell L. Elsberry, Co-advisor

[redacted]

Lester E. Carr, III, Co-advisor

[redacted]

Robert L. Haney, Chairman
Department of Meteorology

ABSTRACT

An interactive tropical wind analysis technique is developed that combines the best features of the automated and subjective analyses over a limited region. An automated, large-scale analysis is used as a first-guess field. Composite observations over two 6-hour synoptic times and synthetic observations are added as increments to the first-guess field. Complete sets of synthetic observations are introduced to represent the upper- and lower-level structure of tropical cyclones, Tropical Upper Tropospheric Trough cells, upper-level anticyclonic cells, weak low-level cyclones, and point outflows from convective clusters. Point synthetic observations are inserted to represent satellite-observed features such as confluent asymptotes, or offset bad observations. A Multi-Quadric interpolation technique that draws closely to the wind observations effectively and efficiently provides an analysis on a 1° lat./long. grid. A sequence of 200 mb and 850 mb interactive analyses that includes Typhoon Robyn and Tropical Storm Steve is used to demonstrate changes from the first-guess and especially the vertical wind shear when synthetic observations are added.

TABLE OF CONTENTS

ACKNOWLEDGMENTS

This research has been partially funded with a grant from the Office of Naval Research Marine Meteorology Program. A number of people at the Naval Postgraduate School have been most helpful. Professor R.T. Williams offered numerical modeling insights, and Professors Wendell Nuss and Pat Harr provided software and code recommendations that were instrumental in the system development. I also wish to thank CDR Les E. Carr, III for his assistance in software development. Finally, I sincerely thank my advisor, Professor Russ Elsberry for the guidance I have received and the patience he has demonstrated over the many months that I have been working on this thesis.

Additionally, I must thank my wife Teresa and my daughter Holly for their love and support during the long hours spent on this work. I dedicate this effort to them.

I. INTRODUCTION

With the advancements in computer technology in recent years, meteorologists are being provided with large observation sets of various types and in many formats that require new procedures to assimilate into analyses and weather forecasts. As these changes in operational procedures continue, meteorologists must take a pro-active role in coordinating new procedures throughout all levels of meteorological applications and training. The primary objective of weather prediction is to provide the user with the best information possible, in a format that is easily understood, with the shortest time delay possible. In the last 20 years, major improvements have been made in analyzing and displaying ever larger amounts of weather information in shorter time periods. This increase in processing speed has lead to numerous new products and services for both forecasters and users.

With the expansion in technology, a polarization into two meteorological groups has occurred: pro-automation versus pro-interaction. Development of a low intensity, adversarial relationship between the pro-automation people and the pro-interaction people has hindered joint development efforts. This type of relationship is counter-productive and leads to delays in scientific advancement (Doswell 1981). The pro-automation people believe that the best way to tackle the 36-48 h and 72-120 h prediction problem is to eliminate all manual intervention in the numerical model initialization and prediction process. The pro-interaction people believe that to analyze the current environment (nowcasting) accurately and predict future changes (medium range), a human must interact with the observational data.

Specifically, the forecaster must have a role in deciding which observations are to be used in describing the current state of the environment for use in numerical models.

The recent application of supercomputer technology to the global numerical modeling problem has significantly increased the speed of data analysis. However, a new trend has been to decentralize the problem by moving regional analysis and forecast efforts to smaller computers. An example is the initiative in the Navy to have shipboard forecast centers that would provide *in situ* weather support. These regional center developments dictate an immediate joint effort between the pro-automation and pro-interaction advocates, or the regional forecasting capability will significantly degrade and the ability to provide weather support to the users will decline.

A. AUTOMATED METEOROLOGICAL ANALYSIS

All global numerical forecast models require the analysis of current observational data as a first step in the development of a prognosis. Each major numerical center has a site-specific procedure to analyze the global observational database and enter the information into the numerical forecast model. For this information to be automatically processed, it must be quality controlled so that the inclusion of erroneous observations is limited. These quality-controlled data are then analyzed in four dimensions (x, y, z, and t) so that a spatially and temporally consistent representation of the current state of the atmosphere is obtained. An essential aspect of this analysis is that the observations are blended with a dynamically-balanced background field that is provided by a short-term integration of a forecast model. At most centers, an additional initialization step is utilized to remove imbalances that would degrade the quality of the forecast model run.

Due to the massive amounts of data that are processed and the limited time available to complete the global numerical model run, the use of automated quality control and analysis techniques for the global numerical model is a must. Because of the automated nature of this procedure and the necessity to complete the analysis-forecast cycle on a tight time schedule, a large amount of observational information may be lost. At various points in the quality control and analysis steps, the data are flagged and further checks are made. At these points, the potential benefit of a man-machine interaction is paramount. Of major concern is the information about the current synoptic conditions that may be lost without the opportunity for the forecaster to review the information before providing direct support to the customer. The inability to review and re-introduce these data into regional and local numerical analyses and forecasts at a later time is potentially detrimental to the customer. That is, all flagged data removed from the global numerical models may be a potential data source that could be reintroduced into a numerical prediction system on a regional or local scale.

B. IMPACT OF DATA LOSS ON TROPICAL WEATHER ANALYSIS

Tropical weather analysis is a complex problem. In tropical latitudes, the horizontal gradients of temperature and pressure are very weak. In general, the fluctuations of the mass field in the tropics are directly influenced by the wind patterns. For these reasons, the tropical weather patterns are best described by the wind field. Areas of low- and upper-level convergence and divergence are key features in developing tropical weather systems. These features are not easily resolved using global-scale, mid-latitude analysis techniques. To depict these features accurately, we need a large amount of observational data with high horizontal and vertical resolution. Herein lies the tropical analysis problem.

The tropics are a mostly maritime environment with few rawinsondes (RAOBS). The data density varies significantly in the horizontal and the vertical. The key data for tropical analysis are from satellite and aircraft observations of the upper- and lower-level wind fields. Little height information is available to describe the mass field and geostrophic balance relationships can not be assumed in the deep tropics.

The main limitation is the lack of data in the middle layers. One option is for a human to fill subjectively this void with human/computer-generated synthetic observations. These observations are created from the subjective interpretation of satellite imagery and introduction of the synthetic observations into the analysis process. This is one potential advantage of the man-machine mix in tropical weather analysis.

II. OBJECTIVE ANALYSIS AND DATA ASSIMILATION

To better understand the advantages of exploiting the man-machine mix in tropical and mid-latitude weather analysis, some weaknesses in data usage in the current system of numerical analysis will be described. The key to a successful data assimilation cycle is to exploit the strengths and avoid the weaknesses. Although procedures employed at the Fleet Numerical Meteorology and Oceanography Center (FNMOC) will be presented, similar deficiencies would be found in the analysis at all major numerical prediction facilities. Thus, this discussion should not be considered to be a criticism of only the FNMOC analysis.

At the FNMOC, the analysis-forecast system is a four-step process called the Data Assimilation Cycle that includes: Data Quality Control; Data Analysis; Model Initialization; and the Forecast Model Run (Goerss and Phoebus 1992). The first three steps will be described in the following sections because they directly impact the tropical analysis problem.

A. DATA QUALITY CONTROL

FNMOC receives 1.25 million (1.1 million meteorological and 0.15 million oceanographic) observations in a 24-h period (Nelson and Aldinger 1992). The data quality control techniques used at FNMOC (Baker 1992) are similar to those used at all numerical modeling centers. As shown in Table 1.1, the primary types of observations that are eliminated in the quality control step are satellite-based. Two primary reasons for these eliminations are the very high data density of satellite observations and the "noise content" of these observations. SSM/I observations have a horizontal resolution of approximately 25 km, which was more

TABLE 1.1 Data types received at FNMOC and percentage of observations eliminated (Nelson and Aldinger 1992; Goerss and Phoebus 1992)

DATA TYPE	NUMBER OBS RECEIVED	PERCENT ELIMINATED	TOTAL OBS LOST
AIREPS	4,000	20%	800
METAR LAND	24,000	1%	240
RAOBS	1,600	2%	32
SSMT/TOVS	22,300	7%	1,561
SSMI	1,000,000	83%	833,333
SAT VECTOR WINDS	10,200	15-20%	1530-2040
PIBALS	1,450	4-5%	58-72
LAND SYNOPTIC	48,000	1%	480
DRIFTING BUOYS	1,200	1%	12
SAT FEATURE BOGUS	1,000	1%	10
TOTAL	1,113,750	75%	838,284

than three times the resolution of the FNMOC numerical forecast model at that time (doubling of the horizontal resolution occurred in June 1994).

If the SSM/I scalar winds were introduced at the full resolution, they would become the primary data source for the model. Before SSM/I scalar winds could be entered at this resolution, they would have to be carefully inspected. A visual type of inspection is not possible on a global scale. Therefore, SSM/I winds undergo two automated data reduction procedures. First, only one of every six observations is retained in the initial review. Next, the data are boxcar-smoothed into 2000 "super obs" with 200 km resolution around the globe (Goerss and Phoebus 1992). This procedure effectively reduces the data density to the horizontal resolution of the global numerical model.

The above procedure greatly impacts the tropical analysis. First, only approximately 10% of the RAOBS received at FNMOC are located in the tropics. Second, the land and ship observations are highly concentrated in a few regions. Therefore, the primary data sources in key areas are the SSM/I scalar winds and the satellite vector winds. Indiscriminate elimination or smoothing of these data can quickly degrade the quality of the tropical weather analysis, and degrade forecast performance.

To overcome this problem, data that have been automatically eliminated from the analysis should be retained for review by the regional forecaster. If upon review the data are still eliminated, knowledge has still been gained. This concept was best stated by Doswell (1986): "Numerical models may dismiss key data that doesn't match the computer first guess. Forecasters must be trained to analyze the weather information as well as the objective analysis."

B. DATA ANALYSIS

Two types of objective analyses are performed at the major numerical modeling centers: the gridpoint, or the data-volume approach. Each of these techniques has strengths and weaknesses. In the gridpoint approach, all analyses are performed at the numerical forecast model gridpoints. All data within an elliptical or circular area around the gridpoint are averaged and a value is assigned to the gridpoint. This information is then blended with the numerical model first-guess field and the data are assimilated into the forecast model.

The data-volume or optimum interpolation procedures specify the grid centers based on the distribution of observations available for analysis. This allows for a large number of small grid volumes over the data-rich land masses and larger grid volumes over data-sparse oceanic regions. At FNMOC, a data-volume approach called the Multi-variate Optimum Interpolation (MVOI) Analysis is used for both the global and regional analyses.

C. FORECAST MODEL INITIALIZATION

Nonlinear normal mode initialization is used to initialize the regional numerical models at FNMOC. Haltiner and Williams (1980) state this procedure removes imbalances generated during the analysis cycle that will degrade the forecast model performance during the first 6 - 12 h of the forecast. Without the use of some type of gravity wave noise elimination during model initialization, the model forecast verification would be degraded to below the skill of an extrapolation forecast during the early portion of the forecast cycle.

One problem with this procedure is the amount of smoothing that occurs, which can result in the loss of small-scale perturbations in the wind field that are key elements for development of tropical weather features. There must exist a

procedure that will allow the on-scene forecaster to assess the effects of the smoothing that result from model initialization. In the tropics, synoptic models are applied based on cloud features and cloud-free areas to imply subjectively the circulation patterns. The following sections describe the tropical synoptic models used in this study.

III. SUBJECTIVE ANALYSIS AND DATA COMPOSITING

Currently, on-scene data are introduced into the operational forecast process through subjective analysis at the regional and local forecast centers. In the tropics, these subjective analyses use conceptual tropical synoptic models, data compositing, and subjective satellite imagery interpretation. In the tropical western Pacific, the main regional forecast center is the Joint Typhoon Warning Center (JTWC). At the JTWC, a manual analysis is performed at 0000/1200 UTC for the 200 mb and gradient levels (3000 ft). The purposes of these analyses are two-fold. First, these analyses provide a nearly continuous update for the forecaster as the observations come in and are plotted. Second, they provide a subjective analysis of the current synoptic situation for comparison with the objective analysis from FNMOC.

The JTWC analyst faces the same data-sparsity problem as FNMOC. To fill the void, FNMOC uses the numerical model first-guess field. The JTWC analyst uses time continuity and a combination of satellite imagery and tropical synoptic models to fill the data voids. The results of this subjective analysis process have long been recognized as superior to numerical analyses in data-sparse regions.

A. TROPICAL SYNOPTIC MODELS

Numerous research projects have performed re-analyses of meteorological events based on experimental data sources that were not available in real-time for the operational analysis-forecast system. With few exceptions, those re-analyses have demonstrated a marked improvement over the weather information that was

available via operational products. In the tropics, synoptic models are applied based on cloud features and cloud-free areas to imply subjectively the circulation patterns. The following sections describe the tropical synoptic models used in this study.

1. TUTT Cells

Chen and Chou (1994) discussed several key features based on a composite of 60 TUTT cells. These TUTT cells generally tracked westward throughout their life cycle. The longest lasting cells were associated with jet streaks that developed around the TUTT. These jet streaks have associated secondary circulations that help to maintain the TUTT cell. In the absence of these jet streaks, the TUTT cell life cycle decreased by nearly one half. These jet streaks are approximately 6° lat. to the northwest and the south of the center. Whereas the mean wind speed in the initial stage is 25 m s^{-1}, it intensifies to 30 m s^{-1} in the mature stage. The streaks that form in the northwest sector propagate around the TUTT and dissipate in the southwest sector. Streaks that form in the south sector also propagate cyclonically and dissipate in the northeast sector.

TUTT cells are cold-core, convergent areas in the upper troposphere that are sustained via a direct secondary circulation of cold air sinking relative to ascent in the adjacent warmer air. That is, the air converging into the TUTT cell sinks and warms. This process would normally cause the TUTT cell to dissipate, but the cells move west-southwestward, which keeps these circulations cooler than the surrounding environment. Thus, the TUTT cell systems are very persistent.

A characteristic cloud signature of TUTT cells in the western North Pacific makes them easily recognizable in animated geostationary satellite imagery. Cirrus cloud shields form on the southeastern side of the circulation and isolated deep convection forms spiral patterns in the center. Once the TUTT is identified

in a data-sparse area, it becomes a prime candidate for synthetic insertion into the analysis.

A TUTT cell will be represented here in the two-dimensional wind field as a convergent area of cyclonic winds with the strongest rotational component at an arbitrary distance from the center of the vortex. This circulation may be represented in cylindrical coordinates centered on the cell as

$$V = \frac{V_{max}}{2}\left(1 - \cos\left(\pi \frac{r}{r_{max}}\right)\right) , \qquad (1)$$

$$U = -0.4V , \qquad (2)$$

where V is the tangential wind, r is the radius from center, V_{max} is the maximum tangential wind at radius r_{max}, and U is the radial wind component. The perturbation wind field is forced to zero at a radius of two times r_{max}. Zero winds near the center are ensured by U and V being set to zero when r is less than 0.5 deg. lat./long. The translation speed is entered as a direction and speed, converted to U and V components, and added as the background flow to the perturbation wind field.

2. Tropical Cyclones

Carr and Elsberry (1994) propose a model based on the partial conservation of absolute angular momentum that may be used to describe the upper- and low-level wind patterns of a tropical cyclone. Equations (3) through

(6) are used to compute synthetic observations that are introduced into the analysis data set

$$V = \frac{M}{r^x} - \frac{1}{2} f_0 r \quad , \tag{3}$$

$$M = \frac{1}{2} f_0 R_0^{(1+x)} \quad , \tag{4}$$

$$U_L = -0.4 V \quad , \tag{5}$$

$$U_U = U_{max} \left(\frac{r_{max}}{r} \right) \tag{6}$$

where V is the tangential wind at either level, R_o is the radius of circulation influence, r is the radius from center, f_0 is the Coriolis value at the latitude of the tropical storm, U_L is the radial component at low levels, and U_U is the radial component at upper levels. U_{max} is the maximum radial wind component and r_{max} is the radius of maximum wind. The value of "x" is set to 0.4 when equations (3) and (4) are used at low levels and set to 1.0 at upper levels. The translation speed is entered as the current storm direction and speed and added as the background flow.

3. Point Outdrafts

Lander (personal communication, 1990) introduced the concept of point outdrafts that are the result of deep convection impinging on an upper tropospheric stable layer or the tropopause. Because of the limited horizontal scale of these convective columns (typically < 100 km), these features are normally

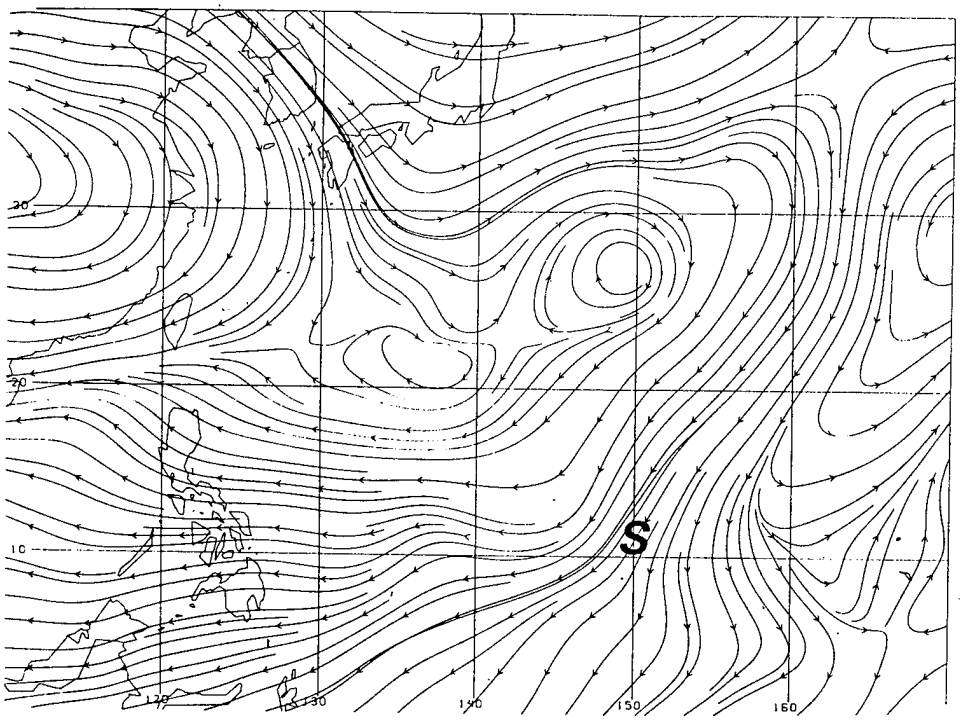

Fig. 1. NOGAPS 200 mb analysis at 2100 UTC 4 Aug 93. "S" indicates the satellite location of the point outdraft associated with pre-Steve that is not present in the NOGAPS analysis.

missing from numerical analyses. The point outdraft from the convective complex that eventually developed into TS Steve (14W, 1993) is not accurately analyzed in the NOGAPS analysis at 2100 UTC 4 Aug 93 (Fig. 1).

If conservation of angular momentum is applied to this problem, the point outdraft can be described by equations (3), (4), and (6) by specifying a value for U_{max} (normally 15 m s^{-1}) and r_{max} (typically 100 km), and setting M to zero in equation (3). This divergent flow must be smoothly blended with the background flow, which produces a 'bow-wave' on the leading side where the outflow and background flow are opposing.

4. Upper-level Anticyclones

In the deep tropics away from the subtropical ridge, counterclockwise flow aloft occasionally develops over regions of deep convection. These small anticyclones develop in response to vertical motions near the monsoon trough or over convective bands associated with tropical cyclones and monsoon gyres. As the air rises rapidly within these convergence regions, it encounters the tropopause and then spreads and subsides. An upper-level anticyclone that develops over deep convection will often persist and can be implied from convection visible on geostationary satellite imagery. These features normally remain in the analysis until the low-level convergence that generates the updrafts, and the favorable upper-level patterns that generate the subsidence, dissipate. One problem associated with these features is the small horizontal scales. The lack of observations in tropical regions often results in these small-scale anticyclones being missed by objective analysis.

In subjective analyses, these features are routinely included based on interpretation of satellite imagery. This procedure can not be duplicated in the current objective analyses due to the lack of procedures for incorporating the subjective interpretation of satellite imagery. Using this interactive analysis, these features are included by using equations (1) and (2) with the simple modification that the right side of equation (1) is multiplied by minus one.

5. Weak Surface Cyclones

Weak surface cyclones occur frequently in the tropics. Most often these cyclones are associated with the inter-tropical convergence zone or monsoon trough. However, weak cyclones do occur outside these zones and are typically associated with areas of low-level convergence in the presence of horizontal wind

shear. In the absence of vertical wind shear, these circulations can develop into tropical cyclones, so continuous monitoring of low-level cyclonic vortices is important. Normally, these cyclones do not become tropical cyclones outside the area of the monsoon trough due to strong vertical wind shear. The most common area where weak vertical wind shear and tropical cyclone development prevails is under the sub-equatorial ridge.

In contrast to tropical cyclones, these surface cyclones are characteristically areas of weak convergence and positive low-level vorticity. Continuous monitoring of these circulations is not possible using the current observation network in the western North Pacific. These features must be subjectively determined from satellite imagery and added to the low-level analysis. The 850 mb level is used for the NPS analysis system. At this level, rawinsonde (RAOBS) and satellite cloud-drift winds (SATWINDS) are the primary observations available for analysis.

To produce these synthetic observations for addition into the numerical analysis, equations (1) and (2) or equations (3) and (4) can be used. Equations (1) and (2) can be used when the radius of maximum winds is known from past history or from observations. Equations (3) and (4) can be used when the value of the maximum winds and the size (Ro) can be inferred from satellite imagery.

B. DATA COMPOSITING

Conventional data used in tropical analysis includes surface winds and pressures from land and ship stations (SFCOBS), rawinsonde winds and heights, SATWINDS and aircraft flight-level winds (AIREPS). Even with the addition of satellite-based observations, the data density is limited.

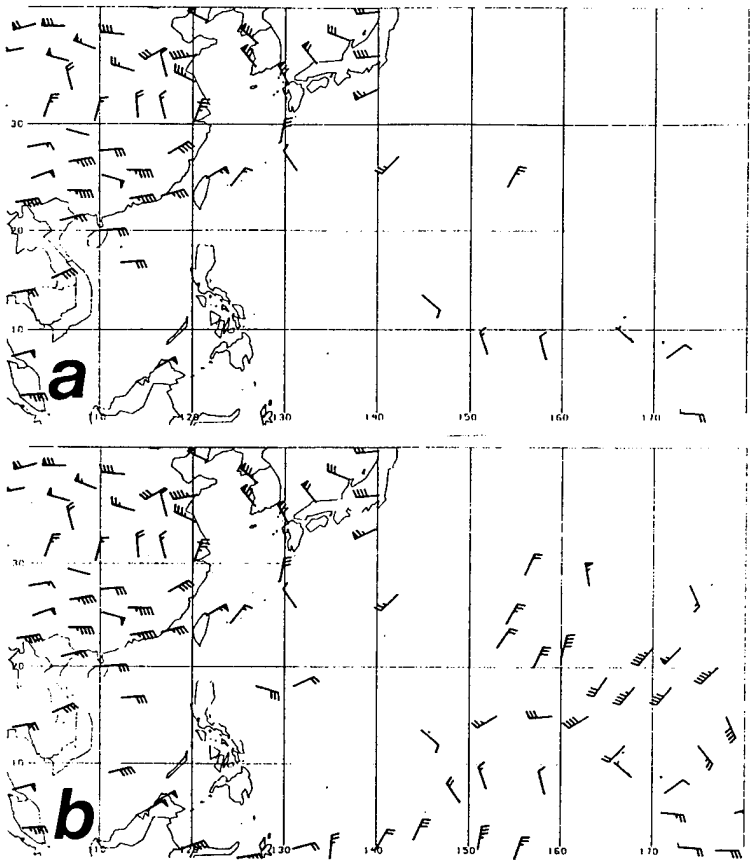

Fig. 2. Real-time set of (a) 200 mb rawinsondes, and (b) 200 mb rawinsondes plus AIREPS, and SATWINDS for 0000 UTC 5 Aug 93.

The RAOBS network in the western North Pacific is shown in Fig. 2a, and a typical complete on-time observation set from the tropical western North Pacific is shown in Fig. 2b. To address the lack of data for the tropical analysis, data compositing is used. That is, data are collected over several hours and/or from several vertical levels to represent conditions at a specific time and fixed level. Although this procedure requires subjective quality control, it will result in a larger data set for both subjective and objective analyses.

1. JTWC

At JTWC, data are hand plotted twice daily to complete subjective analyses of the western Pacific and Indian Ocean. Data compositing is used at 0000 and 1200 UTC for the gradient level (3000 ft or 914 m) and the 200 mb analyses. The JTWC upper-level analysis includes on-time/on-level wind and heights from RAOBS; on-time SATWINDS at 250, 200, and 150 mb; and AIREPS from FL290 to FL410 (FL is flight level in 100's of ft) and within plus or minus 3 h of synoptic time. The JTWC gradient-level analysis includes on-time gradient and 850 mb winds from RAOBS; on-time SATWINDS at 850-mb; on-time winds and pressures from land/ship SFCOBS; and six-hour old winds and pressures from ship SFCOBS. Despite this spatial and temporal compositing, the data coverage is often spotty, and occasionally unsatisfactory, particularly if the on-time SATWINDS are missing (Carr and Jeffries 1993).

2. NPS

The number of data sources in the tropics available for operational analyses is limited. This is primarily due to the large ocean areas in the tropical latitudes. The interactive analyses discussed below will be at the 850 mb and 200 mb levels and use rawinsonde soundings, aircraft reports, and satellite cloud-drift winds. When applying the interactive technique, data compositing is used to create analyses of the area 0°N - 40°N, 100°E - 180°E. As was done during the Tropical Cyclone Motion (TCM-93) field experiment (Carr and Jeffries 1993), the JTWC compositing techniques were modified for this work. A discussion of sounding availability, and both vertical and time compositing of AIREPS and SATWINDS, follows.

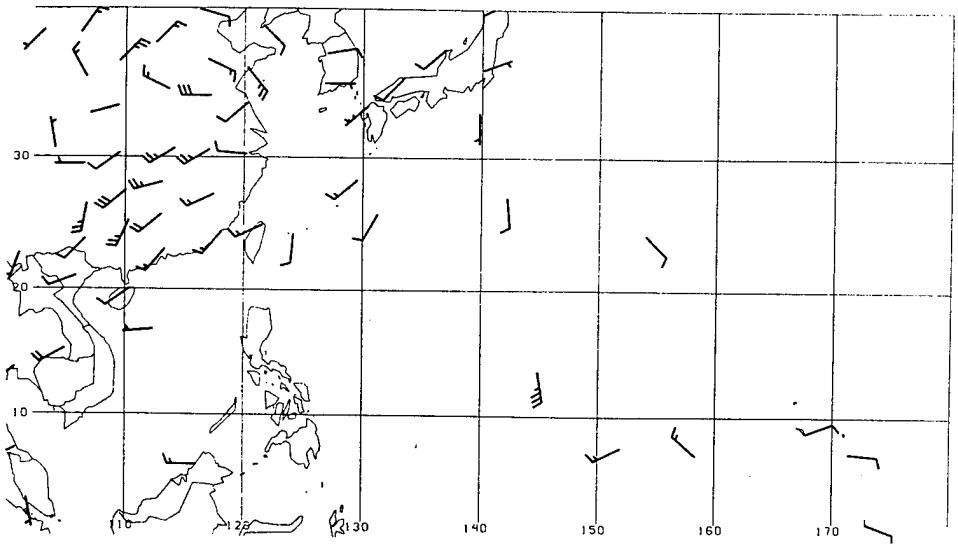

Fig. 3. 850 mb rawinsonde observations at 0000 UTC 5 Aug 93.

A typical set of 850 mb rawinsonde reports for the western North Pacific is shown in Fig. 3. Rawinsonde launches are normally at 0000 and 1200 UTC at the island stations in the western North Pacific. For some stations in the equatorial western North Pacific, additional 0600 and 1800 UTC observations can be initiated by the JTWC, Guam, when tropical cyclones threaten the region. The 1200 UTC soundings were used for the analyses valid at 0900 UTC and the 0000 UTC soundings were used at 2100 UTC.

Upper-level (200 mb) vertical compositing of AIREPS, as with TCM-93 (Carr and Jeffries 1993) follows that used by JTWC, except that the lower limit for the AIREPS was raised to 33,000 ft (10,060 m). Additionally, time compositing of aircraft reports was used for these analyses. All AIREPS received during the period from 0600 UTC and 1200 UTC were valid at 0900 UTC and between 1800 UTC and 0000 UTC were valid at 2100 UTC. These data were given equal weight in the analysis process, without regard to altitude or time

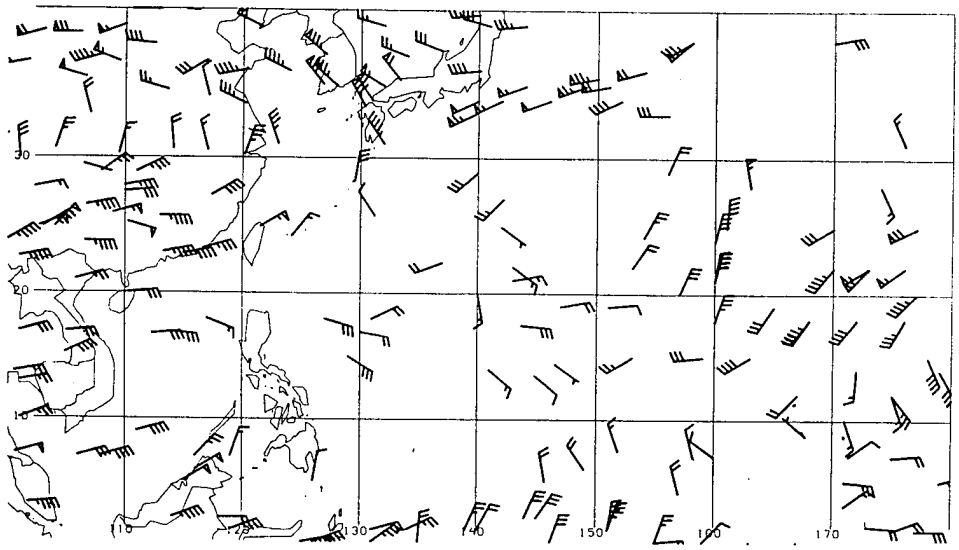

Fig. 4. 200 mb composite observations at 2100 UTC 4 Aug 93.

variations. For the lower-level (850 mb) chart, there is a lack of AIREPS throughout the analysis region.

All cloud-drift winds between 400 mb and 150 mb were considered as 200 mb observations. The SATWINDS were composited in time by using both the 1200 UTC and the 0600 UTC for a 0900 UTC analysis and the 0000 UTC and 1800 UTC observations for the 2100 UTC analysis. All cloud-drift winds above 900 m and below 1950 m are composited as 850 mb winds.

This compositing approach results in analyses 3 h earlier than the corresponding JTWC charts. Compared with the real-time analysis in Fig. 2b, the data coverage is nearly doubled over the tropical oceans using this compositing (Fig. 4), as was the case in the TCM-93 analyses (Carr and Jeffries 1993). This better coverage over the ocean areas permitted more confidence to be placed in the analyses, and compensated in part for the 3-h degradation in timeliness. For Typhoon (TY) Robyn and Tropical Storm (TS) Steve, the observations were

available from the TCM-93 data archives maintained at the Naval Postgraduate School.

C. SATELLITE IMAGERY ANALYSIS

Meteorological satellites are uniquely suited for tropical weather surveillance and analysis. With the advent of geostationary imagery, the near-continuous monitoring of tropical weather phenomenon has greatly increased the understanding of tropical weather events (Rao et al. 1990). Recent improvements of horizontal resolution of geostationary satellite imagery and the addition of animation have significantly increased our knowledge of the motions and interactions between tropical weather events.

The improved understanding of tropical weather phenomenon as it appears on satellite imagery can lead to improved analysis skill if this understanding is applied conceptually to the analysis process. Synoptic models developed based on observations of phenomenon from satellite may be subjectively included in an analysis of the tropical environment.

For this study, a combination of still high resolution geostationary imagery and animated low-resolution satellite imagery will be used to identify these features. Additionally, the location of tropical cyclones will be based on fixes provided by Det 1, 633 Operations Support Squadron (OSS), Anderson AFB, Guam. At this satellite observation facility, the Dvorak satellite analysis procedure is employed.

1. Dvorak

The Dvorak technique outlines rules and procedures for locating the center of the tropical cyclone, measuring cloud features that relate to intensity, classifying cloud systems as to stage of storm development, and applying a model for tropical cyclone development based on satellite analysis experience (Rao et al.

1990). The tropical cyclone position estimate is made by using visual and enhanced infrared high resolution imagery from either geostationary satellites or polar orbiting satellites. These images are analyzed to determine the banding features associated with a mature tropical cyclone, which lead to the determination of the system center. Then a combination of pixel counting to determine cloud top temperatures and an assessment of the banding wrapped around the center is used to determine the current intensity (T-number). After approximately 24 h of fixes have occurred so that an intensity trend has been established, an intensity estimate can be developed. All synthetic observations produced to describe tropical cyclones for the analyses used in this study will be based on the information contained in the position bulletins from the Det 1, 633rd OSS.

2. Animated High Resolution Geostationary Imagery

The time evolution of tropical phenomenon is most easily tracked using animated high resolution geostationary imagery. The hourly images available in the western North Pacific allow a nearly continuous monitoring of synoptic-scale phenomenon in the tropics. Animation of the geostationary imagery provides the analyst the motion and evolution of the synoptic features. In addition, areas of clearing imply upper-level convergence, subsidence, and low-level divergence. Areas of convection imply low-level convergence, upward vertical motion, and upper-level divergence.

Upper-level TUTT cells are easily monitored in animated imagery, due to the cloud edges in the cirrus south of the center and the spiraling "popcorn cumulonimbus" in the center. Sharp upper-level cloud edges are associated with convergent asymptotes and the associated downward motion. Such areas of downward motion imply clearing over time and are expected to be associated with low-level divergence and anticyclonic flow. Areas of baroclinic cirrus leaves are

associated with upper-level divergence and upward motion in the mid-levels. Finally, low-level convergent asymptotes are associated with increasing convection over time and can lead to cyclonic flow and cyclone development. Each of these features is more easily monitored in animated imagery and can be used to improve subjectively tropical analysis.

Polar-orbiting satellite mosaics are available from FNMOC over the Navy Oceanographic Data Distribution System (NODDS) or from the new satellite display software available on Tactical Environmental Support System (TESS) 3.0. At the regional forecast centers and on ships at sea, the forecasters must depend on polar-orbiting satellite imagery for a significant portion of the satellite analysis. This requires a very thorough knowledge of the single image representation of tropical phenomenon. Without the implied motion and system evolution gained from animated imagery, the analyst must have a very comprehensive knowledge of the history of weather elements that are evident on these still images. This history can be gained from various sources and will constitute a good first guess of the location and structure of features subjectively interpreted from the images. Most analysts will mark the locations of the features on the new image, and then make comparisons with the previous image to determine the evolution of the features over time. This procedure will allow for the subjective interpretation of satellite imagery to fill in the data-void regions over the tropical oceans.

IV. TEST CASE

The value of an interactive analysis lies in the ability for the on-scene forecaster to evaluate the observations independent of the objective analysis and compare the results. This will allow for the rapid identification of areas of significant departures between the interactive and objective analyses. These departures may be manifest as differences in relative vorticity, divergence, and vertical wind shear. To demonstrate this process, the development of TS Steve (14W 1993; Fig. 5b) in the trailing region of TY Robyn (13W 1993; Fig. 5a) will be discussed. Both cases involved the development of tropical cyclones in moderate to strong vertical wind shear according to the objective analyses (Smith 1994). Differences between the vertical shear calculated from the objective and interactive analyses will be displayed in Chapter VII. A brief discussion of the synoptic situation associated with each case follows.

Typhoon Robyn formed near 6°N, 162°E on the eastern end of the monsoon trough on 30 July 1993 (JTWC 1993). This tropical cyclone formed in a Standard Synoptic Pattern as described by Carr and Elsberry (1994) and moved generally west-northwestward from 30 July 1993 until 4 August 1993 in the Dominant Ridge Region (Fig. 6). The intensification of Robyn initiated a trailing ridge feature that created a southerly flow pattern near Robyn that is expected to result in a rapid northward translation. A transition to a North-oriented Environment Structure and a dramatic poleward track ocurred on 4 August 1993. However, the developing cyclone associated with TS Steve was situated where it interrupted the trailing ridge intensification and thus slowed the northward translation (Fig. 7). Robyn did

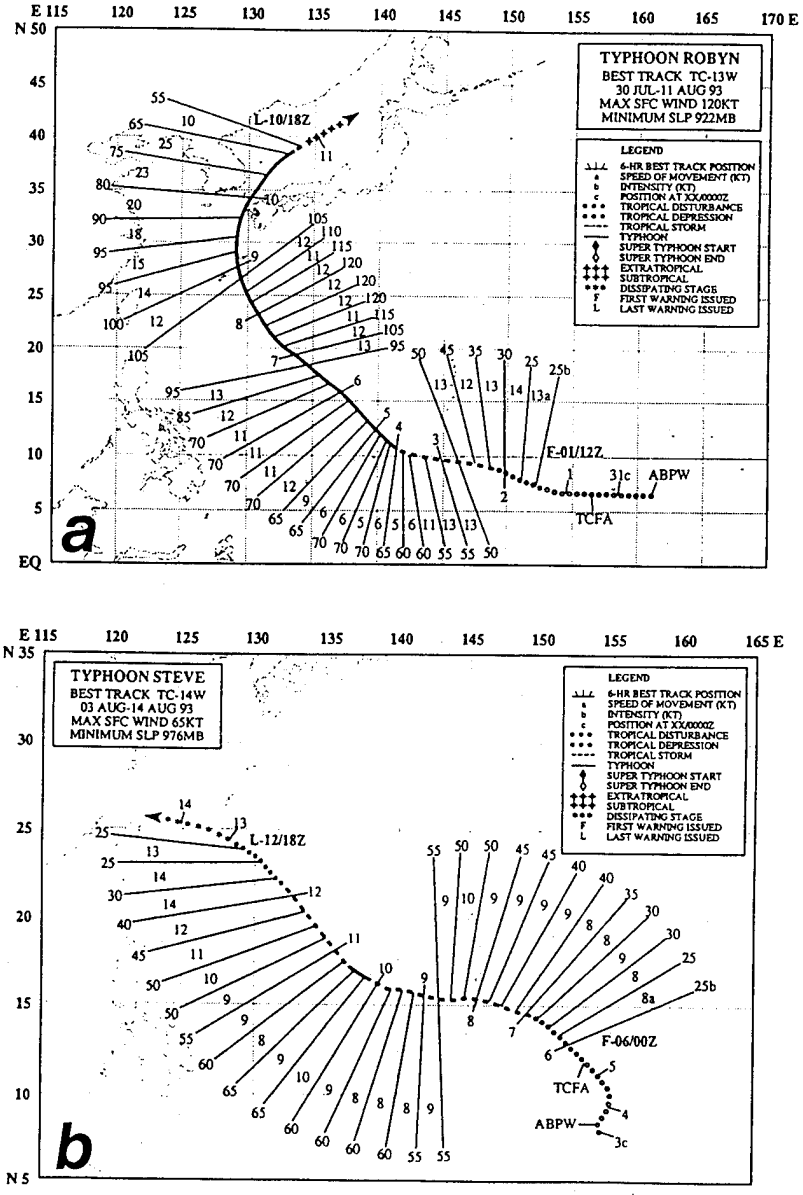

Fig. 5. Joint Typhoon Warning Center best tracks for (a) Typhoon Robyn, and (b) Tropical Storm Steve. Positions at 0000 UTC are indicated along with intensities (kt) indicated at the end of radials extending from intermediate 6-h positions, storm translation speeds over 6 h are indicated between these radials (see inset for explanation of symbols).

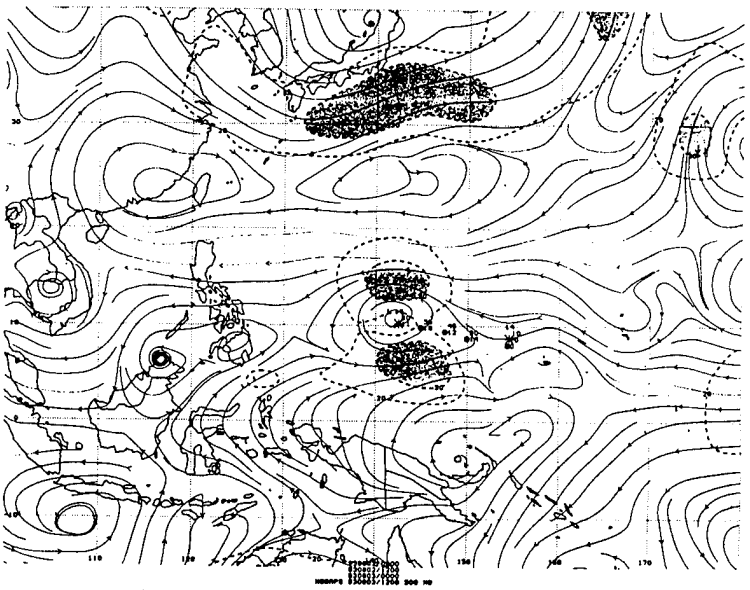

Fig. 6. 500 mb NOGAPS analysis valid at 1200 UTC 3 Aug 93. Solid lines are streamlines and dashed lines are isotachs (kt; contour interval of 10 kt beginning at 20 kt). Asterisk and bold dots near center of figure are the current and past 12-, 24-, and 36-h best track positions of TY Robyn (13 W 1993). Single asterisk to the right is current position of TS Steve.

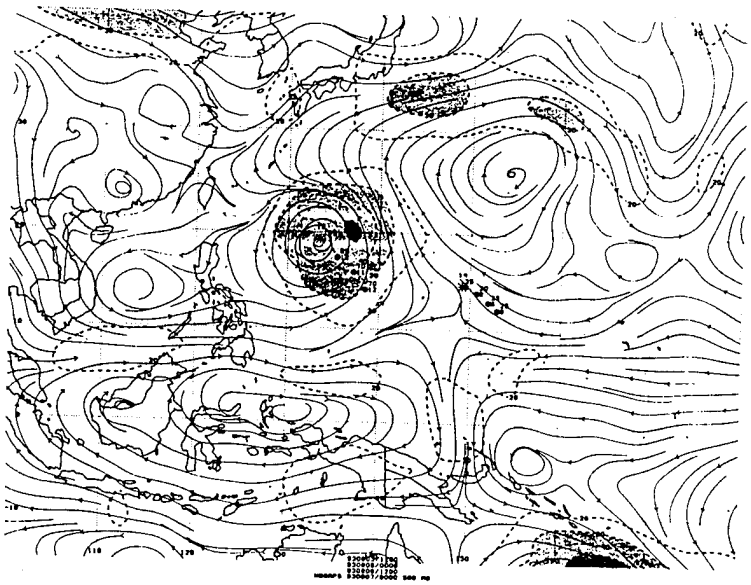

Fig. 7. As in Fig. 6, except analysis valid 0000 UTC 7 Aug 93. Both TY Robyn (13W 1993) and TS Steve (14W 1993) positions are depicted.

continue on a northerly track and passed through the ridge into the mid-latitude westerlies on 9 August and dissipated as a significant tropical cyclone on 11 August.

TS Steve developed as a cyclonic circulation in the eastward end of the monsoon trough near 8°N, 154°W. Steve initially moved north-northeastward under the combined influence of the circulation of TY Robyn and the monsoon trough (Smith 1994). On 4 August, Steve began to develop slowly while it was in a Standard Synoptic Pattern. Steve moved west-northwestward in the Dominant Ridge (DR) Region until it dissipated as a significant tropical cyclone on 14 Aug 93.

V. INTERACTIVE ANALYSIS PROCEDURES

The current Navy numerical analysis procedures limit the ability of the on-scene forecasters to enter local observations into the numerical analysis. As indicated in Chapter I, the on-scene forecaster has numerous data sources that could greatly enhance the weather information that is passed to weapons support systems. However, a capability must be developed to turn satellite-based interpretations into synthetic observations to rapidly update the local or regional analysis and thus improve the numerical analysis from the global and regional forecast centers. This interactive analysis system is designed for this purpose.

The interactive analysis includes three basic steps: (i) An initial objective analysis of a composite data set using the multiquadric interpolation (MQI) technique of Nuss and Titley (1994); (ii) insertion of complete sets of synthetic observations according to various pre-defined conceptual models that are related to cloud and circulation patterns; and (iii) insertion of point synthetic observations to fine-tune the analysis. Steps (ii) and (iii) are iterated as necessary until the MQI analysis agrees acceptably well with the subjective interpretation of satellite imagery.

A. INITIAL ANALYSIS

The first step of this procedure is the insertion of the composite data set described in Chapter IV.B.2, which will provide an initial survey of circulations not present in the first-guess field or the real-time observation set. This first MQI analysis step introduces the full composite observation data set and blends it with the first-guess field. This reanalysis will identify areas where the automated

analysis (first-guess field) lacked (or rejected) key observations around tropical circulations.

B. SYNTHETIC OBSERVATION DEVELOPMENT

During the second step of the interactive analysis, development of satellite-based synthetic wind observations will be accomplished to describe the missing features in the first MQI analysis. As indicated earlier, complete sets of synthetic observations are introduced into the analysis data set based on the conceptual models presented in Chapter II. The upper-level models include: point outdraft; tropical cyclone outdraft; tropical upper-tropospheric trough (TUTT) cell; and upper-level anticyclones. Low-level models include: tropical cyclones; monsoon depression/gyres (available, but not used here); weak cyclones; and low-level anticyclones (available, but not used here).

Once the need for one of these conceptual models has been identified from satellite interpretation, synthetic observations can be rapidly developed. These synthetic observations are then added to the combined data set from step one, and the MQI analysis is repeated.

Application of this interactive analysis technique is an iterative process that involves the insertion of synthetic observations in data-void regions to describe tropical features. Insertion of synthetic observations in each iteration of the second step follows an analysis-evaluation progression. In the first iteration, sets of synthetic observations representing well-defined features such as tropical cyclones and TUTT cells are inserted based on analytical wind models. In the second (and any subsequent) iteration, adjustments to individual synthetic circulations are made as needed. During the reanalysis and evaluation phase, smaller scale features, such as weak surface cyclones and anticyclones may be entered.

C. FINAL ANALYSIS ADJUSTMENT

During the third step, point synthetic observations are inserted to represent, or adjust the location, of key small-scale features, or eliminate the effect of bad observations. For example, these observations are typically introduced to shift the location of singular points (i.e., neutral points) and confluent/diffluent asymptotes based on the satellite imagery. In areas of sparse data, these asymptotes may be missing or be displaced several hundred kilometers from the actual location. The careful placement of wind observations parallel to the asymptote may force the analysis to place correctly these features.

D. DIAGNOSTIC EVALUATION

A useful byproduct of the interactive analysis technique is the ability to rapidly assess the effects of the introduction of satellite-based circulations into the analysis. The vertical wind shear, divergence, relative vorticity, and difference (deviation from the first-guess field) fields are easily calculated from a numerical analyses. Each of these fields provides information that aids tropical analysis and forecasting. Examples of the first and last of these calculations will be shown in discussion of the application of the interactive technique.

1. Vertical Wind Shear

Vertical windshear is defined as the difference between the 200 mb and the 850 mb U and V componenets. It is calculated following Smith (1994), from the 850 and 200 mb MQI wind analyses and NOGAPS (first-guess) wind fields using

$$|\Delta| = \sqrt{(U_{200} - U_{850})^2 + (V_{200} - V_{850})^2} \quad . \qquad (7)$$

2. Relative Vorticity

To assess the effects of adding the synthetic circulations to the upper- and lower-level environmental flow, the relative vorticity values before and after the introduction of synthetic observations may be compared. The relative vorticity is calculated using

$$\zeta_{(i,j)} = \frac{V_{(i+1,j)} - V_{(i-1,j)}}{2\,\Delta x} - \frac{U_{(i,j+1)} - U_{(i,j-1)}}{2\,\Delta y} \quad . \qquad (8)$$

3. Divergence

In the upper levels, mass divergence and convergence are key elements in the ventilation process described by Gray (1968). In areas of strong upper-level convergence, forced subsidence occurs that inhibits convection. By contrast, areas of upper-level divergence tend to enhance convection. The divergence field is calculated using

$$D_{(i,j)} = \frac{U_{(i+1,j)} - U_{(i-1,j)}}{2\,\Delta X} + \frac{V_{(i,j+1)} - V_{(i,j-1)}}{2\,\Delta y} \quad . \qquad (9)$$

4. Difference Fields

A primary task in the forecasting process is the assessment of how well the model analysis represents the actual atmosphere. This procedure has historically been accomplished with the use of hand-drawn subjective analysis of observation data, geostationary and polar-orbiting satellite imagery and the experience of the forecaster in blending these data sources and determining model analysis weaknesses. The interactive analysis system is designed to provide the

user the capability to assess objectively these differences and display the results at each step in the interactive analysis. The difference fields are calculated using

$$Dif = \sqrt{(U_{FINAL}-U_{START})^2+(V_{FINAL}-V_{START})^2} \quad . \qquad (10)$$

Since only significant wind differences are desired, the plots of Dif will be for magnitudes of 10 kt (5 m s^{-1}) or greater.

VI. RESULTS

The following discussion describes a trial application of this interactive analysis system by an experienced tropical analyst. Although the application of the analysis technique is centered around the three steps described in Chapter V, the process is more comprehensive and involves a detailed assessment of the large-scale environment using numerical analysis first-guess fields, satellite imagery, and history of the circulation features. The first analysis in each scenario is necessarily more comprehensive and time consuming to identify representative values of all relevant circulations since no history is available. The other cases in this study follow the procedure described here and do utilize the history during the first-guess review. In each case, only the key synthetic observation insertions will be highlighted to illustrate the interactive analysis system.

A. INITIAL 200 MB ANALYSIS

The following discussion will illustrate a suggested sequence of steps that will result in an analysis that should improve the automated analysis (first-guess field) by insertion of, or re-positioning, tropical circulations. This abbreviated description was derived from the analysis log maintained during the application of the interactive technique.

The first step in the suggested sequence is to review the automated NOGAPS numerical analysis that serves as the first-guess field for the interactive analysis. This review of the synoptic circulations is identical in purpose and scope as the standard operating procedure for the Typhoon Duty Officer at the Joint Typhoon Warning Center (JTWC) beginning each forecast shift. After a

familiarization with the overall situation, a detailed assessment of the individual synoptic circulations is made.

The 200 mb NOGAPS analysis interpolated to 2100 UTC 3 August 1993 (Fig. 8a) has a TUTT that extends from 30°N, 180°E southwestward to 15°N, 160°E. A well-developed subtropical ridge is found over the western North Pacific with two closed cells at 28°N, 148°E and 19°N, 141°E. An additional ridge dominates the circulation over the Asian mainland (not shown). A major long-wave trough lies over Japan (not shown) and easterlies are found in the area from the equator to 18°N between 100°E and 150°E.

The second step is to review the existing Weather Advisories in relation to the synoptic features as analyzed in (or perhaps omitted from) the first-guess field. In the present example, this review of the tropical weather bulletins indicates TY Robyn (13W 1993) is located at 10.3°N, 142.2°E with maximum sustained winds of 65 kt. The cyclone is moving toward 300 degrees at 5 kt. Little or no evidence is found in Fig. 8a of an upper-level outflow associated with TY Robyn.

The third step is to review the satellite imagery to confirm or validate circulations included in (or omitted from) the first-guess field and in the Weather Advisories. In this example, the imagery (Fig. 9) verifies the TUTT cell at 30°N, 180°E. An associated area of clearing extending southwestward is bounded by a sharp cloud edge along the southeastern edge, which is evidence of an upper-level convergent aymptote that extends from 12°N, 155°E to approximately 17°N, 139°E, and is associated with the environmental flow interacting with the outflow from TY Robyn. Convection near 10°N, 153°E covers an area of over 5° latitude. Two other areas of tropical convection lie over southern Mindanao RP and near 7°N, 165°E. A zonal jet streak south of Japan is evident from the cirrus

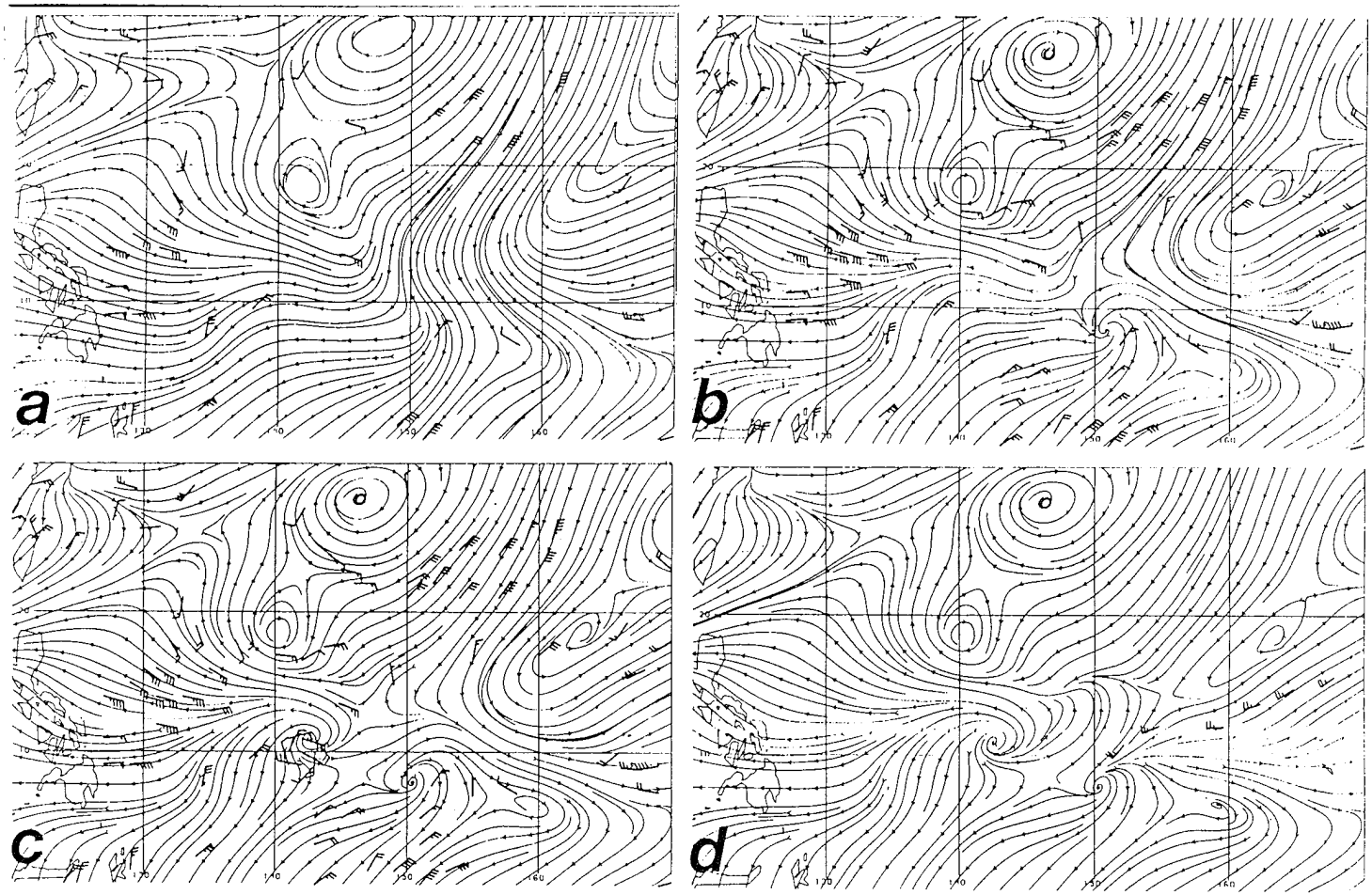

Fig. 8. 200 mb streamline analyses at 2100 UTC 3 Aug 93 of (a) first-guess field, (b) first MQ interpolation blending first-guess field and composite observations, (c) second MQ analysis including synthetic observations for TY Robyn, and (d) final MQ analysis with point synthetic observations overlaid to define convergent asymptote.

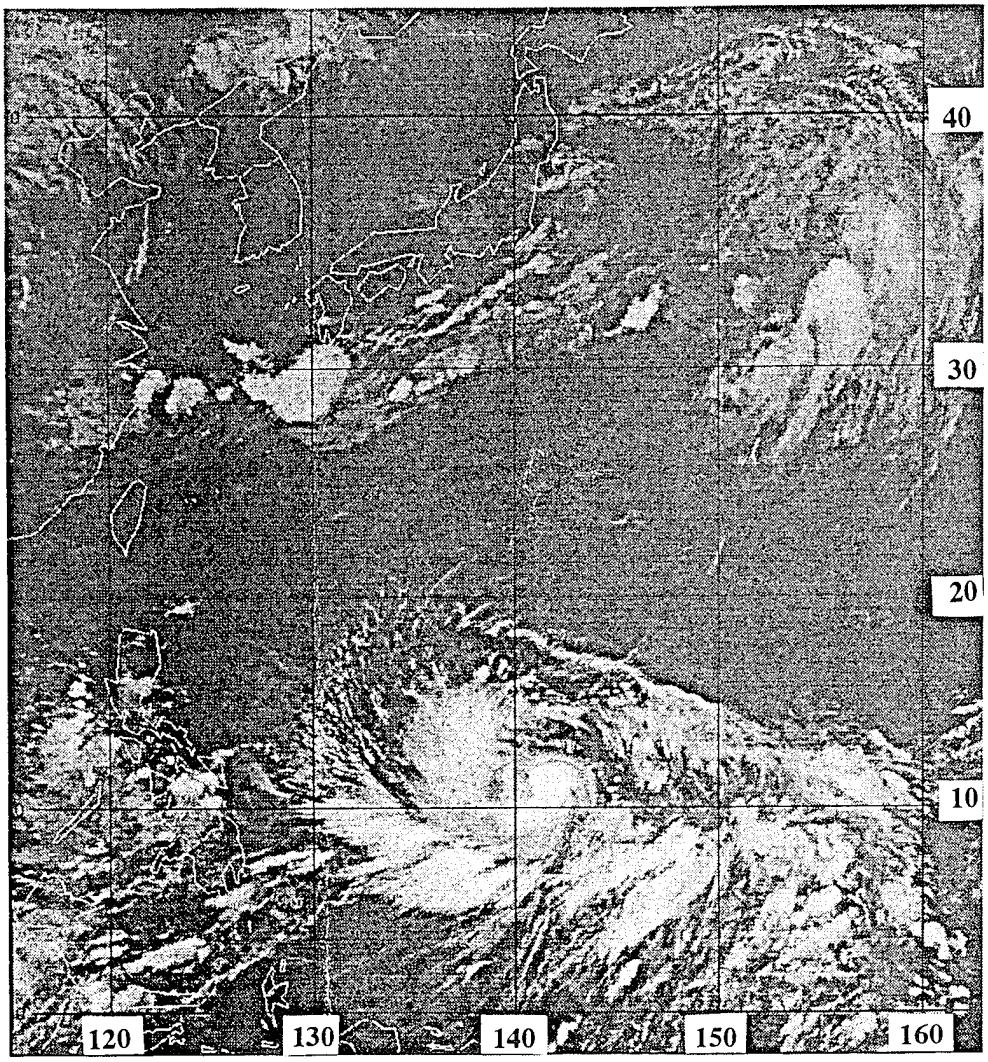

Fig. 9. High resolution Geostationary Meteorological Satellite (GMS) infrared image at 2030 UTC 3 Aug 93.

streaks and evidence of more meridional flow is apparent in the cirrus streaks along 160°E.

The above familiarization and synoptic assessment from the automated first-guess analysis and the satellite imagery is the necessary background to begin the interactive analysis. As indicated in Chapter V, the first step in the interactive analysis is to insert a set of composite observations that is entered as increments

relative to the first-guess field, and the Multi-Quadric Interpolation (MQI) is used to create the first MQI analysis (Fig. 8b). Entering the composite data has resulted in the analysis of two closed TUTT cells located at 27.5°N, 176°E and 19°N, 162°E. A review of the composite observations indicates these analyzed cell positions are well supported. Analysis of a point outdraft near 9°N, 151.5°E dramatically changes the winds in this area from those in the first-guess field. Regions of diffluence are analyzed near the convective areas over Mindanao and 7°N, 165°E. A concentrated flow is analyzed near the jet streak south of Japan (not shown here) and more concentrated meridional flow is analyzed near 160°E. These changes from the first-guess field reflect additional data from the compositing as well as the characteristic feature of the MQI to draw more closely to the observations than does the four-dimensional data assimilation. However, a number of deficiencies remain in the analysis. A well-defined outflow structure of TY Robyn as revealed in the satellite imagery is not reflected in the analysis. Both of the convergent asymptotes in the imagery are missing in the analysis. For example, the asymptote in the satellite image is inconsistent with the strong meridional flow between 150° and 160°E that extends from 40°N all the way to the Equator.

As part of the second step of entering synthetic circulation features in the interactive analysis, a set of synthetic vortex observations to describe the upper-level structure of TY Robyn is created using the algorithms described in the appendix. The Weather Advisory provides the required inputs of latitude (10°N), longitude (142.2°E), maximum winds (65 kt), and present motion of the cyclone (300° at 5 kt). In addition, the analyst must specify a radius of influence of the cyclone circulation (R_o) and a cutoff radius (r_{cut}) of synthetic observations. Because of the large data gap around TC Robyn, the cutoff radius is specified as

200 km, which is then a grid of nine synthetic wind observations. The radius of influence is a characteristic size of the storm circulation and is here estimated from the extent of the cloud shield on the satellite image and the radius of the low-level wind circulation. The radius of influence for Robyn at the 2100 UTC 3 August 1993 is estimated to be 800 km. The second MQI analysis including the composited observations plus the TY Robyn synthetic vortex observations is given in Fig. 8c. A good representation of the TY Robyn outflow is achieved.

The third step (which may involve several areas of the analysis and several iterations) in the interactive analysis is to address missing or incorrectly placed features. For example, the confluent asymptote that extends northeastward from the point outdraft near 9°N, 151.5°E is still missing. A review of the observations used in the analysis indicates a large void between 150° and 170° E along the convergent asymptote. To fill this void, the following synthetic wind observations (direction from north and speed in kt) are entered at the lat./long. shown:

13.0°N 150.0°E 18025
10.0°N 152.5°E 21525
11.0°N 155.0°E 23525
11.5°N 160.0°E 27025
12.0°N 162.5°E 25025
12.5°N 165.0°E 24025
13.0°N 167.5°E 23525
14.0°N 170.0°E 23525

This list of observations is actually the result of three iterations to fine tune the MQI analysis in this region. The speed and directions of these point synthetic observations was assigned based on the surrounding observations and satellite interpretation of the flow field. A comparison of the analysis after step two (Fig. 8c) with the final iteration of the MQI that includes these observations (Fig. 8d) indicates the convergent asymptote is now evident in the wind field. This analysis

correctly indicates that the equatorward current between 140°E and 150°E does not penetrate all the way to the Equator as in the first-guess field (Fig. 8a). Rather, the flow is deflected westward by the Robyn outflow and eastward and then northeastward by the point outdraft near 9°N, 150°E, as revealed by the satellite imagery (Fig. 9).

B. INITIAL 850 MB ANALYSIS

In general, the first-guess field (Fig. 10a) is already in good agreement with the satellite imagery (Fig. 9) for the initial low-level analysis. The first interactive step with the MQI analysis (Fig. 10b) involving the addition of the composite observations results is a good representation of most features on the satellite imagery. Two exceptions are an open wave near 17°N, 113°E (vice linear southwesterly flow), and a low associated with an area of convection near 7°N, 165°E was missing. Additionally, the low-level outer wind field of TY Robyn is too strong. A review of the observations used in the analysis (Fig. 10b) shows a lack of observations near TY Robyn and a 5 kt northerly observation near 17°N, 113°E that does not agree with other observations in the vicinity and is inconsistent with the satellite interpretation. A southerly point observation of 10 kt near 17°N, 113°E to overide the 5 kt northerly observation, and a five synthetic observation cyclone vortex of 15 kt intensity was entered near 17°N, 165°E. To create this vortex, an estimate of the maximum perturbation winds was made from a review of the observations in the vicinity and a cutoff radius of 150 km was entered. The synthetic circulation to correct the outer wind representation of TY Robyn is created using a R_o of 800 km, V_{max} of 65 kt, a motion vector of 300 at 5 kt, and a r_{cut} of 300 km, which results in 18 synthetic observations. The results of the MQI analysis including these synthetic observations is shown in Fig. 10c. This is

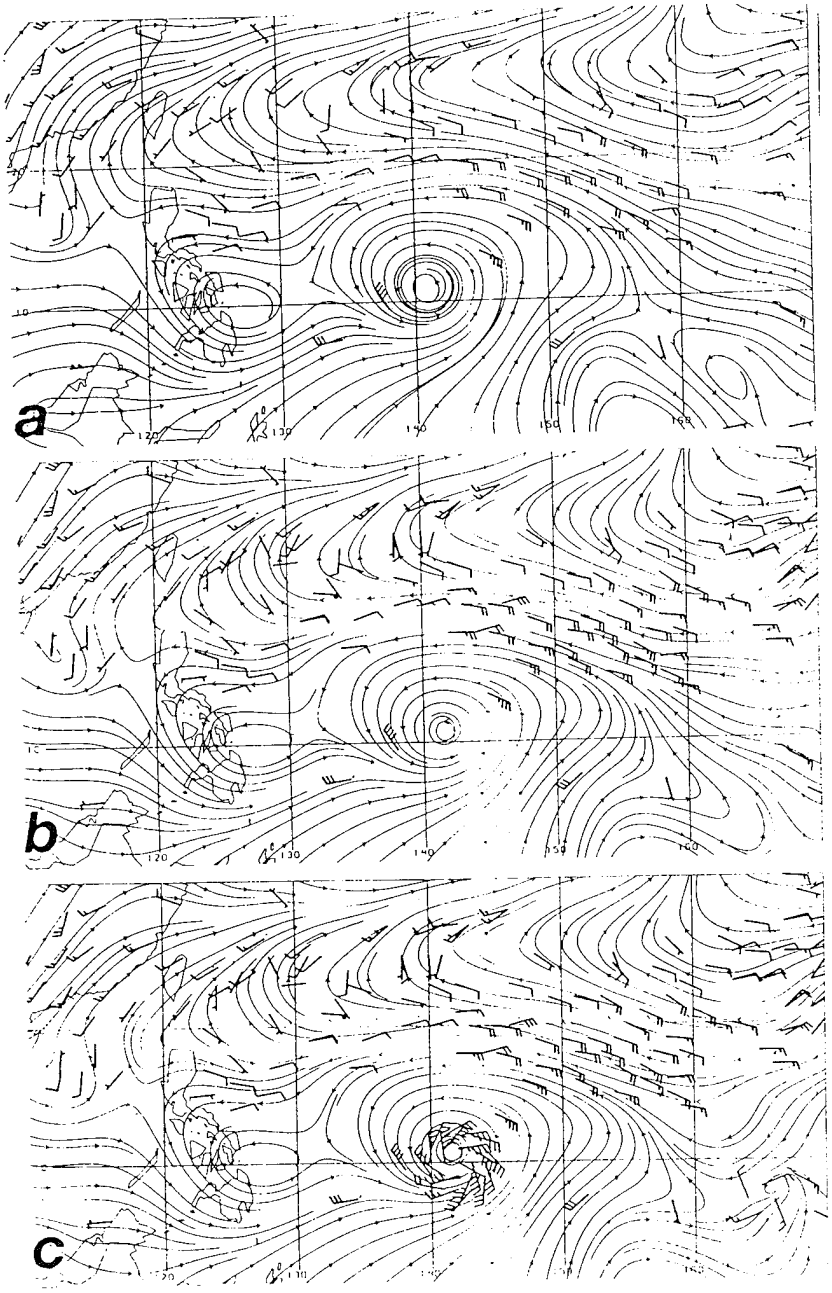

Fig. 10. 850 mb streamline analyses at 2100 UTC 3 Aug 93 of (a) first-guess field, (b) first MQ interpolation analysis blending first-guess field and composite observations, (c) final MQ interpolation including all synthetic observations.

an example of an interactive analysis that required very little intervention because well-placed observations have resulted in a fairly good automated analysis, with the exception of the bad wind observation near 17°N, 113°E.

C. 200 MB ANALYSIS AT 0900 UTC 4 AUG 93

A simple extrapolation from the initial analysis (Fig. 8d) and review of the satellite image valid at 0900 UTC 4 Aug 1993 (Fig. 11) indicates the following features should be present in the analysis: two TUTT cells near 30.5°N, 149°E and 17°N, 160°E; a convergent asymptote that extends from 13°N, 150°E west-northwestward and merges with the outflow of TY Robyn and then extends east-northeastward to 13°N, 160°E and 20°N, 170°E and 23°N, 180°E; an area of strong convection near 10°N between 150°E and 160°E; a weak low-level circulation is possible near 5°N, 175°E; meridional flow along 160°E; and a new low moving into the Yellow Sea. Based on this review, the first-guess field (Fig. 12a) is missing TY Robyn, the point outdraft, one TUTT cell near 17°N, 160°E, and the convergent asymptote.

The first MQI analysis (Fig. 12b) that blends the composite observation set with the first-guess field results in the analysis of a point outdraft near 8°N, 150°E. However, the convergent asymptote along 13°N and the outflow structure of TY Robyn are still missing. A review of the composite observations indicates that no observations exist in the region to describe the convergent asymptote. Although most of the upper-level outflow of TY Robyn is well represented, a key observation is required to describe the upper-level outflow on the south side. As a complete synthetic circulation is not required for this analysis, only the fine tuning step is necessary. The following point synthetic observations (direction clockwise

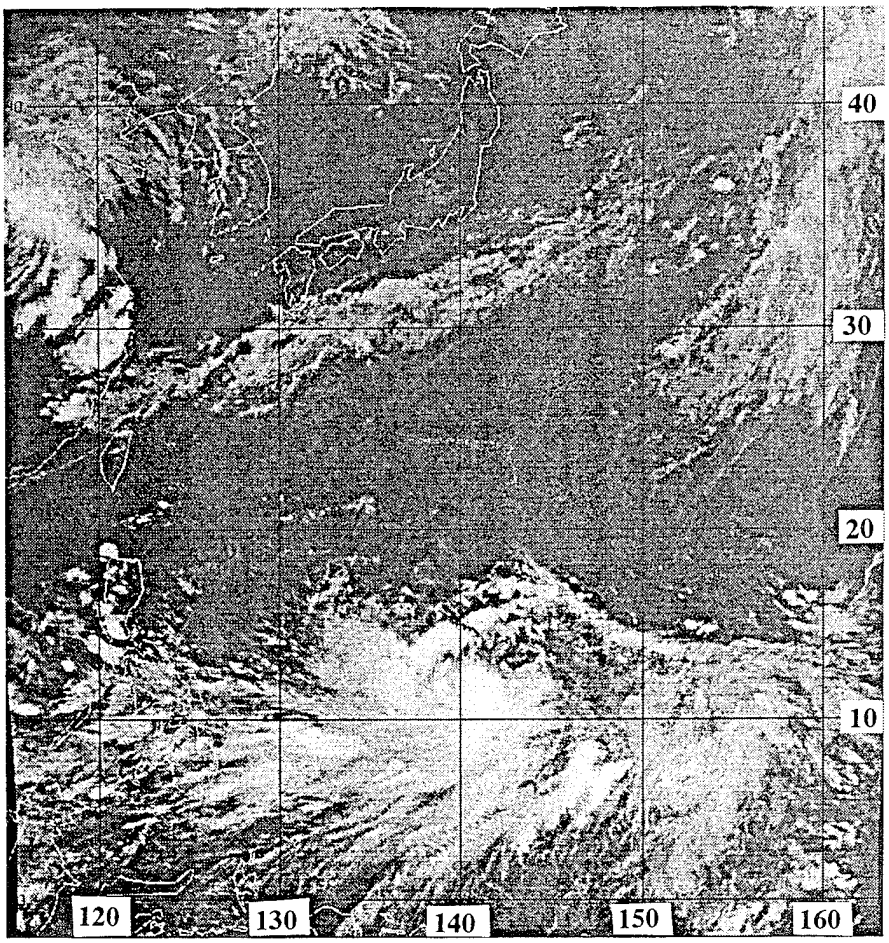

Fig. 11. High resolution infrared GMS imagery at 0830 UTC 9 Aug 93.

from north and speed in m s^{-1}) are entered into another iteration of the MQI analysis:

10.0°N 141.0°E 27025
10.0°N 152.5°E 21525
11.0°N 155.0°E 23525
15.0°N 155.0°E 27025
14.0°N 160.0°E 25025

The final MQI analysis (Fig. 12c) of the first-guess field, composite observations,

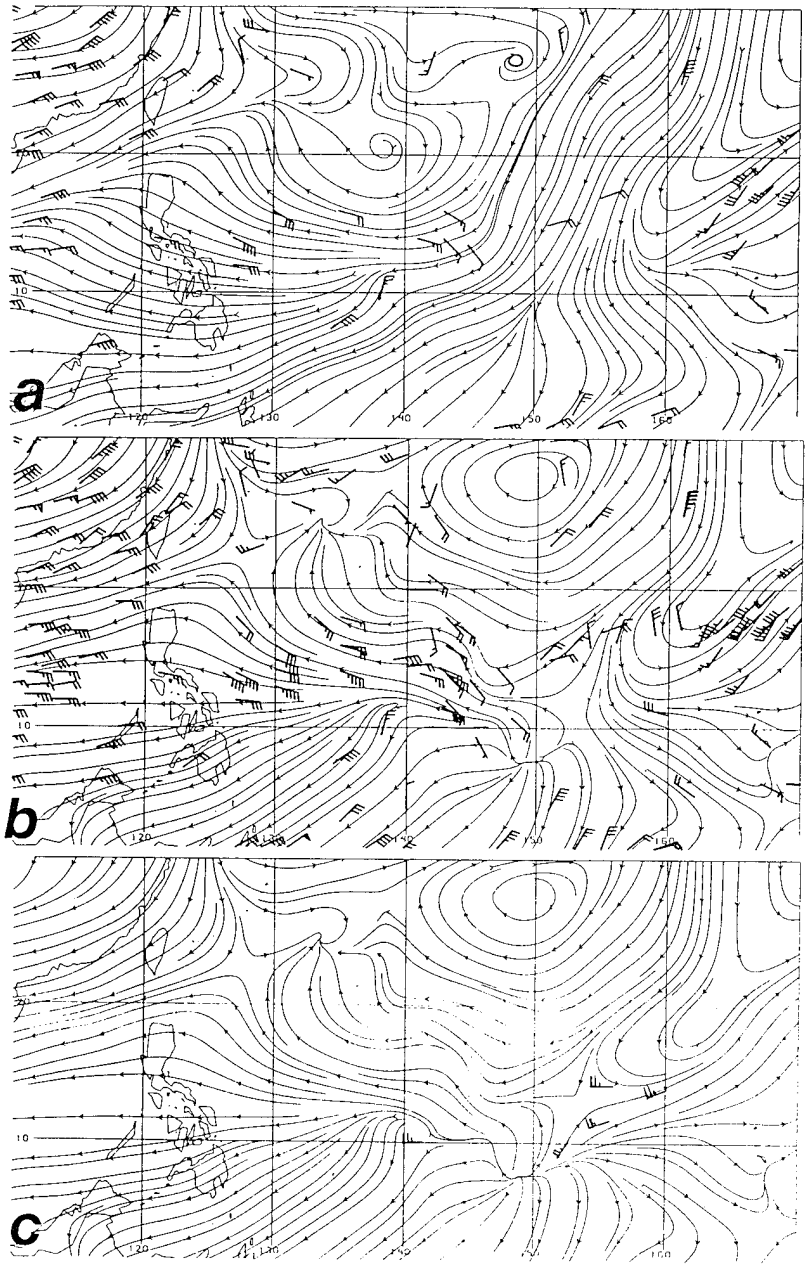

Fig. 12. 200 mb streamline analyses at 0900 UTC 4 Aug 93 of (a) first-guess field with on-time observations overlaid, (b) first MQ interpolation blending first-guess field and composite observations, and (c) final MQ interpolation with point synthetic observations overlaid to adjust analysis.

and point synthetic observations properly depicts the convergent asymptote and the upper-level outflow structure that was missing in the previous iterations.

The final MQI analysis highlights the importance of a thorough review of the observations, and of a complete understanding of the flow fields around features depicted on satellite imagery. In this case, a simple five synthetic observation set results in an analysis that depicts both the proper upper-level outflow structure of TY Robyn and a convergent asymptote where only meridional flow existed in the first-guess field.

D. 850 MB ANALYSIS AT 0900 UTC 4 AUG 93

Beginning with an extrapolation of the previous analysis (Fig. 10c) and comparing it with satellite imagery valid 0900 UTC 4 Aug 93 (Fig. 11), the appropriate analysis features and their locations are identified. A new mid-latitude low, which has moved into the Yellow Sea and dominates the region, is well represented in the first-guess field (not shown). Satellite imagery (Fig. 11) places TY Robyn near 11.3°N, 140.9°E. The latest Weather Advisory supports this position and reports TY Robyn is moving 310° at 5 kt with maximum sustained winds of 70 kt. The motion vector of the previous analysis aligns well with this position, as does the first-guess field (Fig. 13a). However, the first-guess field fails to represent two cyclonic circulations evident in the satellite imagery and over-represents the outer windfield of TY Robyn. The first missing cyclone is embedded in an extensive area of convection near Mindanao that extends over the South China Sea. Cyclonic turning in the low-level cloud lines in this convection (see Fig. 11) indicate two possible placements for this low-level circulation--near 12°N, 113°E or 12°N, 123°E. Neither possibility is present in the first-guess field. The other missing cyclone, which was near 7°N, 165°E in the previous

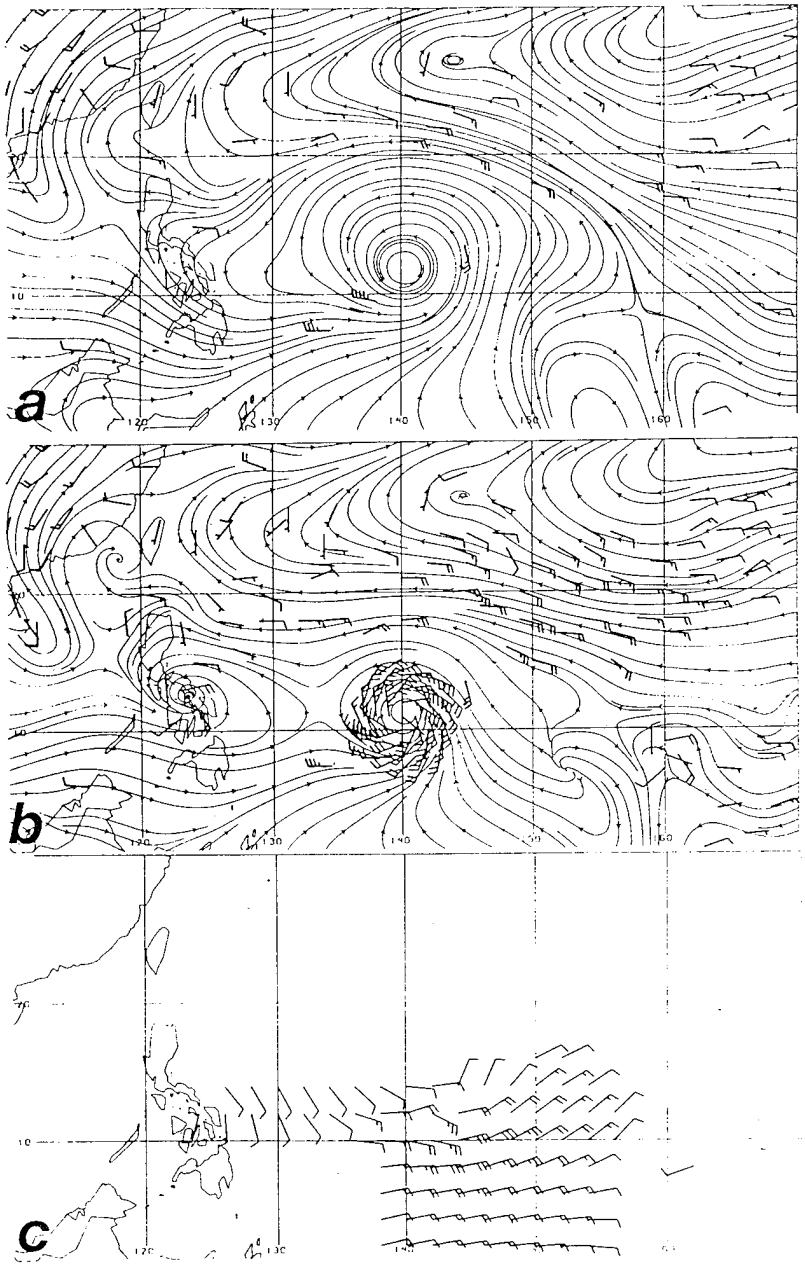

Fig. 13. 850 mb streamline analyses at 0900 UTC 4 Aug 93 of (a) first-guess field with on-time observations overlaid, (b) final MQ interpolation with additional composite and synthetic observations overlaid, and (c) 850 mb final MQI analysis minus first-guess field difference vectors (long barb is 10 kt and only difference vectors exceeding 10 kt are shown).

analysis (Fig. 10c), is found on the current satellite imagery at 8°N, 160°E after having moved 290° at 6 kt.

A composite observation set is blended with the first-guess field and the first MQI analysis (not shown) is performed. This procedure not only fails to add the missing cyclones and correct the outer wind field of Robyn, it produces a new low southeast of Hong Kong that is not supported in the satellite image.

To create the two missing low-level cyclonic features and correct the outer wind field of TY Robyn, complete sets of synthetic circulation observations are added to the composite data set. One of the strengths of this technique is the limited number of observations required to depict weak cyclonic features in the low-level wind field. It is possible to enter as few as five synthetic observations in a data-void region to describe weak low-level circulations. For example, two sets of five synthetic vortex observations are inserted to describe the two missing circulations using a r_{cut} of 150 km, V_{max} of 15 kt, and a r_{max} of 100 km. The outer windfield of TY Robin is corrected with synthetic observations based on a R_o = 800 km, V_{max} = 70 kt, and r_{cut} = 400 km. The final MQI analysis (Fig. 13b) depicts each of these missing features in their proper location.

To eliminate the new low created southeast of Hong Kong, a northerly 5 kt wind observation was replaced with a synthetic southerly wind of 10 kt. The final MQI analysis (Fig. 13b) turns the flow in the region to southwesterly in agreement with the satellite analysis and adjacent observations.

One demonstration of the impact of using this interactive approach to insert composite and synthetic observation is to subtract the first-guess field from the final MQI analysis, which is referred to as the difference field (Fig. 13c). Notice that the first-guess field winds south of TY Robyn were too strong, because anticyclonic flow results in the difference field. The synthetic vortex in the first-

guess field for TY Robyn may be too large because of the coarse grid of the NOGAPS analysis. The single 5 kt southwesterly difference vector near 8°N, 162°E (Fig. 13c) indicates that cyclonic shear was already present in the first-guess field and the introduction of westerly flow south of the vortex is all that is required to depict properly the low-level cyclone near 8°N, 160°E.

A primary finding of this 850 mb analysis is that the MQI analysis will draw to both good and bad observations, and thus manual insertion of point synthetic observations is required to compensate for bad observations. The effect of these bad observations is first realized when the composite observations are blended with the first-guess field. Prior to introducing synthetic data, a thorough review of the previous analysis, satellite imagery, and the first-guess field is necessary, so the analyst can isolate the bad observations. A check of all large wind differences (Fig. 13c) is also an effective way of detecting bad observations.

E. 200 MB ANALYSIS AT 2100 UTC 4 AUG 93

This analysis highlights the procedures necessary when no data exist to describe features indicated on the satellite imagery and further illustrates problems that occur when bad observations are introduced into the MQI analysis. It also shows that when good composite data do exist in the vicinity of missing features, little or no effort is required to depict properly these features. To identify the areas of missing and bad observations, the analyst must first understand the changes in the key features from the previous analysis (Fig. 12c) and required modifications of the flow fields surrounding these features in the current satellite imagery (Fig. 14).

As a first step in this process, the features missing in the first-guess field (Fig. 15a) must be identified (e.g., TY Robyn). Based on the satellite analysis and

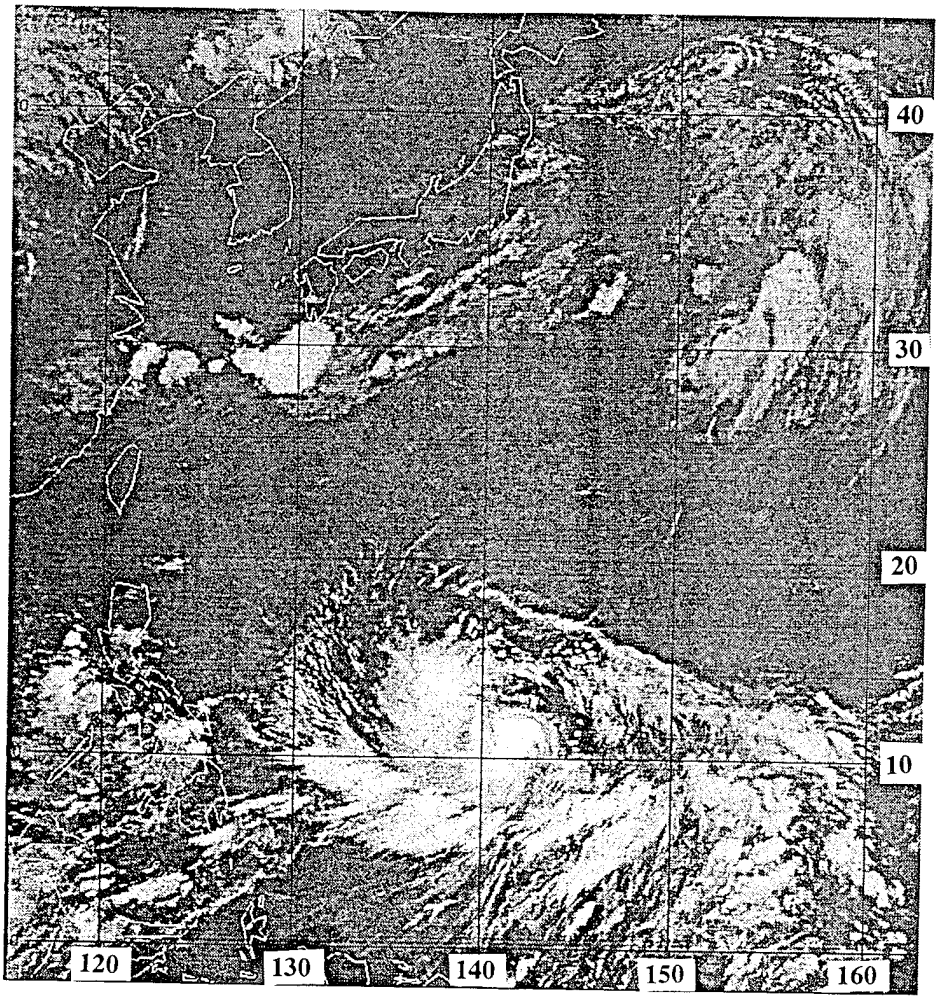

Fig. 14. High resolution infrared GMS imagery at 2030 UTC 4 Aug 93.

reports in the current Weather Advisory, TY Robyn is near 12.3°N, 140.1°E and continues to move west-northwestward (320° at 7 kt) with little change in intensity. A point outdraft from the convection near 11°N, 150°E -160°E is not analyzed. Rather, the first-guess field has a meridional flow between 150°E to 165°E that extends from 35°N to the Equator, which conflicts with the satellite imagery interpretation (recall a similar problem existed in the initial 200 mb analysis). A

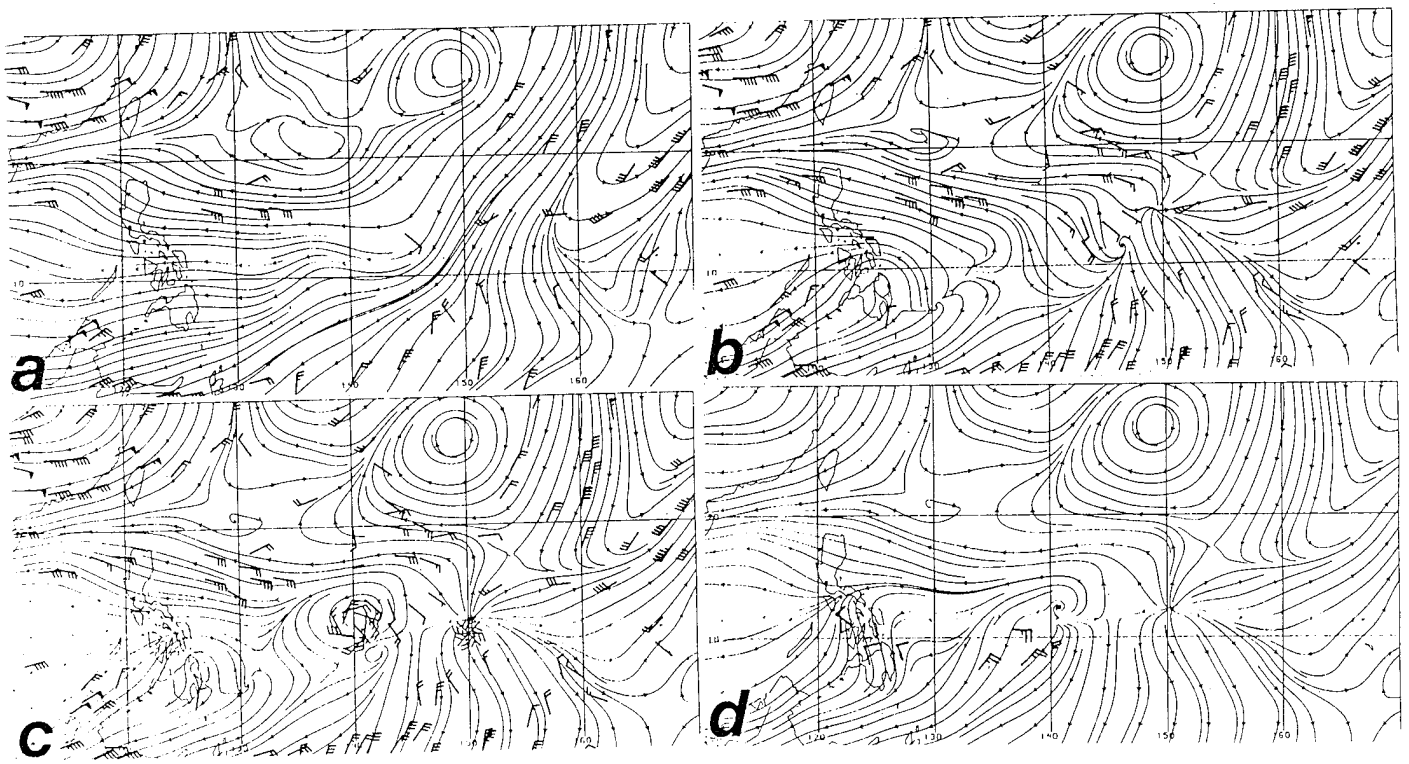

Fig. 15. 200 mb streamline analyses at 2100 UTC 4 Aug 93 of (a) first-guess field with on-time observations overlaid, (b) first MQ interpolation blending first-guess field and composite observations, (c) second MQ interpolation adding synthetic circulations, and (d) final MQ interpolation with point synthetic observations overlaid.

cirrus streak along 160°E in Fig. 14 indicates meridional flow is present north of 15°N, but the convergent asymptote that extends east-northeastward and west-northwestward from 13°N, 155°E indicates this flow becomes more zonal and does not extend to the Equator. Satellite imagery also indicates diffluence in the flow field associated with areas of convection west of TY Robyn between 5°N to 15°N and 130°E to 140°E, west of Mindanao near 12°N, 118°E, and near 5°N, 177°E. These features are poorly depicted in the model analysis.

The first attempt to add these features is blending composite observations with the first-guess field through a MQI analysis (Fig. 15b). Although this first analysis does not result in TY Robyn being represented, an area near 11°N, 147.5°E of upper-level outflow in a spiral convective band associated with TY Robyn is added. A point outdraft near 15°N, 150°E is depicted, although it is not in agreement with the satellite position at 13°N, 150°E. Also added by the composite observations alone is the convergent asymptote. It is significant that simply adding composite observations did introduce the point outdraft and thus the convergent asymptote between this outdraft and the meridional flow toward the Equator in the first-guess field. If these key observations were present in the data set presented to the NOGAPS analysis, they must have been omitted during the quality control step as being too large a deviation from the short-term prediction. However, the introduction of the composite observations also included two bad observations, which result in the analysis of two circulations not supported by satellite imagery analysis. A divergent line analyzed near 7°N, 131°E is based on a bad (zero wind) observation and a weak upper-level anticyclone is depicted based on a single 5 kt wind report near the Philippines. Each of these problems must be addressed with the introduction of synthetic observations.

In the second step, a set of synthetic circulation observations for TY Robyn is developed using a R_o of 800 km based on the value used in the previous analysis

(Fig. 12c) and the size of the convective area in the current imagery, and a r_{cut} of 200 km. The intensity and motion vector are based on the current Weather Advisory. A set of nine synthetic vortex observations results for TY Robyn. To re-position the point outdraft near 13°N, 150°E, a synthetic circulation is developed using U_{rad} =15 m s^{-1}, a r_{max} = 100 km, and a r_{cut} of 200 km.

The MQI analysis (Fig. 15c) with the inclusion of these synthetic circulation observations is successful in placing the point outdraft and the upper-level anticyclonic outdraft of TY Robyn in the proper positions. However, the extent of the anticyclonic outdraft is too large, which is partly a result of the close proximity to the zero observation near 7°N, 131°E. This observation causes a line divergence area south of TY Robyn and a closed circulation feature near Mindanao.

In the third step, four synthetic observations are added (Fig. 15d) to correct the line divergent area. The closed circulation feature near Mindanao is more realistically depicted as an open diffluent wave in the flow field after the insertion of three synthetic observations. Determination of the proper synthetic observation placements to correct these features requires a series of four iterations. The list of point synthetic observations included:

8°N 140.0°E 36025 kt
8°N 137.5°E 04525 kt
11°N 137.5°E 09025 kt
7°N 134.5°E 04525 kt
8°N 122.5°E 36010 kt
8°N 125.0°E 36010 kt
11°N 122.5°E 32510 kt

The final MQI analysis (Fig. 15d) properly depicts the upper-level outflow of TY Robyn, the point outdraft, the diffluent wave near Mindanao, and has

eliminated the effects of the bad observation near 7°N, 133°E. This case highlights the need to add synthetic observations in areas where no data exist and in areas where bad observations are present.

Because the MQI analysis draws closely to all observations, other problems arise in this analysis. Any features not readily identified on satellite imagery require a careful review of the nearby observations to ensure that the effects of bad data are not overlooked. One of the deficiencies of the MQI analysis is that a constant smoothing factor is applied throughout the domain. Thus, it is difficult to blend the real data and synthetic observation in a closely spaced analysis, especially when bad data are present. If a bogus circulation is created near a major synoptic feature, the structure of the synoptic feature will be distorted. A good illustration in Fig. 15 of the need for human quality control is the elimination of the bad circulation near 7°N, 133°E and the resultant reduction of the outflow circulation of TY Robyn. In a truly interactive system, a capability for a "point-and-click" elimination of these erroneous observations would be desirable.

F. 850 MB ANALYSIS AT 2100 UTC 4 AUG 93

As in the previous example, circulations in the previous 850 mb analysis (Fig. 13c) are extrapolated forward based on the current satellite imagery (Fig. 14), which is also reviewed to identify locations of missing or misrepresented features. The primary challenges in this and succeeding 850 mb analyses are to reduce the size of TY Robyn's circulation and introduce low-level circulations that are missing. The recurring problem associated with the representation of TY Robyn in the first-guess field (Fig. 16a) mandates the inclusion of synthetic observations in the MQI analysis. In each case thus far, the circulation of TY Robyn in the first-guess field is too strong in the outer regions. Insertion of the

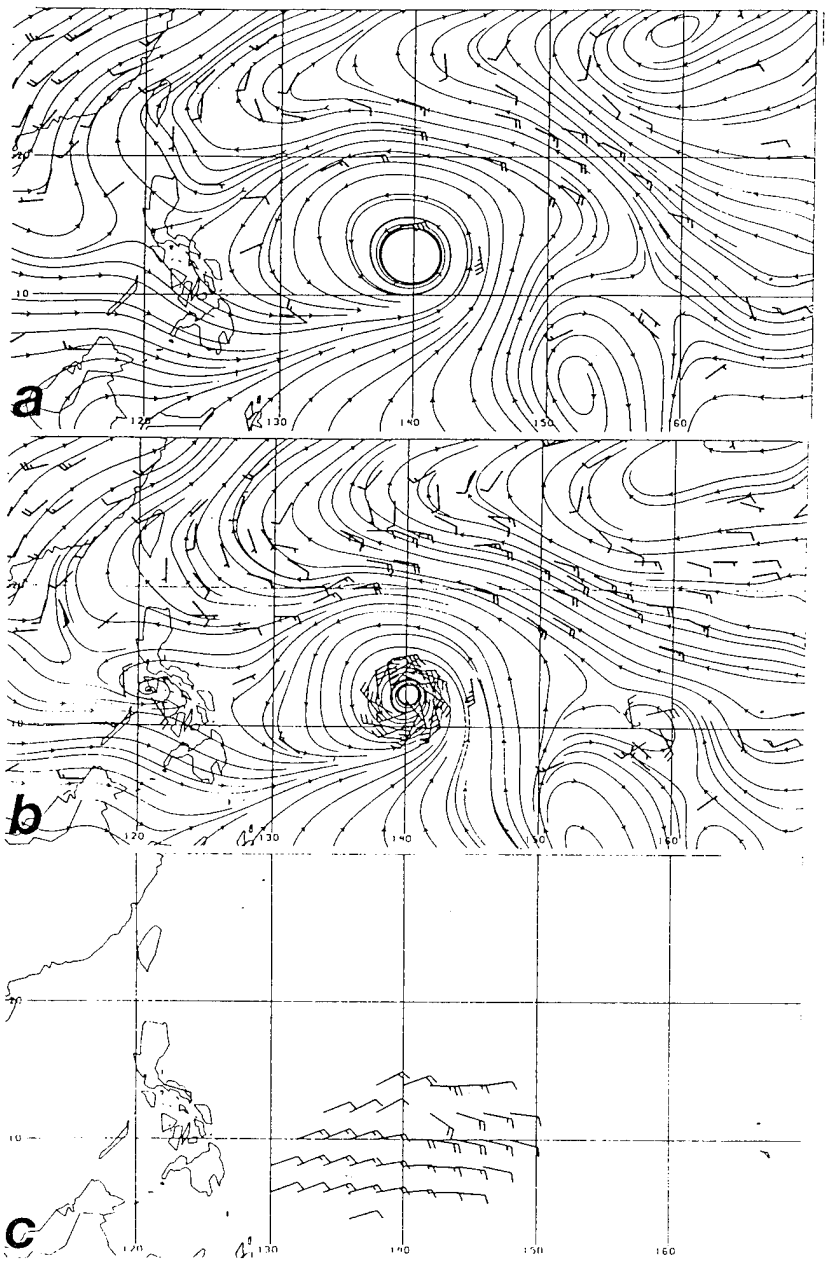

Fig 16. 850 mb streamline analyses at 2100 UTC 4 Aug 93 of (a) first-guess field with on-time observations overlaid, (b) second (final) MQ interpolation blending first-guess field, and composite and synthetic circulation observations, and (c) 850 mb final MQI analysis minus first-guess field difference vectors.

composite observations in the first step did not solve the problem of the missing weak low-level cyclones, so insertion of synthetic vortices is required as in the previous analysis.

Because the outer circulation of Robyn is too strong, a set of synthetic circulation observations will be inserted. The current Weather Advisory indicates TY Robyn is moving 320° at 6 kt with maximum winds of 70 kt. Using this information, synthetic observations for TY Robyn are developed using a R_o = 800 km and a r_{cut} of 300 km. A larger r_{cut} value is used here because no observations existed within a 600 km radius of TY Robyn. As a general rule for developing the low-level synthetic observations for this interactive procedure, the r_{cut} is specified as approximately one-half the distance to the nearest real observations. This specification usually produces a smooth blending of the synthetic observations with the adjacent real observations.

Synthetic circulations to insert the two weak low-level cyclonic circulations were developed using V_{max} of 15 kt, r_{max} of 100 km, and r_{cut} of 150 km, which resulted in five observations each. The second MQI analysis (Fig. 16b) including these synthetic observations has a proper depiction of all features indicated on the satellite imagery and in the composite data set. Notice the radius of max winds for TY Robyn is properly depicted nearer the center as expected in a mature tropical cyclone.

The low-level difference field (Fig. 16c) illustrates that the model first-guess field had stronger winds on the south side of the circulation than is supported by the combination of the composite observations and the synthetic circulation observations. This finding validates the use of a synthetic vortex when dealing with mature tropical cyclone circulations in the first-guess field.

G. 200 MB ANALYSIS AT 0900 UTC 5 AUG 93

This analysis is a good example of inserting complete sets of synthetic circulation observations (vice single synthetic observations) to describe the features missing in the first-guess field. Further support for the use of composite observations is provided. A new feature, an upper-level anticyclone that developed over the main convergent band southeast of TY Robyn, is identified.

As in the previous analyses, a comparison of the previous analysis (Fig. 15d) and the current satellite imagery (Fig. 17) is used to locate the key features of the analysis. Imagery interpretations and the current Weather Advisory indicate TY Robyn is near 12°N, 140.0°E and is maintaining intensity while moving 320° at 7 kt. The point outdraft near 10.3°N, 153.5°E has begun to rotate cyclonically. A Tropical Cyclone Formation Alert (pre-TS Steve) has been issued for this region, and indicates a low-level circulation of less than 30 kt.

Four primary features evident on the satellite analysis (animation assists in these identifications) do not appear in the first-guess field (Fig. 18a): a convergent asymptote along 15°N; a TUTT cell near 17°N, 151°E; the upper-level outflow pattern associated with TY Robyn; and the point outdraft above pre-TS Steve. In the first-guess field, meridional flow is dominating the region where the convergent asymptote and an accompanying zonal flow should be. In addition, two minor TUTT cells near 30°N, 176°E and 25°N, 167°E are evident in the imagery, and diffluence should be analyzed over two areas of deep convection over the South China Sea and near 8°N between 160°E and 170°E.

Blending the composite observations with the first-guess field in the first MQI analysis (Fig. 18b) drastically changed the flow field. For example, the desired zonal pattern emerged near the convergent asymptote along 16°N east of 150°E. A new upper-level anticyclone is analyzed near 10°N, 147.5°E in the

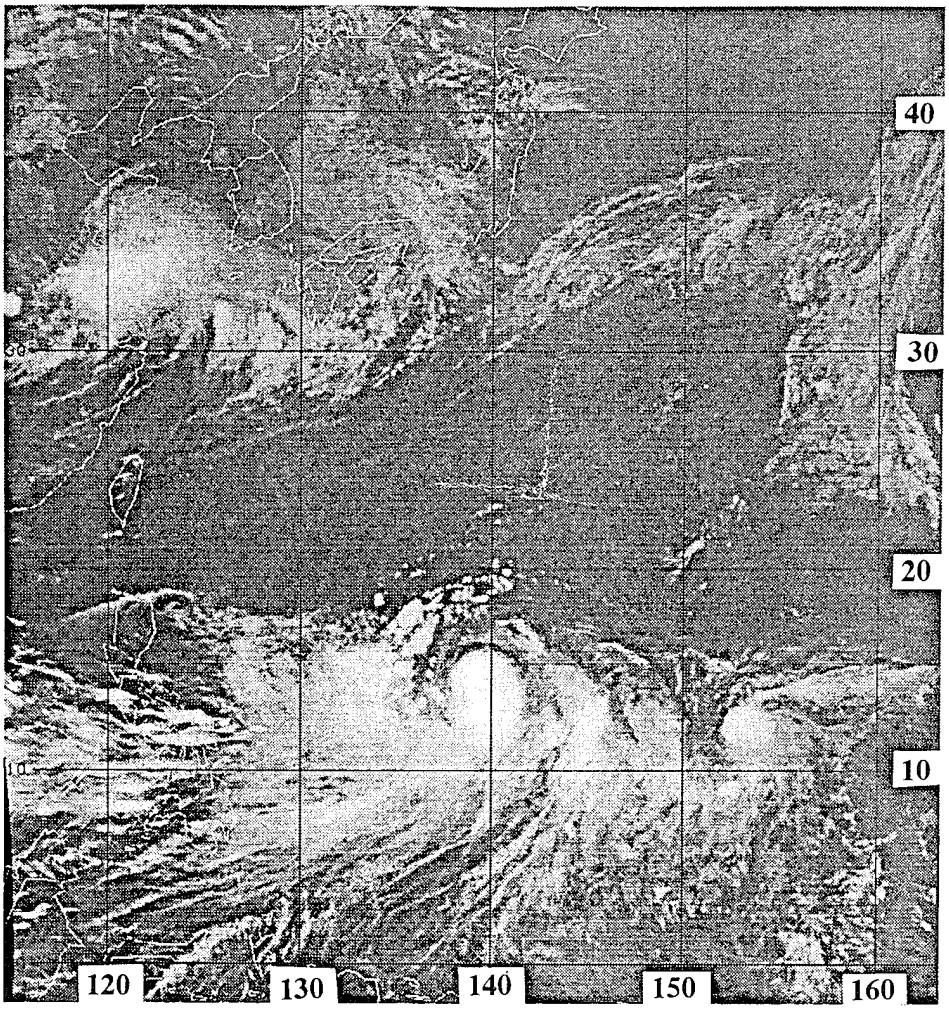

Fig. 17. High resolution GMS imagery at 0830 UTC 5 Aug 93.

vicinity of the strong convection associated with a convergent band southeast of TY Robyn. In addition, the two minor TUTT cells and all of the diffluent regions are now included in the analysis. These marked changes in the flow field, especially along and to the south of 16°N, emphasize the usefulness of composite observations and the need to analyze closely to the wind data in tropical analysis. Presumably, the quality control step in the automated NOGAPS analysis technique has eliminated, or assigned a lower weight to these observation, especially if the

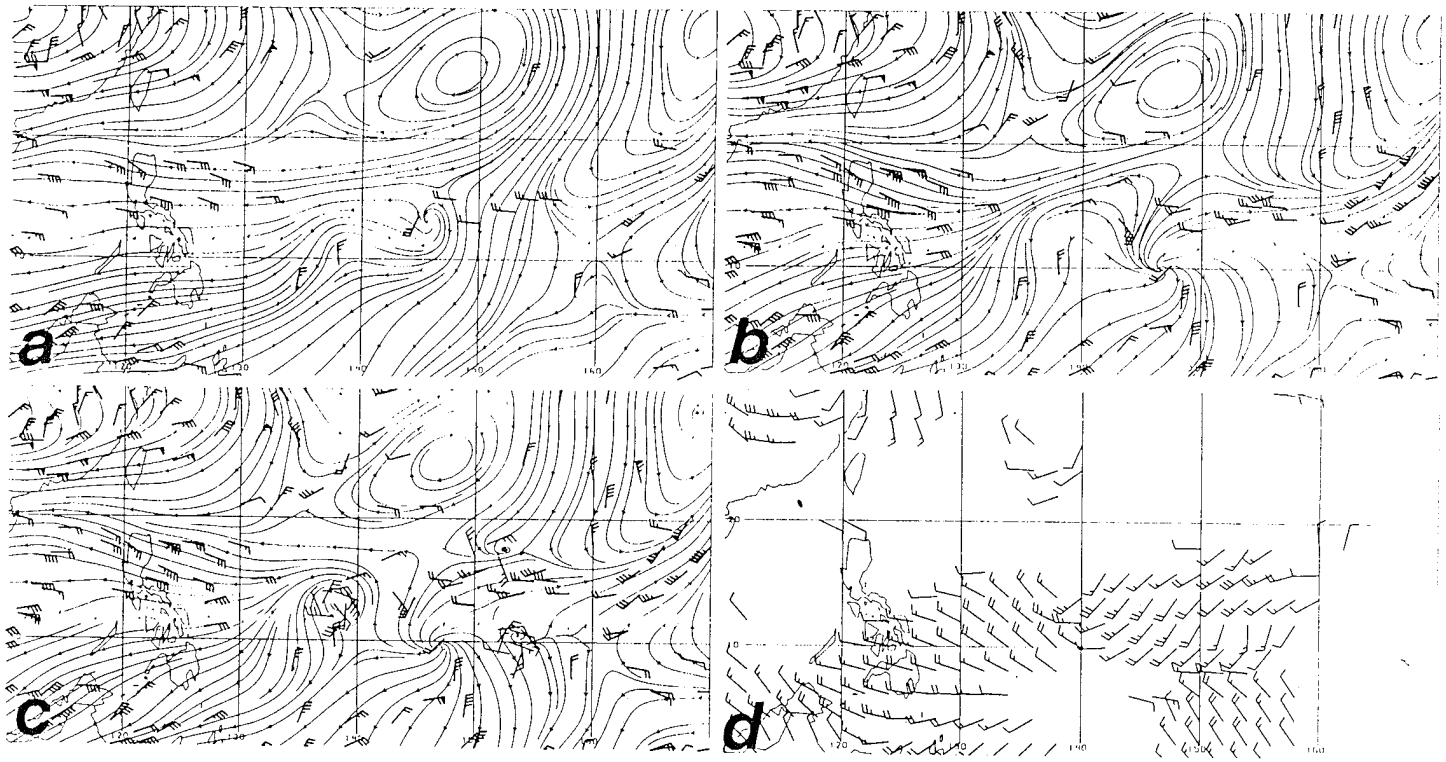

Fig. 18. 200 mb streamline analyses at 0900 UTC 5 Aug 93 of (a) first-guess field, (b) first MQ interpolation blending first-guess fields and composite observations, (c) final MQ analysis including synthetic circulation observations, and (d) 200 mb final MQ analysis minus first-guess field difference vectors.

observations differ significantly from the short-term NOGAPS model prediction used as the first-guess field.

In contrast to these improvements, the upper-level outflow of TY Robyn, the point outdraft, and a weak TUTT cell are still missing due to a lack of key data. The only reflection of the TY Robyn outflow in the initial MQI analysis is an area of diffluence near 12.5°N, 139°E. To create these missing features, application of a single point synthetic observation to force in the TUTT cell circulation is tested. Starting with a zero wind observation at 17°N, 151°E in the vicinity of the cyclonic shear in the initial set, additional single observations are added until a closed circulation is achieved in the MQI analysis. Since this required a minimum of four observations and was a time-consuming process to depict this TUTT circulation, it is thus more efficient to create these circulations using the synthetic circulation observation approach described in the appendix.

Synthetic vortices for TY Robyn, the point outdraft, and the TUTT cell are developed using the synthetic circulation observations approach. The synthetic circulation for TY Robyn is developed using R_o = 800 km, V_{max} = 70 kt, a motion vector of 320° at 11 kt, and r_{cut} = 200 km, which results in nine observations. A synthetic circulation for the point outdraft over pre-Steve is developed using R_o = 500 km, V_{max} = 30 kt, a motion vector of 280° at 5 kt, and r_{cut} = 200 km, which again results in nine observations. The synthetic circulation of the TUTT cell is developed using V_{max} = 25 kt, r_{max} = 100 km, and r_{cut} = 150 km. which results in five observations.

The final MQI analysis (Fig. 18c) has a proper depiction of the convergent asymptote, the weak TUTT cell, and the upper-level structures of both TY Robyn and pre-Steve. This analysis illustrates the efficiency of using complete synthetic

circulations, versus single point synthetic observations, to describe the features missing from the first-guess field.

The 200 mb difference field (Fig. 18d) highlights the changes in the meridional flow field south of 16°N between 140°E and 160°E in the first-guess field. Additionally, the cyclonic flow near 12°N, 140°E in the difference field illustrates that the upper-level cyclonic structure on the south side of TY Robyn was missing from the first-guess analysis.

H. 850 MB ANALYSIS AT 0900 UTC 5 AUG 93

This analysis provides another illustration of the rapid analysis possible with the proper placement of key synthetic observations. In addition, the ability of the interactive analysis to produce a more representative vertical wind shear will be illustrated.

As before, the circulations in the previous analysis (Fig. 16b) are interpreted in view of the current satellite imagery (Fig. 17) and an assessment of the missing features in the first-guess field (Fig. 19a) is completed. As in the previous 850 mb analyses, TY Robyn will require synthetic observations to better represent the outer wind field. The tropical disturbance that later becomes TS Steve is near 10.3°N, 153.5°E in a data-void area, and thus is not reflected in the first MQI analysis (Fig. 19b), which blends composite observations and the first-guess field. TY Robyn's low-level synthetic vortex is developed using R_o = 800 km, V_{max} = 70 kt, a motion vector of 320° at 11 kt, and r_{cut} = 300 km, which results in 21 observations. The synthetic vortex to represent pre-Steve is developed using R_o = 500 km (estimated from satellite imagery), V_{max} = 15 kt, a motion vector of 320° at 11 kt, and r_{cut} = 150 km, which results in five observations. This is another example of an interactive analysis that required minimal iterations because the

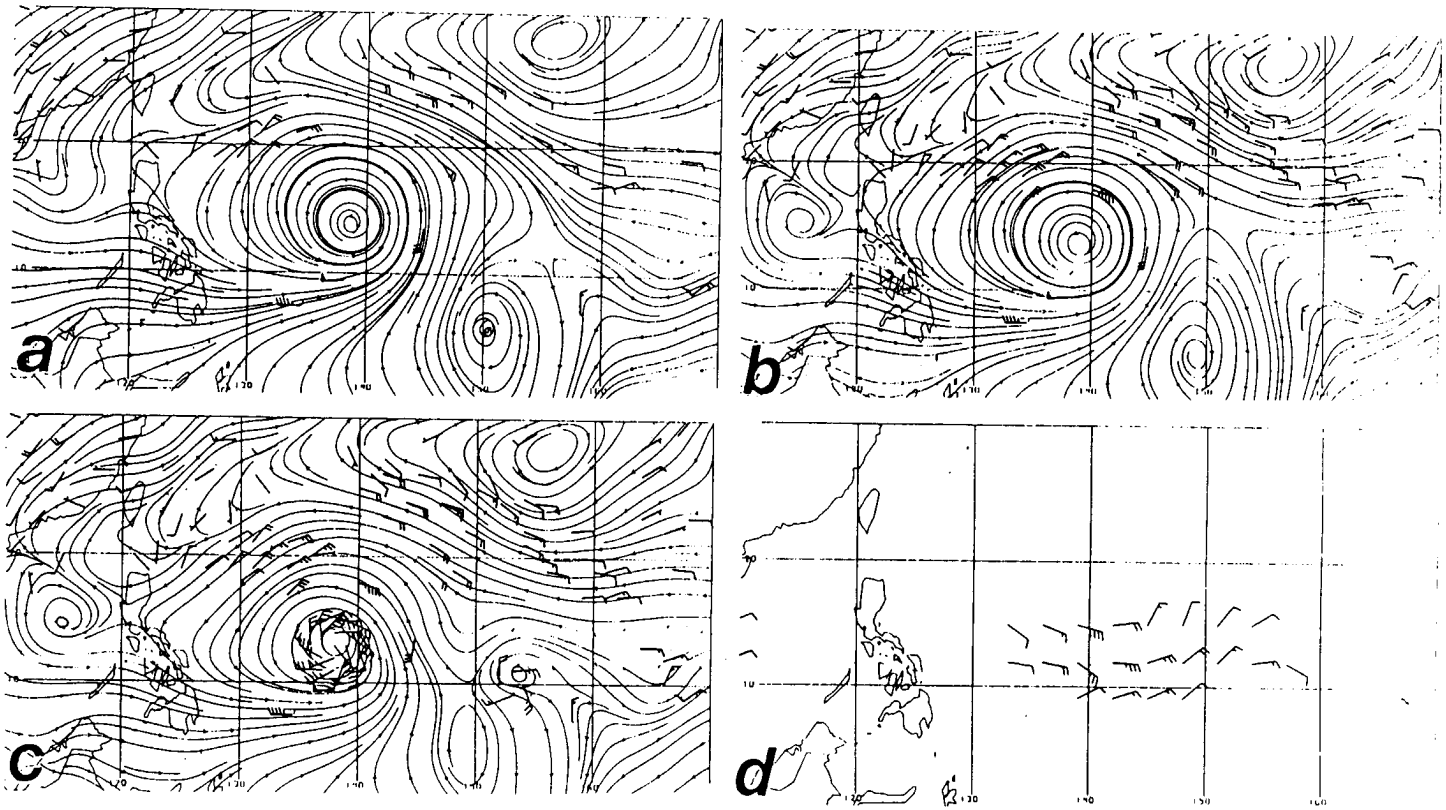

Fig. 19. 850 mb streamline analyses at 0900 UTC 5 Aug 93 of (a) first-guess field, (b) first MQ interpolation blending first-guess field and composite observations, (c) second (final) MQ analysis including synthetic observations, and (d) 850 mb final MQI analysis minus first-guess field difference vectors.

second MQI analysis (Fig. 19c) that includes these synthetic observations has a proper depiction of all features. The 850 mb difference field (Fig. 19d) continues to have cyclonic flow south of TY Robyn, which indicates the excessive outer winds in the first-guess field.

Once the upper- and lower-level final MQI analyses are complete, vertical wind shear calculations are made. The vertical shear (Eq. 7) is defined here as the difference (m s^{-1}) between the 200 mb and 850 mb winds. In the final interactive analyses, the tropical disturbance that develops into TS Steve (near 10°N, 152°E) is in an area of minimal vertical wind shear (Fig. 20a). In contrast, the vertical wind shear in the first-guess field (Fig. 20b) over pre-Steve has values between 5 and 8 m s^{-1}. Although the magnitudes of vertical wind shear are similar in the vicinity of pre-Steve, the differences are larger near the center of TY Robyn and near 16°N in the region of the convergent asymptote. Such differences in vertical wind shear are critical factors in determining which tropical cyclonic circulations or convective complexes will develop into significant tropical cyclones.

I. 200 MB ANALYSIS AT 2100 UTC 5 AUG 93

This analysis is another illustration of the positive impact of composite observations alone in adjusting the first-guess field. As in the previous cases, composite observations made a major adjustment in the meridional flow field and the depiction of the convergent asymptote near 16°N. Lessons learned from the previous analyses made it possible to introduce all necessary synthetic observations in only two steps, which makes this the most rapid upper-level analysis in this sequence thus far.

Using the previous analysis (Fig. 18c) in conjunction with the current satellite imagery (Fig. 21) and the current Weather Advisories confirmed TY

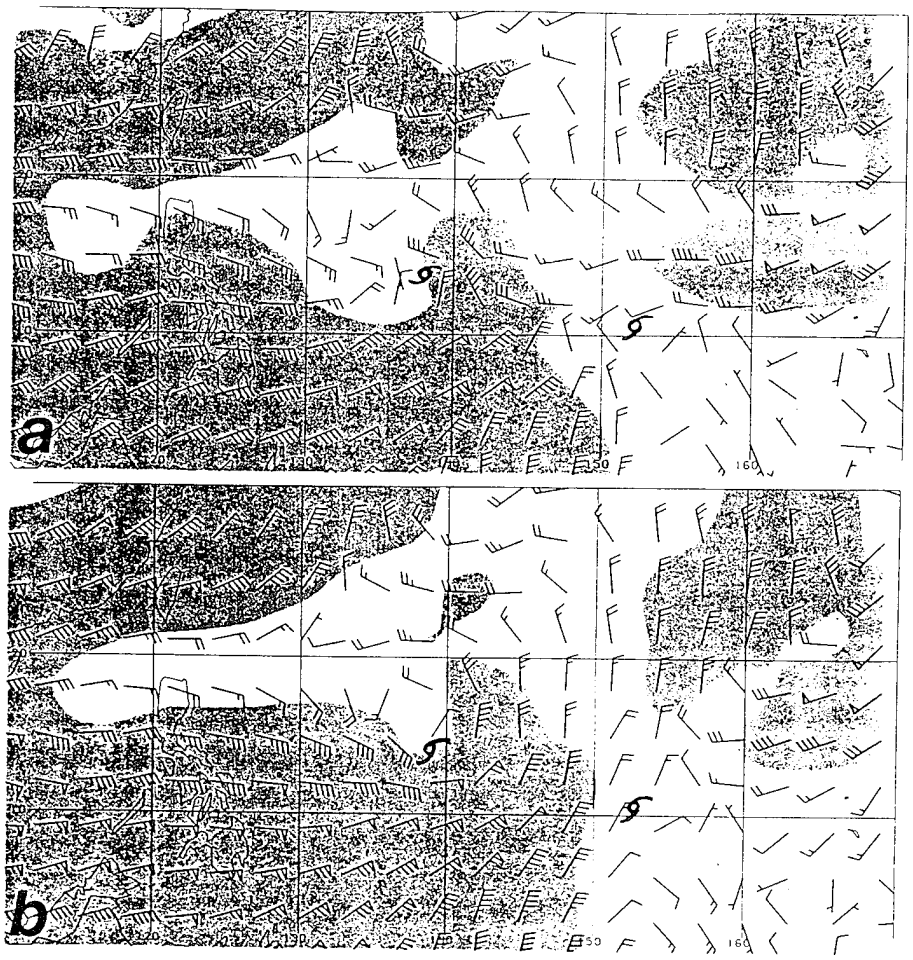

Fig. 20. Vertical wind shear (m s^{-1}) between 200 mb and 850 mb at 0900 UTC 5 Aug for (a) final MQ interpolation analysis, and (b) first-guess field. Western and eastern TY symbols indicate positions of TY Robyn (13W 1993) and TS Steve (14W 1993),and shear values greater than 12.5 m s^{-1} are shaded.

Robyn was located near 15°N, 137.0°E, with maximum winds of 80 kt, and moving 330° at 11 kt. Although the current Weather Advisory positions TD Steve at 8°N, 152°E (with maximum winds of 25 kt and moving 330° at 8 kt), the interpretation of the satellite imagery suggests a position near 11°N, 152.5°E. Neither TY Robyn or TD Steve is reflected in the 200 mb first-guess field

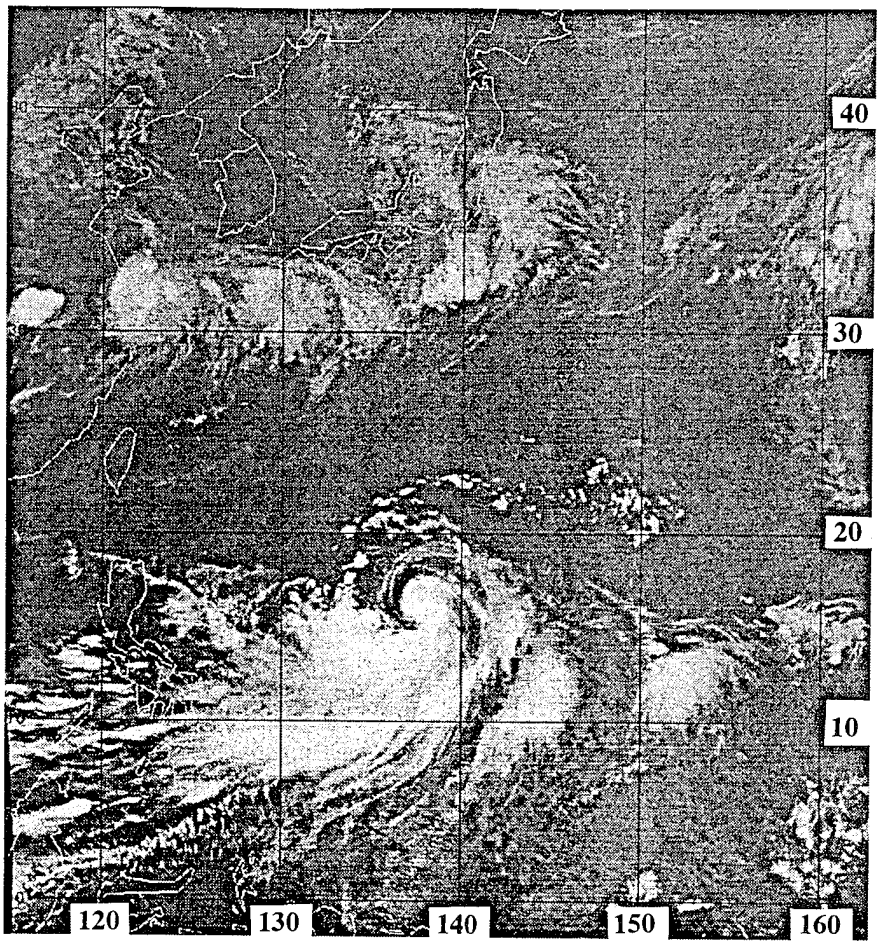

Fig. 21. High resolution GMS imagery at 2030 UTC 5 Aug 93.

(Fig. 22a), except for an area of weak diffluence in the vicinity of TY Robyn. As in the previous analyses, the convergent asymptote indicated in the satellite imagery near 16°N conflicts with the meridional flow between 140°E to 160°E, from 40°N to the Equator shown in the first-guess field.

The first MQI analysis (Fig. 22b) blending the composite observations and the first-guess field adds several features into the analysis. A weak convergent asymptote at 16°N east of 150°E is well supported by the satellite imagery

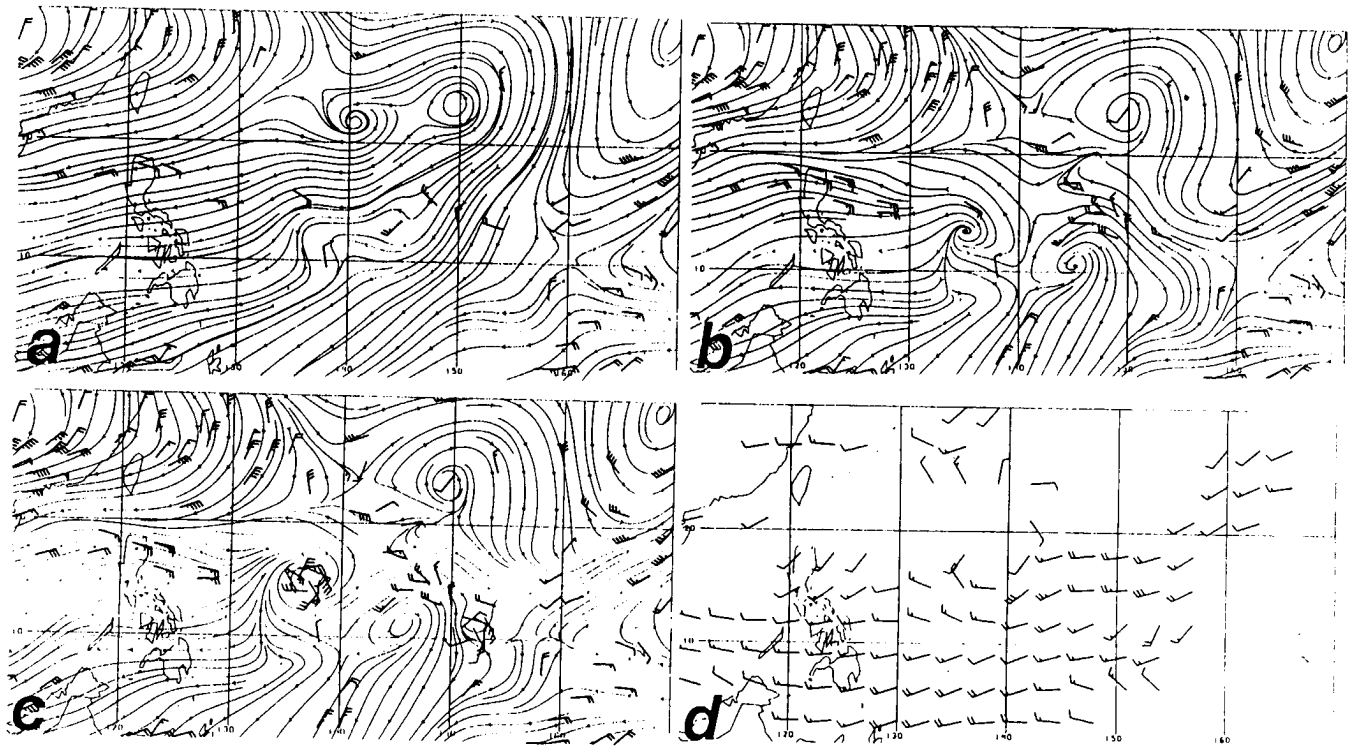

Fig. 22. 200 mb streamline analyses at 2100 UTC 5 Aug 93 of (a) first-guess field with on-time observations overlaid, (b) first MQI analysis blending first-guess field and composite observations, (c) final MQI analysis including synthetic observations, and (d) 200 mb final MQI analysis minus first-guess field difference vectors.

(Fig. 21). An upper-level anticyclone near 10.5°N, 145°E is added over a main convective band associated with TY Robyn. Although an anticyclonic outdraft associated with TY Robyn is added near 14.0°N, 135°E, it is displaced to the west of the position in the satellite imagery. The two features that composite observations fail to describe are the upper-level circulation associated with pre-Steve and a weak TUTT cell near 20°N, 151°E.

Starting from the parameters specified in the previous upper-level analyses, synthetic vortices for both TY Robyn and TD Steve are easily developed and inserted in the composite data set. No synthetic vortex for the TUTT cell is entered at this step, because it lies in an area of cyclonic shear and the effects of entering synthetic vortex observations for TY Robyn and TD Steve must first be assessed. The synthetic vortex for the upper-level outflow of TY Robyn is developed using R_o = 800 km, V_{max} = 80 kt, a motion vector of 330° at 11 kt, and r_{cut} = 200 km, which results in nine observations. TD Steve's synthetic vortex is developed with R_o = 500 km, V_{max} = 30 kt, and a motion vector of 330° at 8 kt, and r_{cut} = 200 km, which also results in nine observations.

A second MQI analysis (not shown) using these additional synthetic observations has the desired effect near TY Robyn, TD Steve, and the weak TUTT, but shifts the convergent asymptote southward. Two additional synthetic observations are entered: 270° at 25 kt near 15°N, 155°E; and 250° at 25 kt near 12°N, 153°E. A final MQI analysis (Fig. 22c) that includes all composite and synthetic observations results in the proper positioning of this convergent asymptote.

The 200 mb difference field (Fig. 22d) highlights the major changes in the flow field south of TY Robyn and along the convergent asymptote north of TD Steve. However, the majority of the wind differences in Fig. 22d result from the

composite observations, which emphasizes the importance of using an augmented data coverage in the analysis.

J. 850 MB ANALYSIS AT 2100 UTC 5 AUG 93

This analysis highlights the advantages that will be realized as the analyst gains experience using this procedure. The first MQI analysis is not shown because the composite observations improved the first-guess field very little. Rather, two erroneous features were introduced because of a bad observation south of Hong Kong, and a weak 850 mb wind displaces the TUTT cell southeast of the satellite position.

All synthetic observations necessary to complete this analysis are produced and entered in one step. The synthetic vortices from the previous analysis (Fig. 18b) are used as the basis for insertion of the missing features in the first-guess field (Fig. 23a) in comparison with the current satellite imagery (Fig. 21). As in the previous 850 mb analysis, TY Robyn is properly positioned, but the outer circulation is too strong. TD Steve is again missing, along with a weakening low-level cyclone west of Mindanao, and the 850 mb reflection of the TUTT cell near 30°N, 174°E. TY Robyn's synthetic vortex is produced using R_o = 800 km, V_{max} = 80 kt, a motion vector of 320° at 11 kt, and r_{cut} = 300 km, which introduces a set of 21 observations. TD Steve's synthetic vortex is developed using R_o = 500 km, V_{max} = 15 kt, a motion vector of 320° at 11 kt, and r_{cut} = 150 km, which inserts only five observations. In addition, four synthetic observations are created to eliminate the effects of the bad observations: one south of Hong Kong, and three near the 850 mb reflection of the TUTT cell.

Because all of the synthetic observations described above are developed and inserted in one step, only one iteration is necessary to compute the final MQI

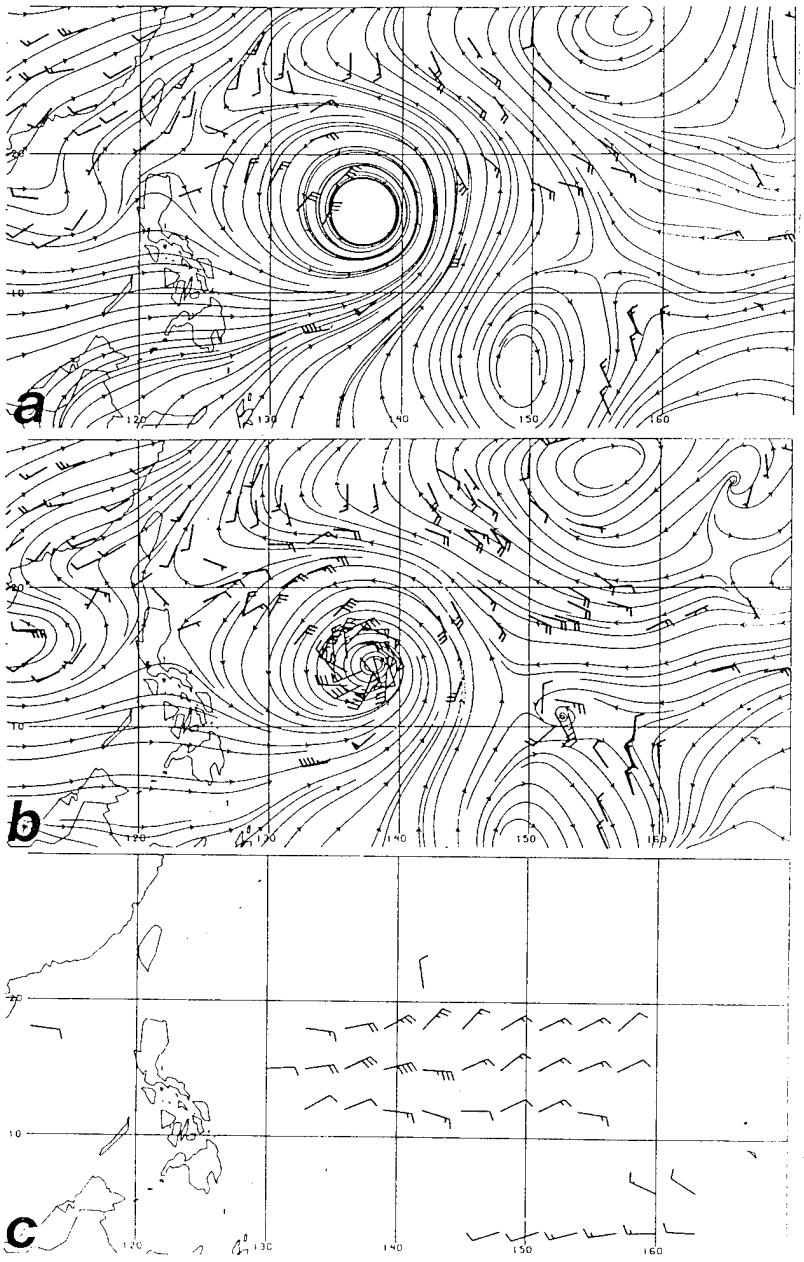

Fig. 23. 850 mb streamline analyses at 2100 UTC 5 Aug 93 of (a) first-guess field with on-time observations overlaid, (b) second (final) MQI analyses with composite and synthetic observations overlaid, and (c) 850 mb final MQI analysis minus first-guess field difference vectors.

analysis (Fig. 23b). All missing features and the corrections of the problems introduced by the bad observations are possible due to the application of lessons learned in the previous analyses. The 850 mb difference field (Fig. 23c) indicates that the first-guess field continues to have too strong outer winds south of TY Robyn as in the previous analyses.

K. 200 MB ANALYSIS AT 0900 UTC 6 AUG 93

A major change in the synoptic environment coupled with the complexity of the circulations near the significant synoptic features make this the most difficult upper-level analysis yet. More synthetic observation insertions and several difficult iterations are required to adjust the longwave pattern, introduce TY Robyn's and TD Steve's outflow patterns, insert a missing anticyclone, and align the circulation patterns.

Comparison of the previous analysis (Fig. 22c), current satellite imagery (Fig. 24), and first-guess field (Fig. 25a) reveals the major changes in the past 12 h. The outflows of TY Robyn near 15°N, 136.0°E and TD Steve near 13°N, 152.5°E are not well represented in the first-guess field. The current Weather Advisories indicate maximum winds of 80 kt and movement of 330° at 12 kt for TY Robyn, and TD Steve has maximum winds of 30 kt and movement of 330° at 8 kt. Meridional flow in the first-guess field continues to penetrate through the (weakening) convergent asymptote as in the previous analysis, except a break is present in the cirrus between TY Robyn and TD Steve. Notice also the weakening of the ridge north of TY Robyn. The shift to meridional flow and the weakening ridge are major synoptic changes not well represented in the first-guess analysis. The first-guess field also does not reflect the convergent asymptote and exaggerates the weakening of the ridge so that meridional flow extends throughout the region

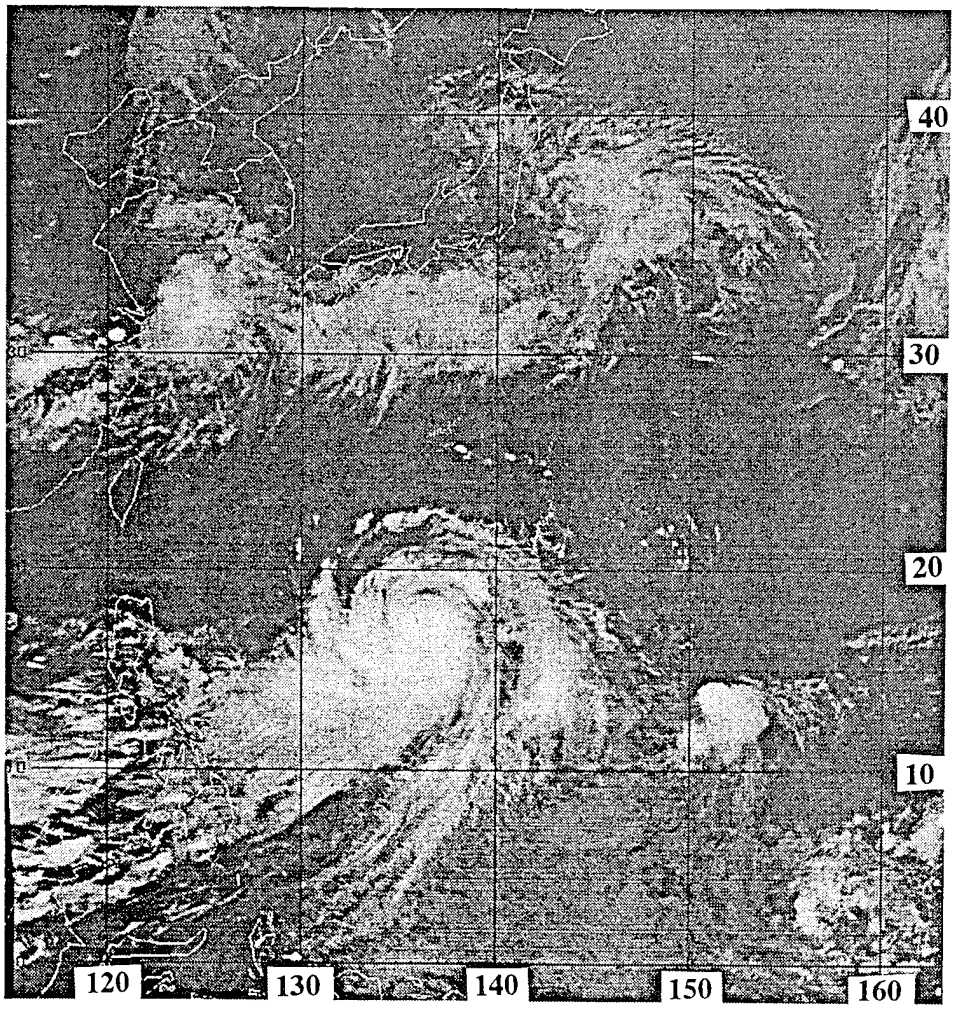

Fig. 24. High resolution GMS imagery at 0830 UTC 6 Aug 93.

from the 30°N to the Equator. The first-guess field is also missing the anticyclone over the convective band between TY Robyn and TS Steve, and two weak TUTT cells near 21°N, 150°E and 25°N, 140°E.

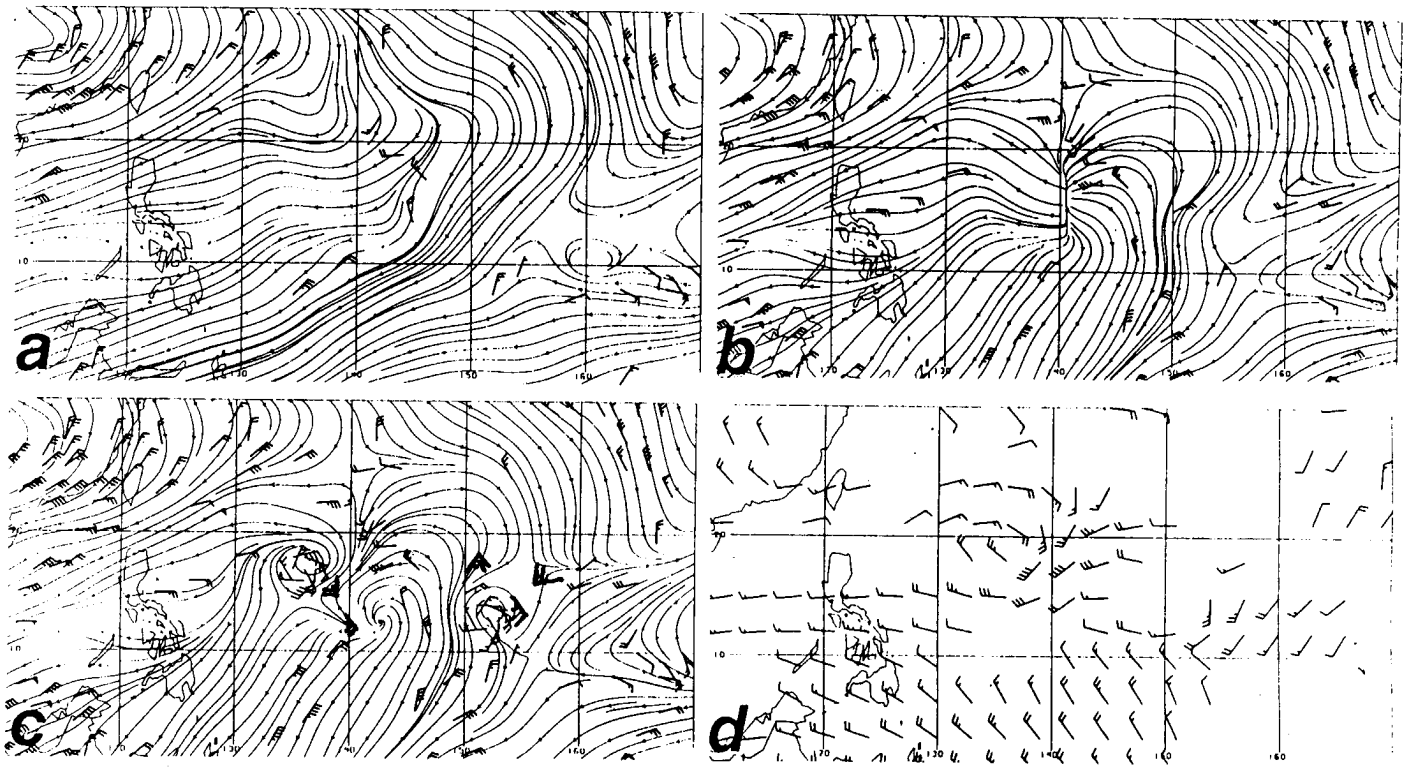

Fig. 25. 200 mb streamline analysis at 0900 UTC 6 Aug 93 of (a) first-guess field with on-time observations overlaid, (b) first MQI analysis blending first-guess field and composite observations, (c) final MQI analysis including all synthetic observations, and (d) 200 mb final MQI analysis minus first-guess field difference vectors.

A major change to the first-guess field is made by adding the composite observations during the first step of the interactive analysis. Although the first MQI analysis (Fig. 25b) has a disruption of the meridional flow between 140°E and 150°E, it includes a rather strange north-south oriented divergent line along 140°E. The composite observations (Fig. 25b) are consistent with the MQI analysis of the divergent line, but the flow does not agree with the satellite interpretation in the region. An experienced analyst would recognize that the additional composite observations are a reflection of three separate features: TY Robyn, TD Steve, and the anticyclone between them. Because these features are only partially represented in the data (resulting in the divergent line), introduction of synthetic observations is required to depict properly the entire flow pattern.

Because of the large number of changes required, and the potential for multiple insertions causing interactions at a point, this analysis is broken into small parts. In the first part, synthetic observations for TY Robyn and TD Steve are introduced and the impact is assessed. TY Robyn's synthetic vortex is developed using R_o = 800 km, V_{max} = 80 kt, a motion vector of 330° at 12 kt, and r_{cut} = 200 km, which results in a set of nine observations. A synthetic vortex for TD Steve is developed with a larger R_o = 600 km based on satellite imagery, V_{max} = 30 kt, a motion vector of 330° at 8 kt, and r_{cut} = 200 km, which also results in nine observations. The second MQI analysis (not shown) including these synthetic vortices has upper-level outflow structures for TY Robyn and TD Steve, but the anticyclone over the convective line southeast of TY Robyn is still missing and the upper-level circulation of TD Steve is too large. Five point synthetic observations are entered to fine tune the analysis around TD Steve and include the anticyclonic feature:

13°N 140°E 14025 kt
17°N 138°E 15025 kt
17°N 150°E 03025 kt
15°N 154°E 15025 kt
16°N 156.5°E 27025 kt

The resulting MQI analysis (not shown) blending these synthetic observations with the previous data set result in the proper depiction of the anticyclone near 15°N, 142°E. However, the upper-level circulation of TD Steve remains too large.

The final MQI analysis (Fig. 25c) with a proper depiction of all features results from replacing the synthetic vortex of TD Steve with one based on R_o = 500 km. This result indicates that the analyst should be careful when increasing R_o, because a small increase in R_o may increase the cyclonic flow in the outflow layer too much, and also distort the surrounding anticyclonic region.

The interactive analysis procedure radically changes the first-guess field in this case. Not only are cyclonic structures introduced near the center of both tropical cyclones, the dominant easterly flow is decreased to the south and west of these two circulations. The 200 mb difference field (Fig. 25d) documents these changes.

L. 850 MB ANALYSIS AT 0900 UTC 6 AUG 93

This example illustrates again how rapid the analysis can be completed when all synthetic observations for the missing features may be inserted in a single step. Based on the previous analysis (Fig. 23b), current satellite imagery (Fig. 24), and the first-guess field (Fig. 26a), three misrepresented or missing features are discovered: TY Robyn near 16.5°N, 135°E is misrepresented; and TD Steve near 12°N, 152°E and a weak low-level cyclonic circulation between 5°N and 10°N,

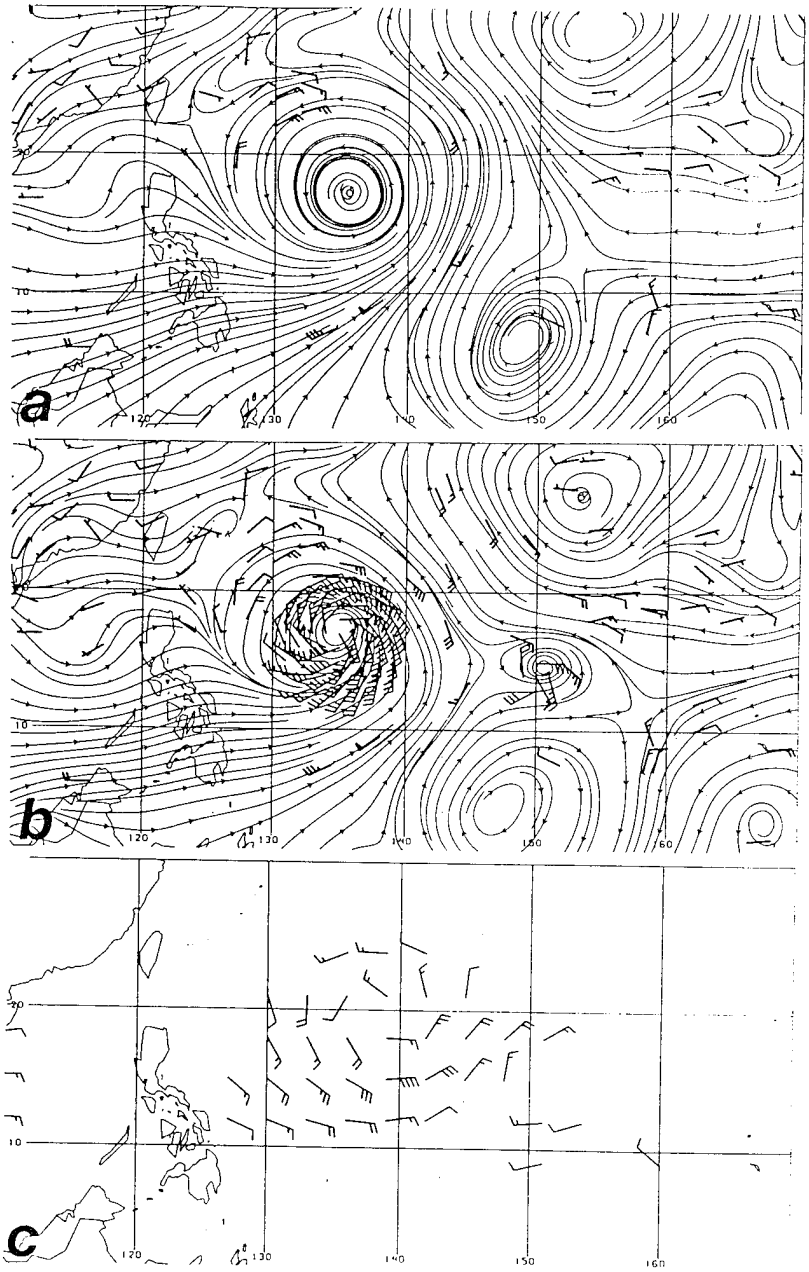

Fig. 26. 850 mb streamline analyses at 0900 UTC 6 Aug 93 of (a) first-guess fields with on-time observations overlaid, (b) second (final) MQI analysis with synthetic observations included, and (c) 850 mb final MQI analysis minus first-guess field difference vectors.

160°E and 180°E are missing. Again, the circulation for TY Robyn in the first-guess field is too large.

The first MQI analysis (not shown) blending the composite observations and the first-guess field depicts the missing cyclonic circulation near 6°N, 168°E, but does not include the low-level circulation of TD Steve and still over-represents the circulation of TY Robyn. Using R_o = 800 km, V_{max} = 80 kt, a motion vector of 320° at 11 kt, and a r_{cut} = 500 km, a synthetic vortex for TY Robyn is developed that has 59 observations. A synthetic vortex for TD Steve is produced using R_o= 500 km, V_{max} = 15 kt, a motion vector of 320° at 8 kt, and a r_{cut} = 150 km, which results in only five observations. The second MQI analysis (Fig. 26b) using these synthetic observations properly depicts all features without the need for point synthetic observations. The 850 mb difference field (Fig. 26c) highlights the improvements in the analysis. As was the case previously, the low-level circulation in the first-guess field south of TY Robyn is too strong, and the circulation of TS Steve is missing from the first-guess field.

M. 200 MB ANALYSIS AT 2100 UTC 6 AUG 93

As in the previous analysis (Fig. 25c), major adjustments to the first-guess field (Fig. 27a) are required. Based on the current satellite imagery (Fig. 28), TY Robyn near 19°N, 135°E and TD Steve near 13.5°N, 149.5°E are missing. Current Weather Advisories have TY Robyn with maximum sustained winds of 100 kt and a motion vector of 330° at 13 kt, and TD Steve with maximum sustained winds of less than 30 kt and moving 295° at 8 kt. The convergent asymptote near 15°N described in previous analyses has nearly dissipated in the satellite imagery. Evidence of meridional flow between TY Robyn and TD Steve continues, as does the clear zone reflecting the ridge to the north of TY Robyn.

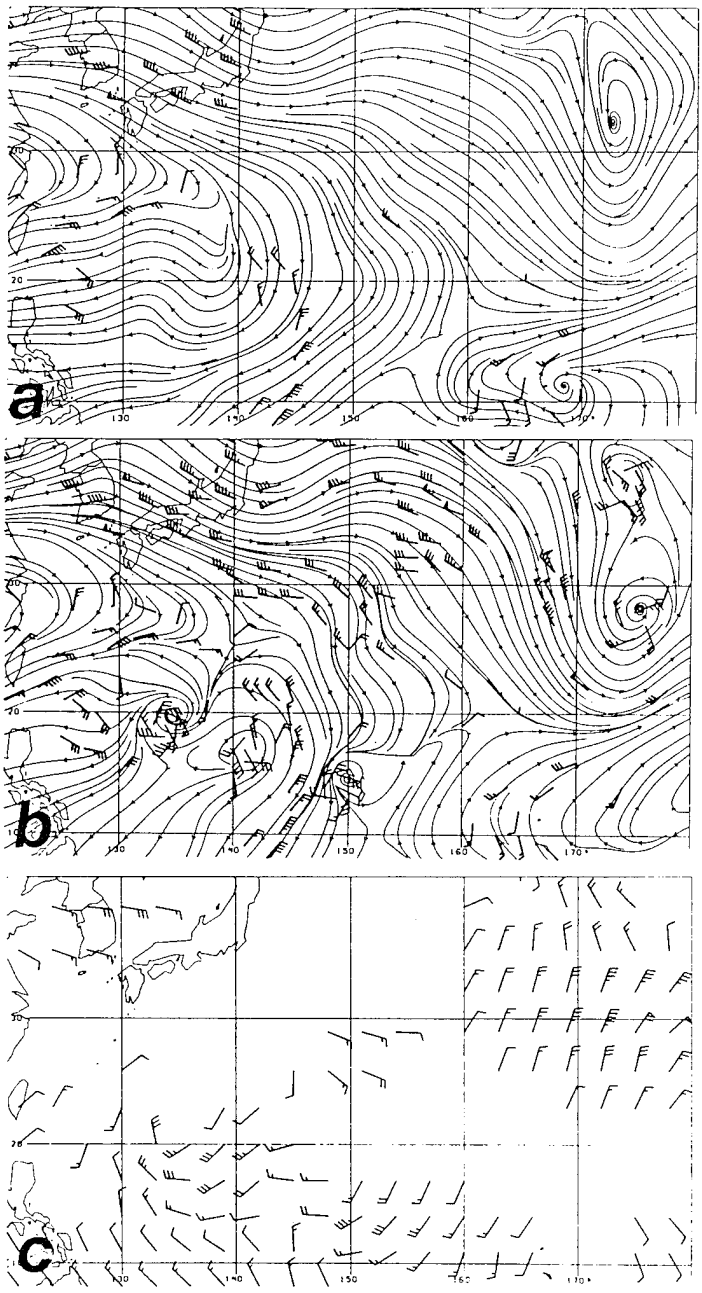

Fig. 27. 200 mb streamline analyses at 2100 UTC 6 Aug 93 of (a) first-guess fields with on-time observations overlaid, (b) second (final) MQI analysis with all synthetic observations included, and (c) 200 mb final MQI analysis minus first-guess field difference vectors.

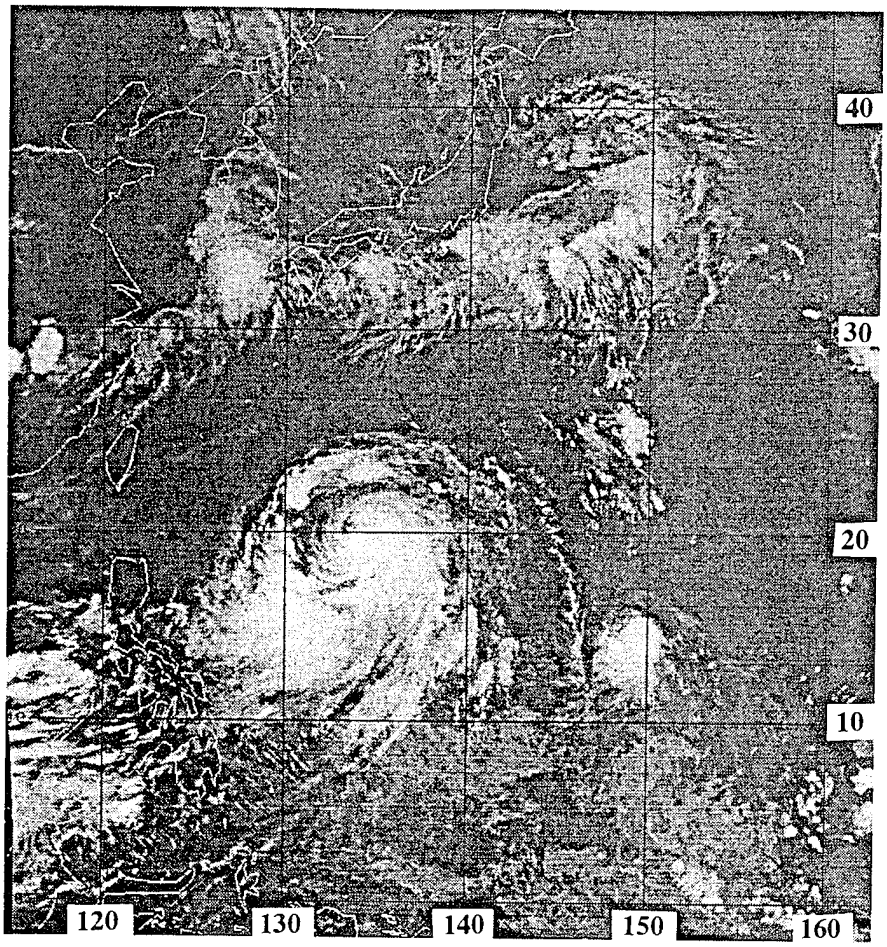

Fig. 28. High resolution GMS imagery at 2030 UTC 6 Aug 93.

The first-guess field is missing the convergent asymptote and the ridge north of Robyn, and again exaggerates the extent of the meridional flow between 140°E and 150°E across the tropical cyclones. The satellite imagery also indicates diffluence associated with an area of convection over the South China Sea, and near 7.5°N, 176°E.

As in the previous analysis, the composite observations do not provide a significant improvement in the depiction of the missing circulation features.

Blending the composite observations and the first-guess field in the first MQI analysis (not shown) did interrupt the meridional flow in the first-guess field north and east of TY Robyn with a closed anticyclonic cell near 29°N, 138°E. In addition, a new area of diffluence near 17°N, 132°E is produced over the strong convection west of TY Robyn.

As in the previous 200 mb analyses, synthetic circulations are inserted to introduce circulations associated with TY Robyn and TD Steve, an anticyclone near 17°N, 141°E, a weak TUTT cell near 38°N, 174°E, another TUTT cell near 29°N, 129°E, and an anticyclone between the tropical cyclones. Nine synthetic observations representing TY Robyn are developed using R_o = 800 km, V_{max} = 100 kt, a motion vector of 330° at 13 kt, and a r_{cut} = 200 km. The synthetic vortex for TD Steve has R_o = 500 km, V_{max} = 30 kt, a motion vector of 330° at 8 kt, and a r_{cut} = 200 km, which results in a set of nine observations. For both TUTT cells and the upper-level anticyclone, a V_{max} of 25 kt and r_{max} of 100 km are used, and with a r_{cut} of 150 km this requires only five observations. The anticyclonic circulation between TY Robyn and TD Steve is entered based on persistence and the continued presence of the convection southeast of Robyn. The second MQI analysis (Fig. 27b) properly depicts all features indicated in the satellite imagery.

In the previous analysis, several iterations had been required because of the major changes required. As the analyst learned from that case, the necessary corrections to the first-guess field were evident, and the final analysis is created more rapidly with a minimum of iterations.

As shown in the 200 mb difference field (Fig. 27c), introduction of the composite and synthetic observations significantly changes the flow field throughout the analysis domain. The difference field indicates the cyclonic upper-

level structures of TY Robyn and TD Steve were not in the first-guess field. Additionally, the easterly flow over the Philippines and the South China Sea was too strong in the first-guess field, and major changes in wind field in the northeast corner of the domain were introduced by the composite and synthetic observations.

N. 850 MB ANALYSIS AT 2100 UTC 6 AUG 93

This analysis is another example of how the inclusion of well-placed synthetic observations leads to the proper depiction of the low-level tropical synoptic features that are obscurred by cirrus. As before, the previous analysis (Fig. 26c) is extrapolated and compared with current satellite imagery (Fig. 28) to determine the location of the missing features in the first-guess field (Fig. 29a): TY Robyn near 15°N, 138°E; TD Steve near 13.5°N, 149.5°E; a weak low-level cyclone near 6°N, 166°E; and the 850 mb reflection of a TUTT cell near 27°N, 175°E (displaced westward in the first-guess field). The first MQI analysis (not shown) blending the composite observations and the first-guess field had little impact.

Parameters needed to create synthetic circulations for Robyn and Steve are derived from current Weather Advisories and satellite imagery for the R_o estimates. The synthetic vortex for TY Robyn is developed using R_o = 800 km, V_{max} = 100 kt, a motion vector of 320° at 13 kt, and a r_{cut} = 500 km, which again results in a large set of 59 synthetic observations. TD Steve's synthetic vortex is developed using R_o = 500 km, V_{max} = 30 kt, a motion vector of 320° at 11 kt, and a r_{cut} = 150 km, which results in only five observations. Satellite interpretation in combination with surrounding observations is used to insert the circulation near 6°N, 166°E with V_{max} = 15 kt, r_{max} = 100 km, and r_{cut} = 150

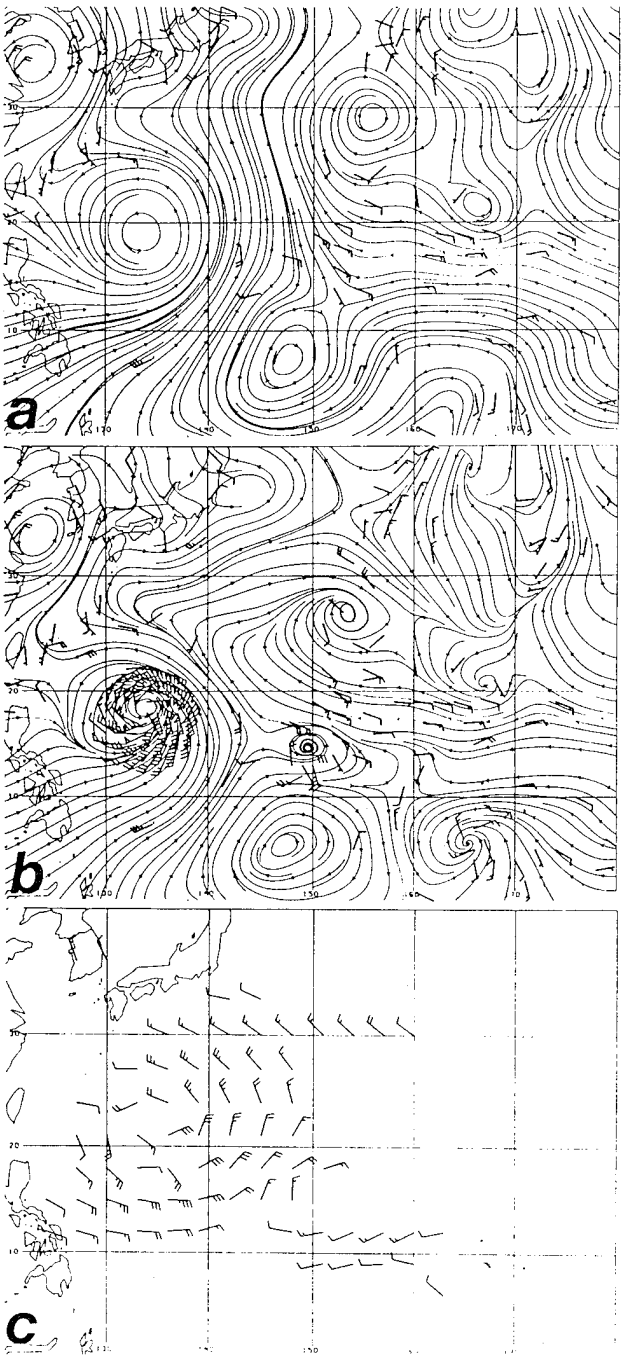

Fig. 29. 850 mb streamline analyses at 2100 UTC 6 Aug 93 of (a) first-guess field with on-time observations overlaid, (b) second (final) MQI analysis with composite and synthetic observations overlaid, and (c) 850 mb final MQI analysis minus first-guess field difference vectors.

km. The second MQI analysis (Fig. 29b) has all of the features that were missing or misrepresented.

As a consequence of the intensification of TY Robyn over the past 12 hours, the first-guess field has an even stronger cyclonic circulation at outer radii, which is corrected in the MQI analyses as shown by the anticyclonic wind in the 850 mb difference field (Fig. 29c). This recurring over-representation of the TY Robyn outer wind field in the first-guess field is attributed to the extrapolation of the inner vortex structure that is used in creating the synthetic observations for tropical cyclones in the FNMOC global model.

A potential tropical cyclone intensity forecast impact is revealed by a comparison of the 200-850 mb vertical wind shear from the final MQI analysis (Fig. 30a) and from the first-guess field (Fig. 30b). Whereas an approximately 25 m s^{-1} shear is depicted over TD Steve in the first-guess field, the shear over TD Steve in the final MQI analysis is less than 10 m s^{-1}. A shear value of 25 m s^{-1} is approximately twice the threshold value for developing tropical cyclone (Zehr 1992). However, the MQI analysis shear of less than 10 m s^{-1} would not be too unfavorable, and TD Steve intensified during this period. Further discussion of the relationship between intensity changes and the vertical wind shear estimates is given in Chapter VII.

O. 200 MB ANALYSIS AT 0900 UTC 7 AUG 93

In many of the previous upper-level analyses, a minimum number of observations could be used to insert the synthetic circulation. This analysis demonstrates a situation in which lack of observations for a large distance around the outflow from TY Robyn resulted in a larger upper-level cyclonic circulation around the cyclone than was desired.

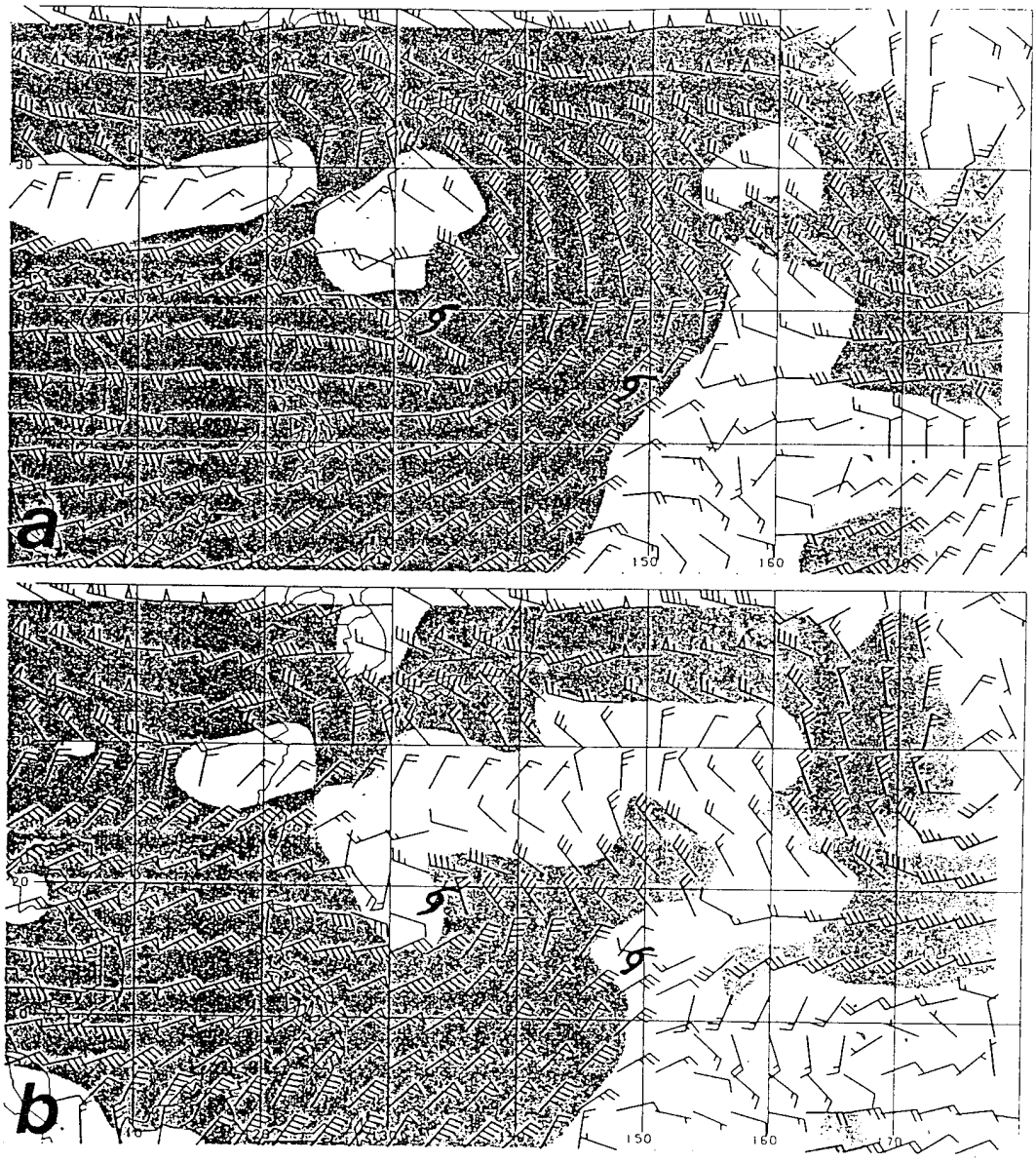

Fig. 30. Vertical wind shear (m s^{-1}) between 200 mb and 850 mb at 2100 UTC 6 Aug 93 for (a) final MQ interpolation analysis, and (b) first-guess field. Western and eastern TY symbols indicate positions of TY Robyn (13W 1993) and TS Steve (14W 1993).

As above, the circulations from the previous analysis (Fig. 27b) are roughly translated 12 h and compared with the current satellite imagery (Fig. 31) and the

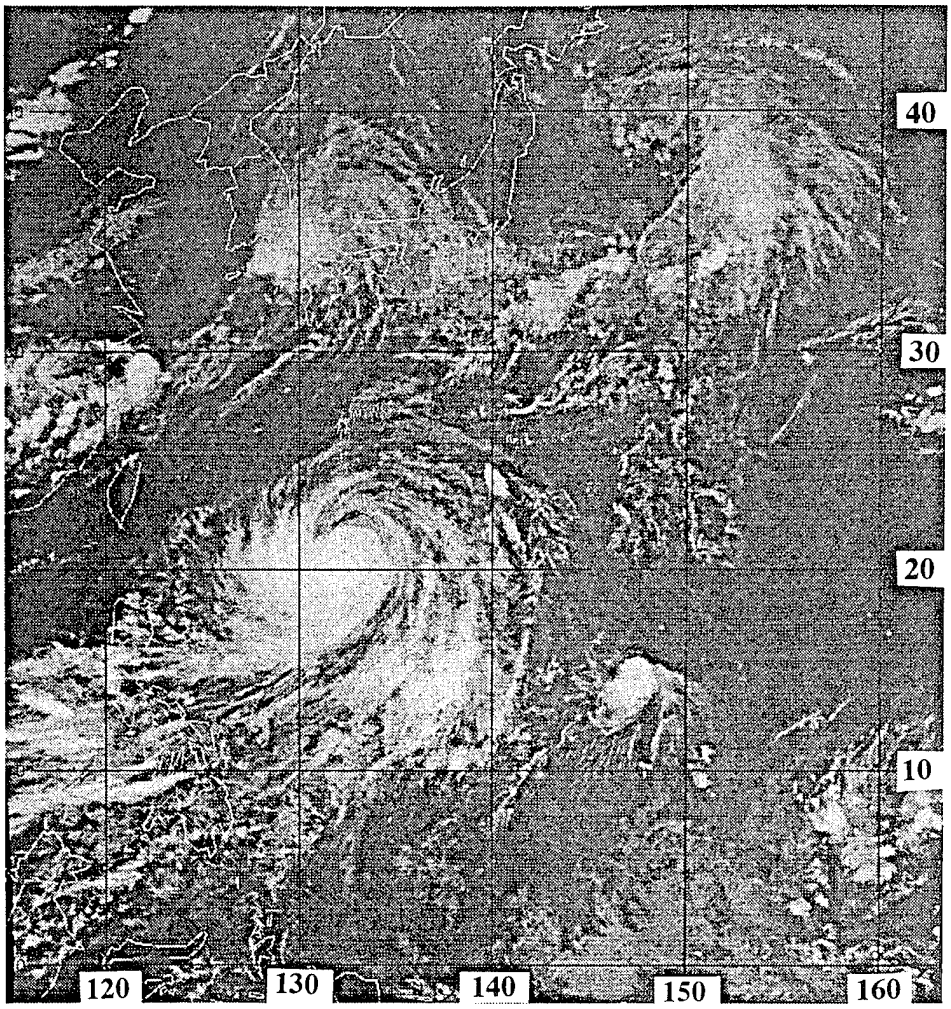

Fig. 31. High resolution GMS imagery at 0830 UTC 7 Aug 93.

first-guess field (not shown). Some differences are found between the current Weather Advisory positions for TY Robyn (20.6°N, 132.3°E) and TS Steve (14.9°N, 147.8°E) and the satellite interpretation positions here (19.8°N, 133.0°E, and 14°N, 147°E, respectively). These differences would be more important for a low-level analysis than for this 200 mb analysis. As a test, the latter positions are used with the translations (330° at 11 kt, and 295° at 9 kt, respectively) and intensities (115 kt and 40 kt, respectively) from the Weather Advisory. The first-

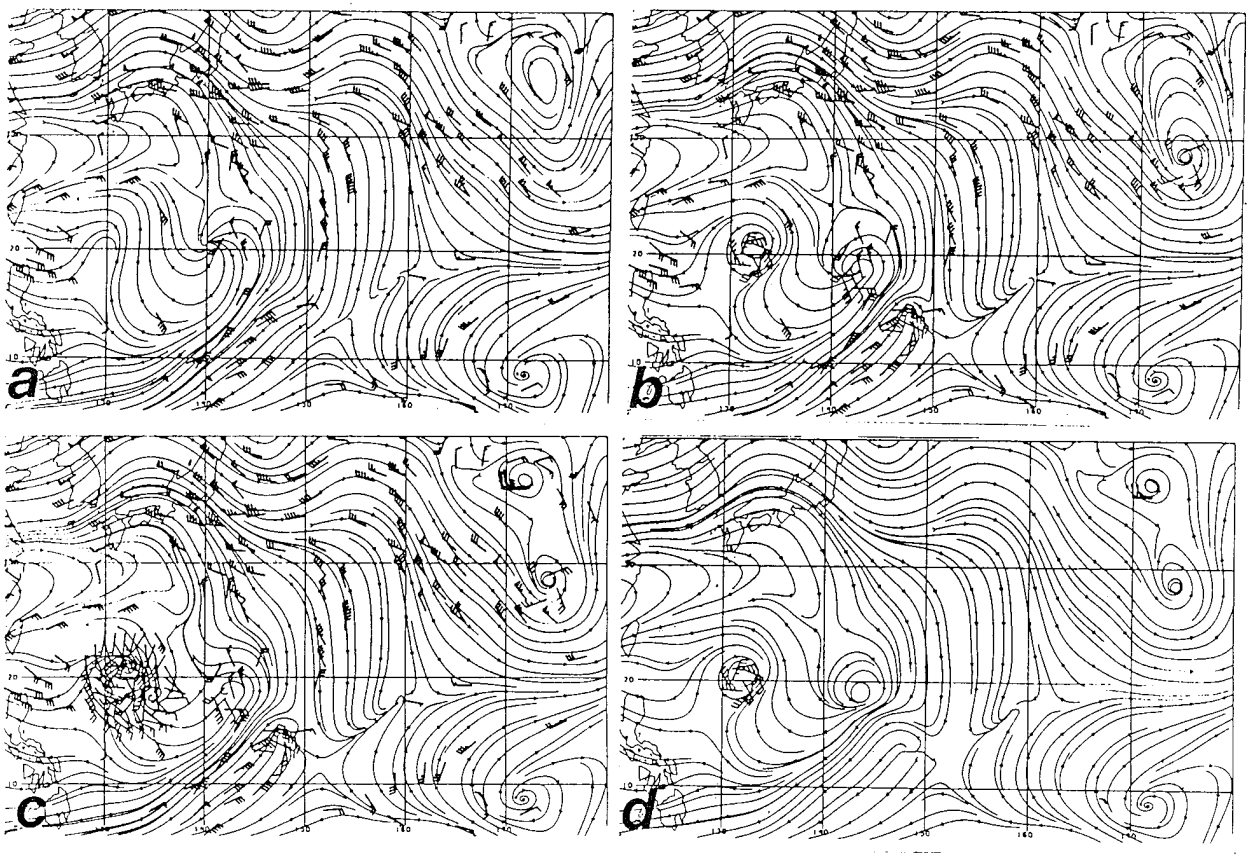

Fig. 32. 200 mb streamline analyses at 0900 UTC 7 Aug 93 of (a) first MQI analysis blending the first-guess field and composite observations, (b) second MQI analysis including synthetic circulation observations, (c) third MQI analysis with a larger synthetic circulation for TY Robyn, and (d) final MQI analysis with smaller synthetic circulation for TY Robyn with a point synthetic observation overlaid.

guess field has a closed anticyclone near 25°N, 138°E that does not reflect the cyclonic outflow expected near the center of TY Robyn. No upper-level circulation above TS Steve is present; rather, the first- guess field has strong meridional flow between 140°E to 155°E from 30°N to the Equator. Whereas meridional flow is evident in the satellite imagery north of TS Steve, this flow is actually being deflected around the upper-level circulation. Two TUTT cells near 28°N, 174°E, and 37°N, 172°E are evident in the satellite imagery, but only the northern cell is found in the first-guess analysis.

The first MQI analysis (Fig. 32a) that blends the composite observations and the first-guess field again has major changes in the synoptic circulations. The anticyclone near 25°N, 135°E is relocated to near 20°N, 140°E, and thus lies over the strong convective band east of TY Robyn. A new area of diffluence is analyzed near 19°N, 130°E, which is near the location of TY Robyn, but is displaced somewhat to the west. Steve and the southern TUTT cell are still absent from the analysis.

The required inputs for the synthetic vortices are determined using persistence and current Weather Advisories. Inputs for TY Robyn are R_o = 800 km, V_{max} = 115 kt, a motion vector of 330° at 11 kt, and a r_{cut} = 200 km, which produces a set of nine observations. Inputs for TS Steve are R_o = 500 km, V_{max} = 40 kt, a motion vector of 295° at 9 kt, and a r_{cut} = 200 km, which also results in nine observations. A V_{max} of 25 kt, a r_{max} of 100 km, and a r_{cut} of 150 km are used to create the five synthetic observation circulation for the TUTT cell near 28°N, 174°E. The second MQI analysis (Fig. 32b) resulting from the inclusion of these synthetic observations has cyclonic flow to a large radius near TY Robyn. In this case, no observations are available in the vicinity to force the circulation to become anticyclonic aloft. To correct this problem, a larger r_{cut} of 500 km (59

observations) was tested to introduce the anticyclonic outer structure of the synthetic tropical cyclone circulation. This larger circulation disrupted the flow pattern (Fig. 32c), so the original synthetic circulation (r_{cut} = 200 km) was re-entered. Additionally, the northern TUTT cell is no longer closed (Fig. 32b), so a 25 kt point synthetic observation is entered near 37°N, 171°E to close this circulation. In the final MQI analysis (Fig. 32d) the cyclonic inner structure is still too large, but the upper-level circulations of TY Robyn, TS Steve, and the anticyclone between these features is better represented than in Fig. 32c.

As in previous analyses, the upper-level difference field (Fig. 33) has significant modifications to the first-guess field due to the outflow structures of TY Robyn and TS Steve. Additionally, the easterly flow south and west of these features is also too strong in the first-guess field.

This analysis highlights problems associated with specifying the upper-level circulation of a mature tropical cyclone located in a very large data-void area. Due to the problems (discussed in appendix) associated with blending composite observations and synthetic observations in the MQI analysis the analyst must not enter too large a set of synthetic circulation observations in too small an area or the flow field will be disrupted.

P. 850 MB ANALYSIS AT 0900 UTC 7 AUG 93

Using the previous analysis (Fig. 29b) as a guide, the current satellite imagery (Fig. 31) is used to identify regions that require adjustment in the first-guess analysis (not shown). Although TY Robyn is correctly placed near 19.8°N, 133°E, the outer circulation of TY Robyn again is too strong. Similiarly, the 850 mb reflection of the TUTT cell near 28°N, 174°E appears satisfactory. However,

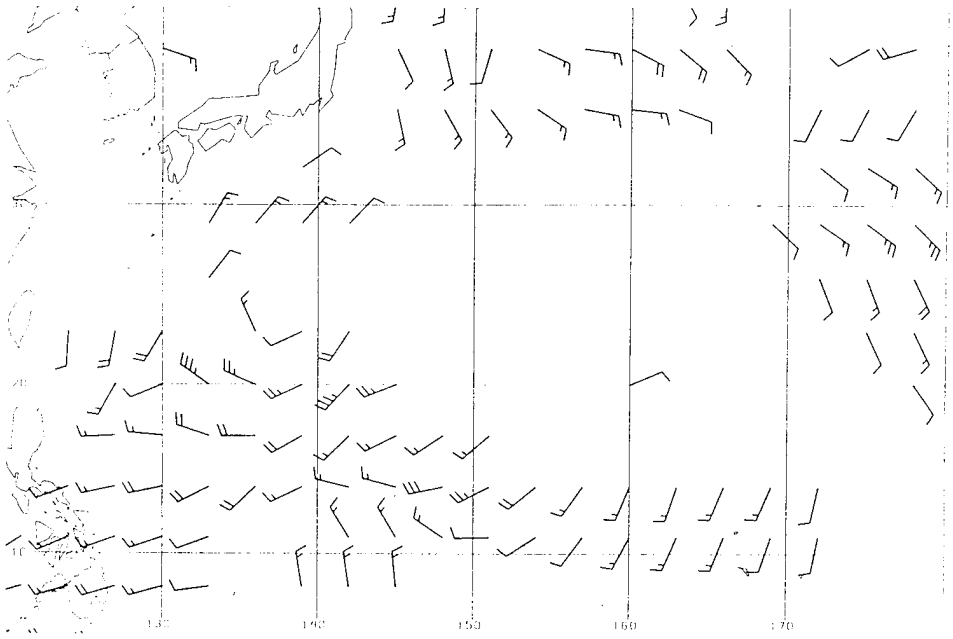

Fig. 33. 200 mb final MQI analysis minus first-guess field difference vectors at 0900 UTC 7 Aug 93.

the circulations for TS Steve near 15°N, 148°E and a low-level cyclone near 4°N, 162°E are missing. The blend of the composite observations and the first-guess field in the first MQI analysis (not shown) introduces the cyclone near 4°N, 162°E based on a limited number of composite observations.

A synthetic circulation of 35 observations for TY Robyn is generated with R_o = 800 km, V_{max} = 115 kt, a motion vector of 320° at 11 kt, and r_{cut} = 400 km. The synthetic vortex for TS Steve is developed using R_o = 500 km, V_{max} = 40 kt, a motion vector of 295° at 9 kt, and r_{cut} = 150 km, which results in only five observations. All of the circulations are found in the second MQI analysis (Fig. 34) using these synthetic observations. This case again illustrates how an interactive analysis can be completed in two steps with the insertion of complete synthetic circulations based on satellite interpretation. No 850 mb difference field is shown here because of the similiarity with the previous analysis (Fig. 29d).

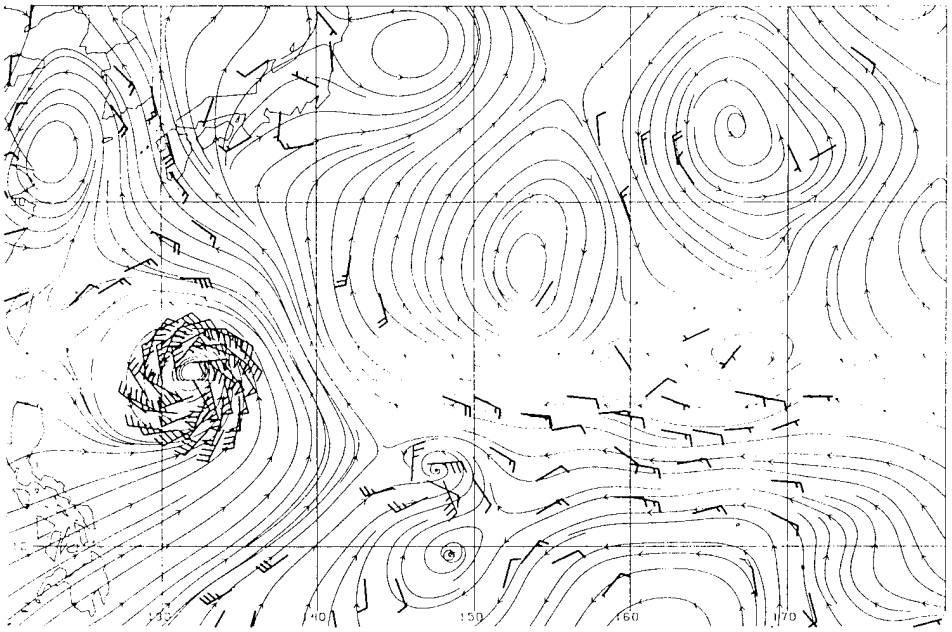

Fig. 34. 850 mb streamline analysis at 0900 UTC 7 Aug 93 of the final MQI analysis blending the first-guess field with composite and synthetic observations.

Q. 200 MB ANALYSIS AT 2100 UTC 7 AUG 93

This final upper-level analysis provides a different view of the advantages of using composite observations, which results in the depiction of all but one of the missing features. Although the locations of these features did require some fine-tuning, it is significant that just the inclusion of composite data correctly depicts most of the features. In addition, insertion of the composite observations introduced a convergent asymptote 5° long. to the east of TS Steve that the analyst had missed due to its weak signature on the satellite imagery.

The regular routine is followed of projecting forward the previous analysis (Fig. 32d) and comparing the current satellite imagery (Fig. 35) with the first-guess field (Fig. 36a). TY Robyn near 23°N, 132.5°E is only depicted as a diffluent wave in the first-guess field and TS Steve near 15°N, 146°E is missing. By contrast, the satellite imagery indicates the upper-level circulation of TS Steve is interacting with meridional flow from the north. The first MQI analysis (Fig.

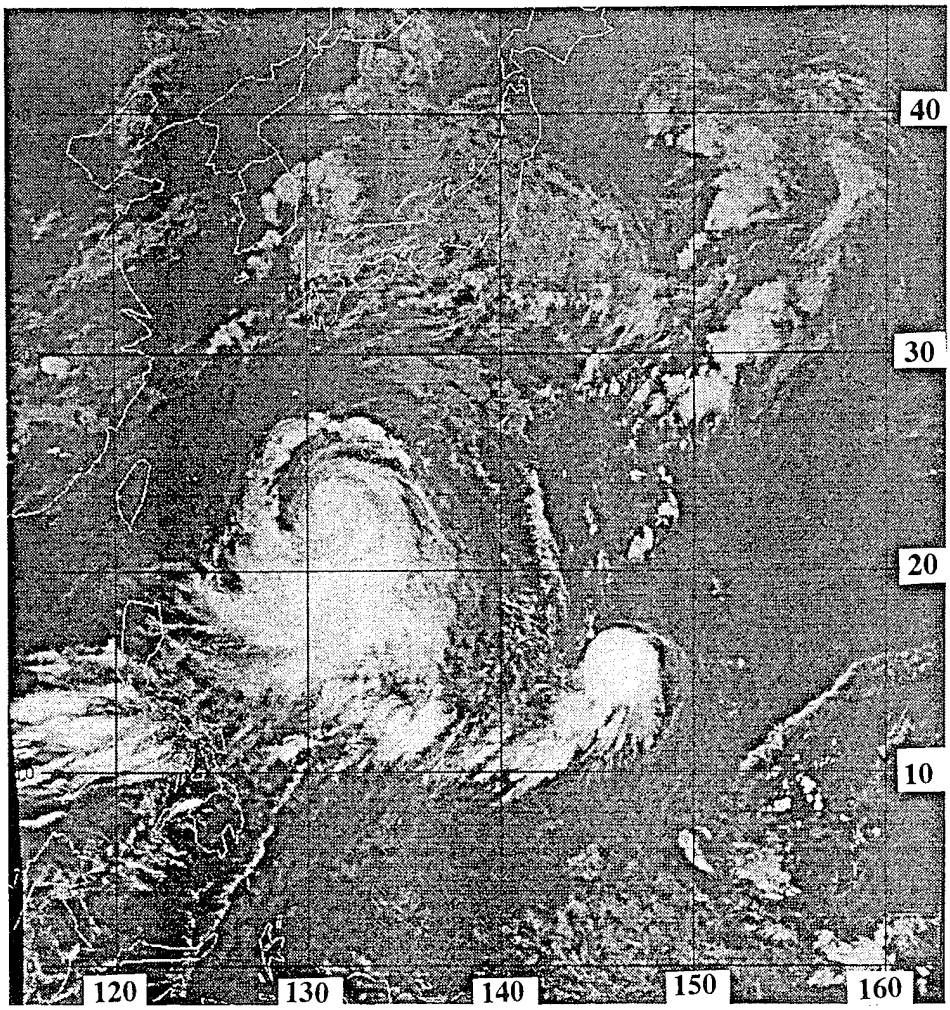

Fig. 35. High resolution GMS imagery at 2030 UTC 7 Aug 93.

is interacting with meridional flow from the north. The first MQI analysis (Fig. 36b) that adds the composite observations as increments to the first-guess field results in major changes: a closed TUTT cell near 22°N, 158°E; an upper-level anticyclone near 18°N, 138°E over the convective band southeast of TY Robyn; a weak cyclonic outflow for TY Robyn, which is displaced west of the actual location; and an area of diffluent flow over the Philippines. However, the upper-level circulation associated with TS Steve is still missing.

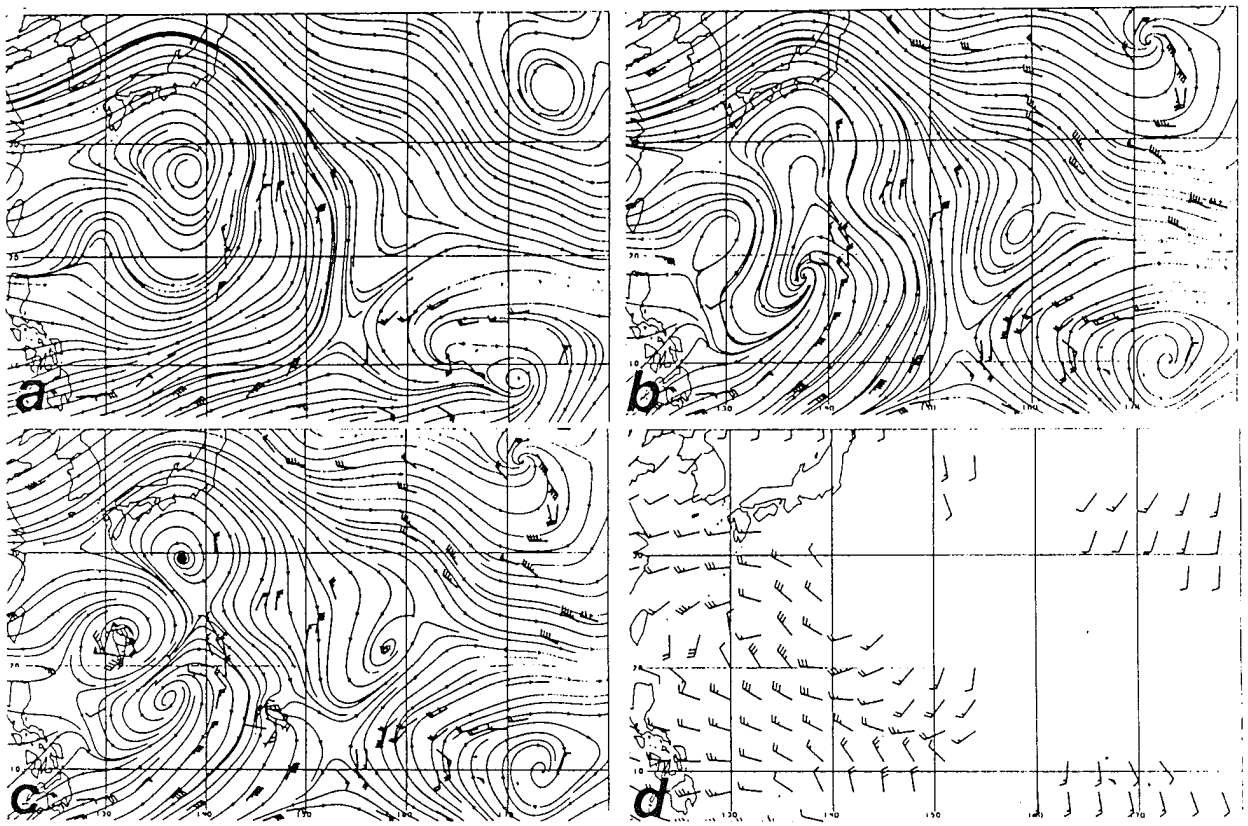

Fig. 36. 200 mb streamline analyses at 2100 UTC 7 Aug 93 of (a) first-guess field with on-time observations overlaid, (b) first MQI analysis blending first-guess field and composite observations, (c) second (final) MQI analysis including all synthetic circulation observations, and (d) 200 mb final MQI analysis minus first-guess field difference vectors.

As indicated above, a new convergent asymptote that was initially considered suspect is analyzed east of Steve in the first MQI analysis (Fig. 36b). A reanalysis of the satellite imagery (Fig. 35) in this region then identified an area of thin cirrus with a sharp cloud edge near 14°N, 170°E to 180°E that is consistent with a developing convergent asymptote.

As before, the current Weather Advisories are used to create the synthetic circulations. TY Robyn is inserted using a R_o = 800 km, V_{max} = 120 kt, a motion vector of 340° at 12 kt, and a r_{cut} of 300 km, which results in 19 observations. The synthetic observations to describe TS Steve are developed with R_o = 500 km, V_{max} = 45 kt, a motion vector of 295° at 9 kt, and r_{cut} = 200 km, which results in a more normal set of nine observations. The second MQI analysis (Fig. 36c) blending these synthetic observations with the composite data set and the first-guess field properly displays all features in the satellite imagery.

This case illustrates the need for sensitivity tests to determine an appropriate r_{cut} value for the upper-level structure of tropical cyclones in large data-void areas. Smaller r_{cut} values of 200 km and 300 km resulted in little change in the cyclonic region around the upper-level outflow of TY Robyn. This is the direct result of a lack of composite observations near this synthetic vortex to create the proper anticyclonic flow at a distance from the cyclone. These initial tests and the results described with the upper-level analysis from 12 h earlier dictate that in the absence of observations near the upper-level outdraft of a mature tropical cyclone, a larger synthetic observation cutoff radius must be set to describe properly the outflow structure.

The 200 mb difference field (Fig. 36d) highlights the major deviations between the first-guess field and the final MQI analysis. Insertion of both the cyclonic and anticyclonic portions of TY Robyn outflow create large differences

from the first-guess field. The changes in the field near TS Steve are less organized due to the weak synthetic observations entered. The other large regions with more than 5 m s^{-1} differences are associated with the introduction of the composite observations.

R. 850 MB ANALYSIS AT 2100 UTC 7 AUG 93

This last analysis illustrates the positive contributions of composite observations and the rapid correction of the analysis in data-void areas using complete sets of synthetic observations based on the experience gained from the previous low-level analyses. The extrapolation and comparison of the previous analysis (Fig. 34) with current satellite imagery (Fig. 35) and the first-guess field (Fig. 37a) again indicates that TY Robyn is too strong at outer radii and TS Steve near 15°N, 146°E is missing. Although the first-guess field does identify a weak low-level circulation near 6°N, 155°E, it fails to depict a circulation near 8°N, 168°E.

The first MQI analysis (not shown) blending the composite observations and the first-guess field shifts the weak low-level cyclone to a position near 5°N, 159°E, which is likely a better placement than the position from the satellite image. TY Robyn is still too large, and the low-level circulations associated with TS Steve and the cyclone near 8°N, 168°E are missing. The persistent lack of data near these missing features again dictates the use of synthetic observations. Using the current advisories, a synthetic vortex for TY Robyn is derived using R_o = 800 km, V_{max} = 120 kt, a motion vector of 340° at 12 kt, and r_{cut} = 400 km, which results in 34 observations. TS Steve's synthetic vortex uses R_o = 500 km,

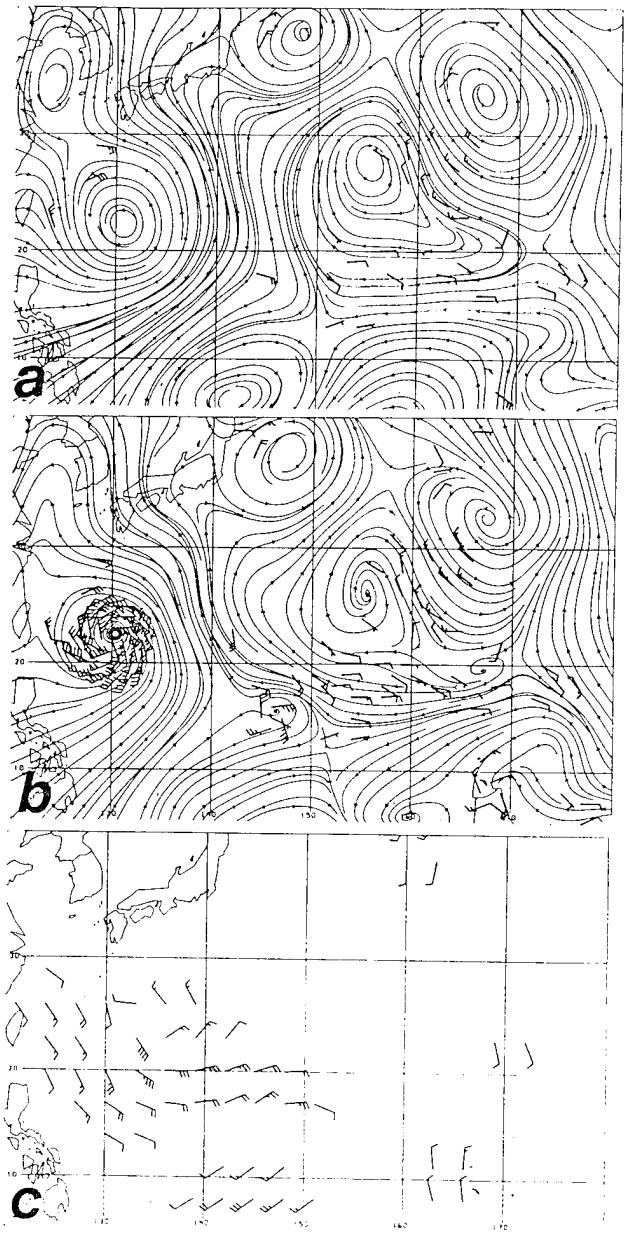

Fig. 37. 850 mb streamline analyses at 2100 UTC 7 Aug 93 of (a) first-guess field with on-time observations overlaid, (b) second (final) MQI analysis blending first-guess field, composite observations, and synthetic observations, and (c) 850 mb final MQI analysis minus first-guess field difference vectors.

V_{max} = 45 kt, a motion vector of 295° at 9 kt, and r_{cut} = 150 km, which again results in five observations. The missing low-level cyclone at 8°N, 168°E is developed based on the surrounding wind observations using r_{cut} = 150 km, V_{max} = 15 kt, and r_{max} = 100 km.

The second MQI analysis (Fig. 37b) including these synthetic observations now has all the desired circulations. Again, this two-step interactive analysis demonstrates that a good low-level analysis can be produced quickly with the insertion of complete sets of synthetic circulation observations once experience is gained.

The improvement in the outer wind field realized in the final analysis is quite evident in the 850 mb difference field (Fig. 37c). The anticyclonic difference vectors at the outer edges of TY Robyn indicates that the first-guess winds are higher than those based on the tropical cyclone model by Carr and Elsberry (1994). The cyclonic difference vectors near the center indicate the coarse grid first-guess field under-represents the strength of the winds near the center. These results suggest that a better representation of the low-level wind distribution of a tropical cyclone is possible using this interactive analysis.

Comparison of the 200-850 mb vertical shear calculations indicates the vertical wind shear from the first-guess field (Fig. 38a) over TS Steve near 15°N, 146°E is approximately 20 m s^{-1}. Calculations from the interactive analyses (Fig. 38b) indicates the shear is only 5-8 m s^{-1}. The impact of such shear differences on the formation and intensification of TS Steve will be described in the next chapter.

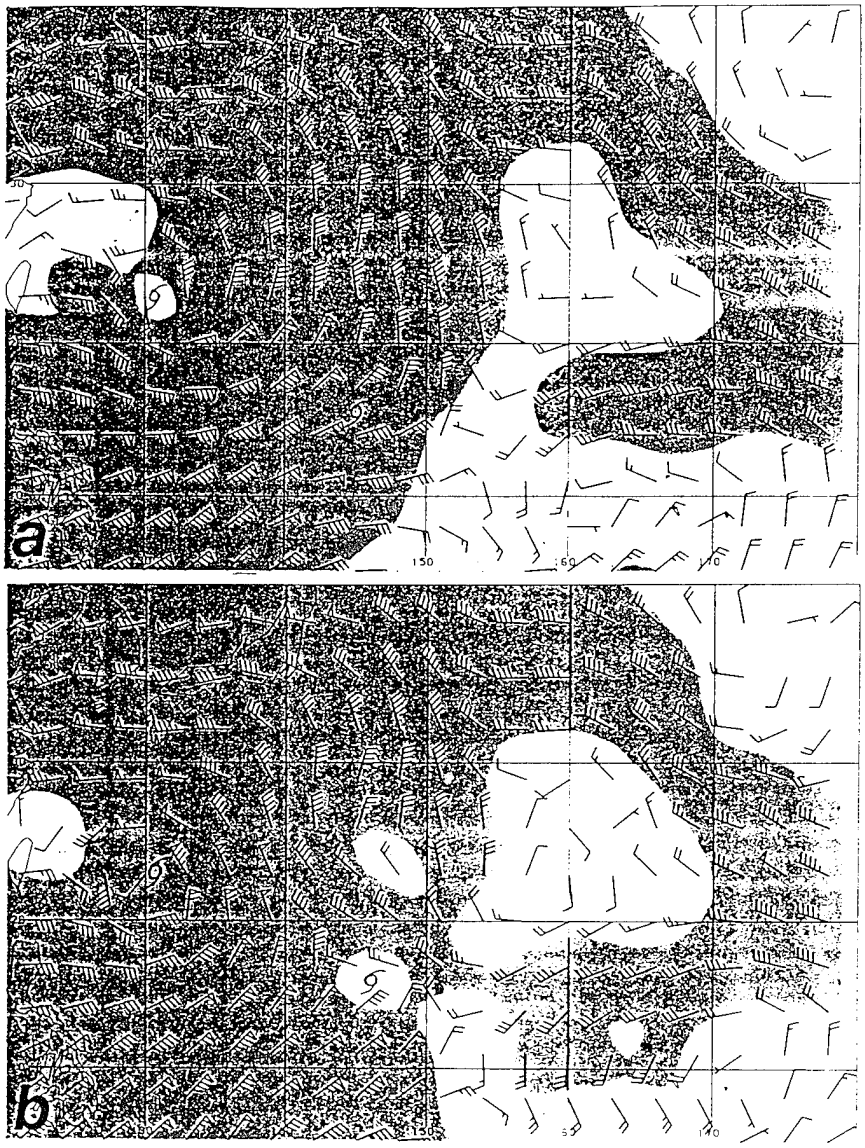

Fig. 38. Vertical wind shear (m s^{-1}) between 200 mb and 850 mb at 2100 UTC 7 Aug 93 for (a) first-guess fields, and (b) final MQ interpolation analyses. Western and eastern TY symbols indicate positions of TY Robyn (13W 1993) and TS Steve (14W 1993).

S. SUMMARY

Based on this first application of the interactive MQ analysis, several lessons have been learned. It is clear from the above daily descriptions that many circulations required repeated introduction of synthetic observations. Once such a circulation was identified, the initial estimate of user-specified values was based on the previous application of the interactive MQ analyses. For example, repeated introductions of upper-level synthetic vortices for TY Robyn and TS Steve were required since the first-guess fields seldom had data to represent the upper-level tropical cyclone wind structures. This should be expected as the FNMOC tropical cyclone synthetic observations are between 1000 and 400 mb only.

The low-level wind circulation in the first-guess field around TY Robyn was consistently misrepresented. Because the outer winds were too strong and the inner winds were too weak, a synthetic vortex was required in each analysis. In the case of TS Steve, inadequate observations were available to represent accurately either the upper- or lower-level circulation in the first-guess fields. No synthetic observations are included at FNMOC until the tropical cyclone is a TS (35 kt), and the coarse resolution of the model analysis, are probable contributors to the poor representation of weak tropical cyclones in the NOGAPS analyses. Thus, synthetic vortices had to be inserted in each MQ analysis. It is curious that TS Steve was missing after 00 UTC 6 August, when synthetic observations should have been automatically entered in the NOGAPS analysis. Because no reflection of TS Steve appeared, it is concluded that either the synthetic observations were never entered, or the strong circulation associated with TY Robyn overwhelmed the TS Steve synthetic observations.

During the entire analysis period, a large region of meridional flow from around 35° - 40°N to the Equator in the central western North Pacific was present

in the first-guess field. This caused a significant degradation of the analyses in those regions where the satellite imagery indicated point outdrafts were developing near a convergent asymptote. With only two exceptions, the first step of insertion of the composite data set corrected most of the degradations. Evidently, these observations had been consistently rejected in the quality control step at FNMOC. In the other two cases, synthetic observations of point outdrafts were required. Point synthetic observations were occasionally required at 200 mb to reposition the convergent asymptote, the point outdraft, and the meridional flow in the first-guess field.

The introduction of synthetic circulation observations was accomplished with a minimum of effort with only two exceptions. In large data-void regions at upper levels, a larger set of synthetic circulation observations is desired to describe the outflow structure of a mature tropical cyclone. However, other circulations in the vicinity will be disrupted if the circulation is too large. Insertion of a small set of synthetic observations in such a case results in only the cyclonic portion of the outflow pattern being entered, but is preferred over the disrupted field. The MQI technique then spreads these cyclonic winds over too large of an area and does not blend well with the anticyclonic real observations at larger radii. Synthetic observation sets at low levels for tropical cyclones are often quite large due to the large data-void regions around these circulations. The MQI technique did not have a problem blending the cyclonic synthetic observations near the center with the real observations at larger radii because the latter were also cyclonic.

Specifying circulations with single point observations is very time consuming because it often requires multiple iterations. In all but one case, the use of single observations to specify a closed circulation failed. However, single point

observations were very effective in compensating for bad observations or for fine-tuning the analyses, e.g., in the region of a convergent asymptote.

Based on this example, the upper-level structure of all tropical cyclones, and the low-level structure of mature tropical cyclones as well as weak low-level cyclones will require the introduction of synthetic vortices. Introduction of complete sets of synthetic circulation observations has proven to be effective and efficient. The best use of single point observations is to adjust the flow fields near convergent asymptotes and to compensate for the effects of bad observations.

VII. VERTICAL WIND SHEAR CALCULATIONS

Smith (1994) discusses the continued development of TS Steve (14W 1993) even though weak to moderate vertical wind shear was being analyzed over the pre-Steve disturbance. In particular, a northeasterly wind associated with the TUTT cell northeast of the disturbance appeared to interact with the point-source divergence over pre-Steve. A key feature of the Robyn-Steve tropical cyclone pair was the small separation distance of 9° to 13° lat., which allowed the large upper-level outflow pattern of Robyn to affect Steve. If the separation had been larger, Steve presumably would not have been affected as much, and the development of the pre-Steve disturbance would have occurred earlier. On 6 - 7 August as Steve became a tropical storm, the TUTT axis to the northeast shifted away from Steve and strong northeasterly flow from the outflow of Typhoon Robyn caused strong vertical shear over Steve until it dissipated on 14 August.

Gray (1968) identified weak vertical windshear as one of six favorable environment conditions for tropical cyclone development. Zehr (1992) specified a threshold vertical wind shear value of 12.5 m s^{-1} that is sufficient to prevent tropical cyclone development. Smith (1994) examined the TS Steve development with the NOGAPS analyses as a first-guess field, and re-analyzed rawinsondes, satellite cloud-track winds, and aircraft reports using a 50 km MQ interpolation. Using equation (6), she calculated the vertical wind shear for TS Steve (Fig. 39).

Smith (1994) suggested a mechanism by which the circulation of TD Steve might have been maintained against the inhibiting effects of vertical shear. She describes a diurnal variation in deep convection over or just south of the low-level

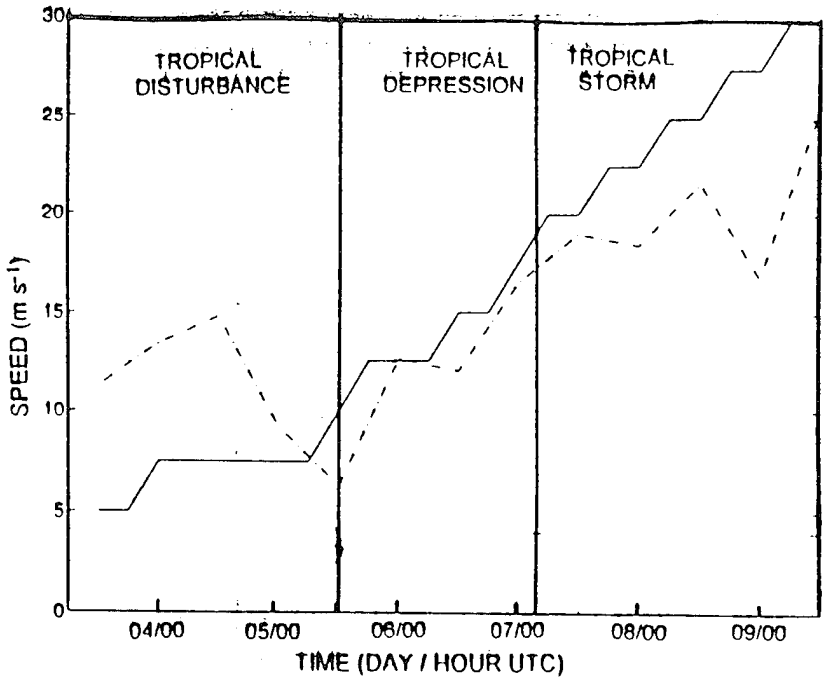

Fig. 39. Vertical wind shear (m s^{-1}) between 200 mb and 850 mb over TC Steve (solid) for 1200 UTC 3 August to 1200 UTC 9 August 1993 calculated from the multi-quadric analyses, and over Guam (dashed) for 1200 UTC 3 August to 0000 UTC 8 August 1993 calculated from upper air soundings (Smith 1994).

center that maintains vertical coupling of the circulation and prevents destruction of the warm core by the vertical wind shear. As the convection reaches diurnal maximum, the associated point divergence aloft will resist the effects of vertical wind shear over the developing tropical cyclone. This is evident in the satellite imagery as a bow-wave where the convection outflow aloft and the upper-level environmental flow meet. During the deep convection diurnal minimum, the upper-level flow penetrates close to the center, which results in forced subsidence near the center of the cyclone, warming in the vertical column and pressure falls. She states this warming combined with the latent heat released by the convection must be strong enough to offset any heat lost due to the ventilation effects of the

vertical wind shear. She concludes "The location of a the tropical cyclone within a very active monsoon trough environment appears to be the key factor for determining the ability of a developing system to overcome the inhibiting vertical shear" (Smith 1994).

To re-assess the shear calculations of Smith (1994), interactive MQ analyses for the period 2100 UTC 3 Aug 93 to 2100 UTC 7 Aug 93 were used in the vertical wind shear equation (6). These shear values are averaged over a radial extent of 333 km centered on the storm position. A comparison of the vertical shear calculations from the first-guess field and from the final MQ analysis is given in Fig. 40. Notice that the vertical wind shear calculations of Smith (1994) were very near those of the first-guess fields (NOGAPS) for the MQ analyses. Because the Smith reanalysis also used the NOGAPS analysis as a first-guess field, it is clear that her reinsertion of the observations made only a small change from the NOGAPS. Smith did not composite the observations for two synoptic periods (06 and 12 UTC; 18 and 00 UTC) as in this research, so that the amount of data available to her MQI analysis was much smaller. In addition, the smoothing factor she used in the MQI reanalysis was too large (see the appendix for sensitivity tests that justify the value in this research). Consequently, the vertical shear calculations of Smith (1994) do not differ significantly from the first-guess (NOGAPS) values, which also apply here.

The vertical wind shear values from this interactive MQ analysis demonstrate that the pre-Steve disturbance was not under the influence of strong vertical wind shear during the early development stages. Whereas the Smith (1994) and first-guess field (NOGAPS) shear values even exceed the Zehr (1992) threshold value of 12.5 m s^{-1} on 0900 UTC 4 August, the final MQ analyses at 200 mb (Fig. 12c) and 850 mb (Fig. 13b) lead to a shear value of less than 5 m s^{-1}.

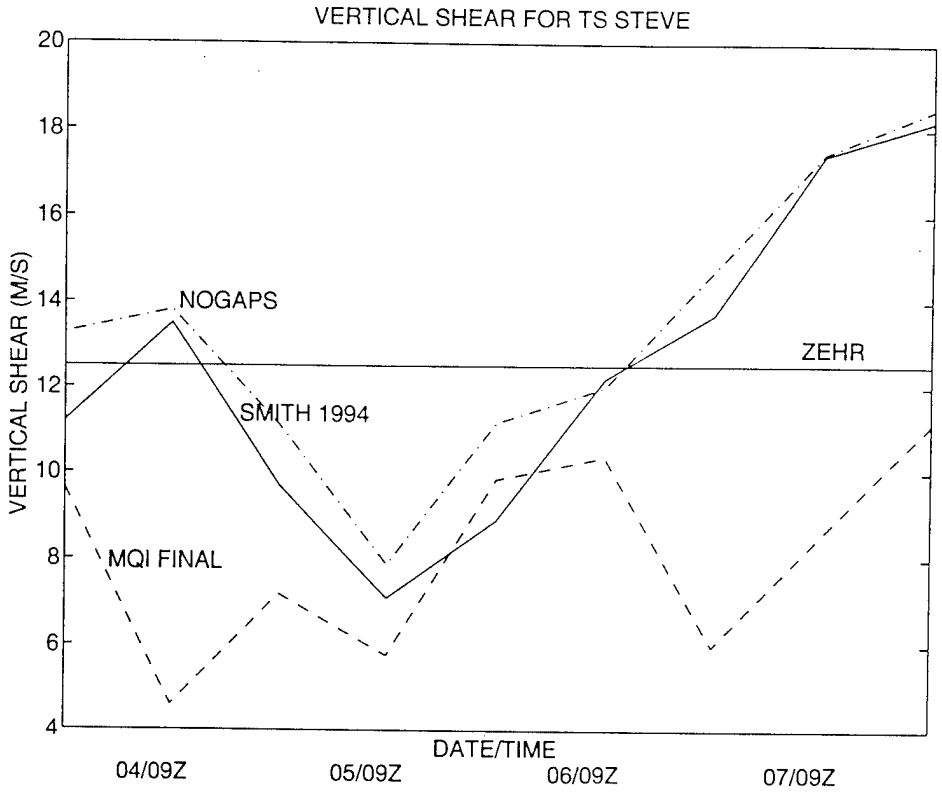

Fig. 40. Averaged (radius = 333 km) vertical wind shear (m s^{-1}) between 200 mb and 850 mb over TC Steve for 2100 UTC 3 August to 2100 UTC 7 August 1993 calculated from final MQI analyses (dashed), Smith (1994) (dash/dot), and NOGAPS first-guess fields (solid). Solid line at 12.5 m s^{-1} is the Zehr (1992) vertical wind shear threshold for developing disturbances.

All analyses have small shear around 0900 UTC 5 August, and then increase over the subsequent 24 h. However, the MQI shear does not exceed the Zehr threshold shear value as do the Smith and NOGAPS analyses. Rather, the MQI analyses at 21 UTC 6 August for 200 mb (Fig. 27b) and 850 mb (Fig. 29b) lead to a shear of only 6 m s^{-1}.

The vertical windshear values of Smith (1994) and the interactive MQI analysis are compared with the intensity variations of TS Steve in Fig. 41. The pre-Steve disturbance was initially classified as a tropical disturbance (winds $\leq$ 25

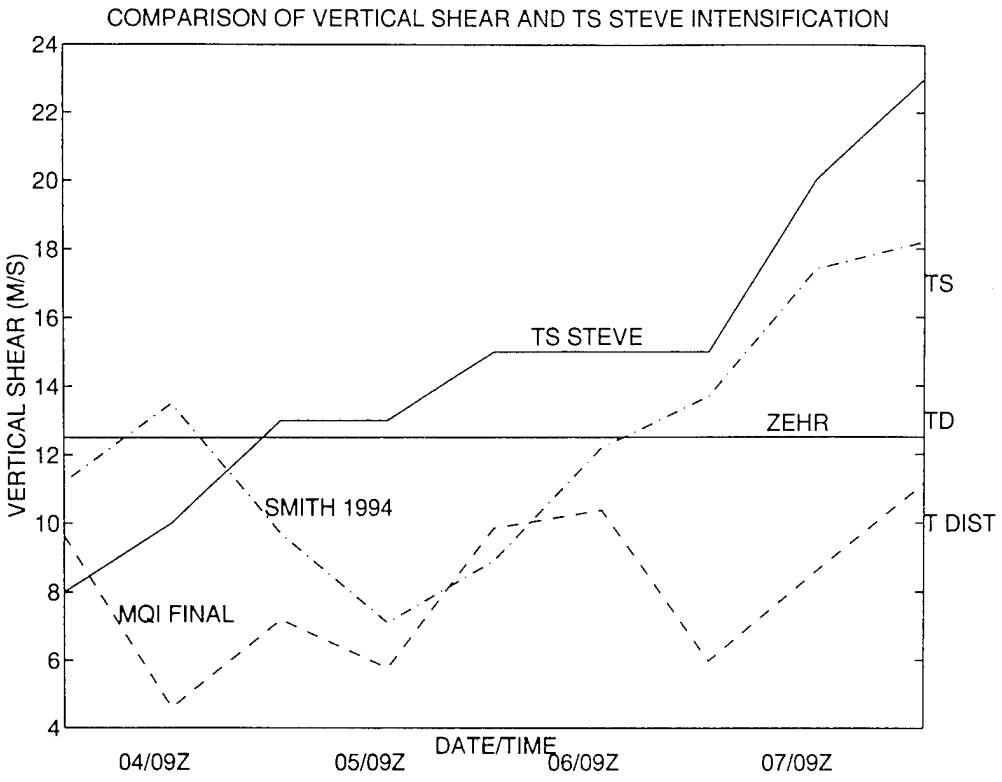

Fig. 41. Low-level maximum velocity (intensity) in m s^{-1} of TC Steve (solid), 850/200 mb vertical wind shear from final MQI analyses (dashed) and Smith (1994) (dot/dash), and the Zehr (1992) threshold for developing tropical disturbances.

kt or 13 m s^{-1}) at 1200 UTC 4 Aug 93, which immediately followed a period of minimum vertical wind shear in the MQI analyses. Additionally, the upgrades to tropical depression (30 kt or 15 m s^{-1}) at 1200 UTC 5 Aug 93 and to tropical storm (35 kt or 17 m s^{-1}) at 0600 UTC 7 Aug 93 immediately followed periods of minimum vertical wind shear in the MQI analysis. When the upper- and lower-level wind fields in the vicinity of TS Steve are properly analysed, the values of vertical wind shear correlate better in the sense that a period of weakening vertical wind shear precedes each increase in intensity classification.

Based on the first-guess field (NOGAPS) analyses, TS Steve would appear to have developed under weak to moderate vertical wind shear. According to the final MQI analysis, this tropical cyclone development may have been inhibited, but was not prevented, by vertical wind shear as might have been expected from the NOGAPS analyses. TS Steve did eventually weaken and dissipate (not shown here) as a tropical cyclone by 14 Aug 93 due to strong vertical wind shear (JTWC 1993).

Although this is a single case, it provides an example of the potential usefulness of the interactive MQ analysis for improving forecasts of tropical cyclone formation and intensification. Existing analyses (e.g., the NOGAPS analyses used as a first-guess field here) may not resolve the upper-level structure above the tropical cyclone, and particularly may imply larger winds aloft as in this case. Statistical equations for tropical cyclone intensity changes (e.g., DeMaria et al. 1993) that are based on such large-scale analyses may then fail during these situations.

VIII. CONCLUSIONS, IMPACTS, AND RECOMMENDATIONS

A. CONCLUSIONS

Through the use of data compositing and introduction of synthetic circulation features, the interactive analysis procedure provides an analysis that blends the best features of both the objective numerical analysis and the subjective analysis and results in an assessment of the tropical environment that is superior to either method. This interactive numerical analysis scheme builds upon (and thus improves) the tropical wind analysis provided by the four-dimensional data assimilation technique and incorporates satellite interpretation information in the same manner as a human subjective analyst in the tropical warning centers. Data compositing is used here to provide nearly twice the data available to the four-dimensional analysis. These extra data combined with synthetic observations developed from the interpretation of satellite imagery provide a more complete picture of the atmosphere than could be otherwise obtained. Comparison of the 200 mb subjective hand analysis (Fig. 42) and the MQI analysis (Fig. 15d) at 2100 UTC 4 Aug 93 validates this subjective insertion of features interpreted from satellite imagery into the interactive analysis.

The automated numerical analysis often does not represent the highly divergent and rapidly changing tropical weather circulations, perhaps due to rejection of observations in the data quality control or by inclusion of a model first-guess field that has too small divergence. This data rejection often eliminates smaller scale tropical features from the model analyses. Current practice at tropical warning centers requires careful scrutiny of all available observations and careful interpretation of satellite imagery to determine what features have been

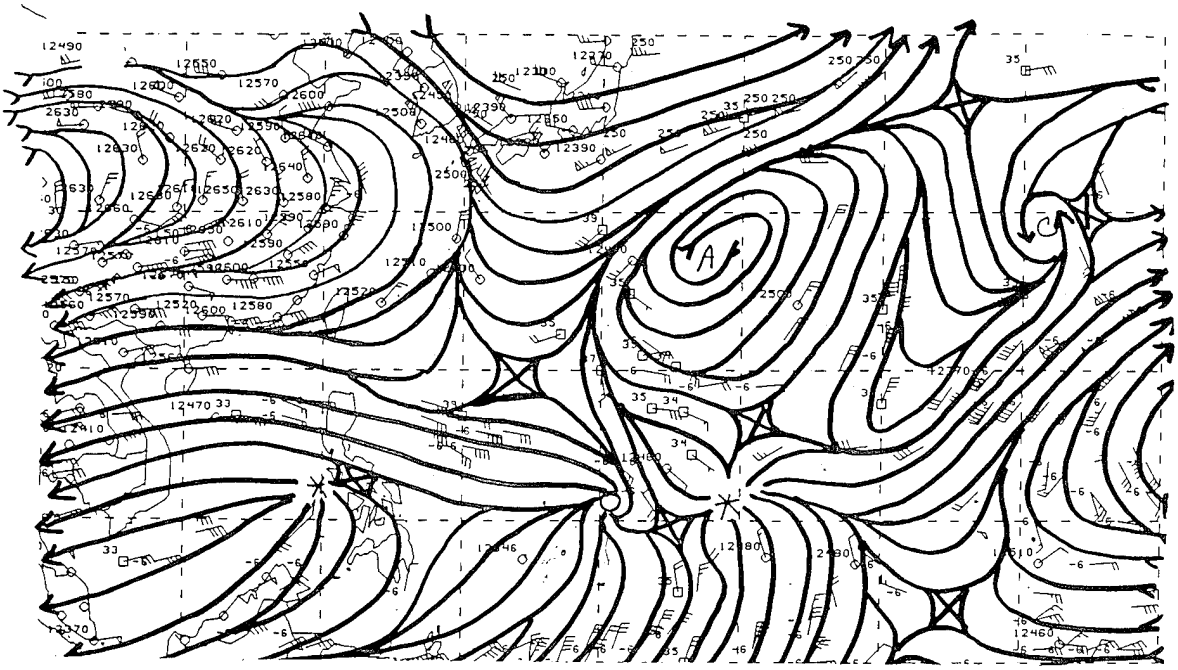

Fig. 42. 200 mb hand-drawn streamline analysis at 2100 UTC 4 Aug 93 from TCM-93 (Carr and Jeffries 1993).

eliminated. However, no interactive procedure has existed to re-incorporate these missing features or reanalyze the discarded data.

A key aspect of this research is the use of data compositing to increase the data available for tropical wind analysis. An increased data set can improve the numerical representation of the highly divergent features in a tropical analysis. Satellite cloud-drift wind and aircraft data composited over six-hour periods centered on 0900 UTC and 2100 UTC results in nearly twice the observations as data composited on the individual synoptic times (0600 and 1200 UTC; 1800 and 0000 UTC). Incorporating these composited data sets alone results in a significantly improved numerical analysis. However, data compositing does not solve entirely the tropical data-sparsity problem.

Once a tropical cyclone warning is issued, the regions around these severe storms typically become data-void. Ships and aircraft avoid these areas, dense

cirrus limits upper- and lower-level cloud-drift wind retrievals, and radiosonde launches in the vicinity often fail. Additionally, the lack of clouds near TUTT cells or along convergent asymptotes (subsiding, cloud-free air preventing satellite cloud-drift winds) limits the data quantity near these features. Another problem discovered in this research is the low-level structure of the tropical cyclone synthetic observations currently inserted in the NOGAPS analysis are too strong in outer regions and too weak near the center. This misrepresentation of the tropical cyclone vortex in the NOGAPS analysis can be attributed to the size of the vortex that is entered into the analysis and the coarse resolution of the model. A lack of data near these synoptic circulations prevents adjustment of the synthetic circulation by the numerical analysis. This lack of data leads to the requirement for synthetic observation insertions to fill data voids and adjust the model analysis.

Insertion of complete sets of synthetic observations to represent tropical cyclones, TUTT cells, point outdrafts, anticyclones, and weak tropical waves is a rapid method of inserting missing, or repositioning misplaced, circulations. The number of synthetic observations that are required to be inserted depends on the position of the circulation in a data-void area, the size of the data-void, and the quality of the first-guess field in the region. The number of synthetic observations is a user-specified value that limits an overlap between synthetic and real observations. Repositioning, or an insertion of missing, weak low-level cyclone, TUTT, or anticyclonic circulations can usually be accomplished with as few as four synthetic observations.

The use of point synthetic observations is necessary to adjust (fine-tune) the interactive analysis and to eliminate the effects of bad observations identified during human quality control. The MQI analysis draws closely to all observations. Thus, bad observations or a wind $\leq$ 5 kt may cause a poor depiction of a

circulation feature. Human quality control is necessary to detect these bad circulations, and to insert compensating point synthetic observations. Additionally, a distinct confluent asymptote in the satellite imagery can be depicted in the interactive analysis by input of a series of 25 kt point synthetic observations along the convergent line.

Another aspect of this interactive analysis is the useful diagnostic fields that can be readily computed during the iterative process. Vertical wind shear calculations from the interactive analysis are more closely consistent with observed TC intensity changes than are those from an automated analysis. A review of the vertical wind shear, vorticity, divergence, and increment (final MQ analysis minus the first-guess) fields during the analysis process can lead to new insights into the flow field and its relationship to features identified on satellite imagery. This new insight can improve the tropical synoptic models, improve understanding of the environment, and aid in forecasting future changes.

Doswell (1986) states a combination of education and task-oriented training is the best solution to the problems associated with training new forecasters. He also points to the process of diagnosing weather information that leads to models of current weather features and a prognosis of future weather events. These models are a key element in the forecast process. This interactive analysis system could aid in training of new personnel for tropical analysis and forecasting.

Another feature of this interactive system identified during the development process is the application of this interactive approach to the university training environment. Doswell (1981) cites the problem of lack of practical training in meteorology/forecasting at the universities as a major drawback to the advancement of meteorology as a science. This interactive system is designed around the numerical representation of tropical synoptic features discussed in the NPS

curriculum and offers a practical application of these features. The ability to simulate quickly these features and enter them as perturbations or eddies into the environmental field may lead to an improved understanding of the environmental interactions in the tropics.

The diagnosis of vertical wind shear, vorticity, divergence, and difference fields on a local workstation provides significant flexibility to the on-scene forecaster. The re-introduction of observations, addition of new observations, or the introduction of synthetic observations is particularly useful for regional or smaller scale analyses in support of the on-scene forecaster. Although the global analysis is useful for large-scale circulations, it often does not depict the small-scale features that impact a local area forecast. This interactive analysis is a step toward giving the local forecaster a higher resolution analysis that makes maximum use of observations and satellite imagery interpretation techniques.

B. IMPACTS

A discussion of the impacts of this work may be divided into science and operations. Whereas the science impacts center on the new knowledge gained from the procedure, the operations impacts are directed toward improvements in forecast and warning services provided. Each of these considerations are inter-twined and will overlap in the applications of this technique.

For the sciences, the interactive analysis improves representations of upper- and lower-level tropical circulations. For example, these analyses provided an improved vertical wind shear assessment during the formation and intensification of TS Steve. Improvements in tropical analysis should lead to a better understanding of the interactions of the tropical circulations and the large-scale environment.

For operational impacts, the interactive analysis provides a more uniform analysis procedure that honors all of the available data unless specifically discarded by the analyst. Compositing of data over two 6-h synoptic times as applied here almost doubles the satellite cloud-drift winds and aircraft reports. Even though the analysis is valid 3 h earlier, it is a better analysis because data sparsity is a major problem for the tropical analysis. The same procedure could be used each 6 h to produce analyses valid at 0300 UTC, 0900 UTC, 1500 UTC, and 2100 UTC if desired. The interactive analysis improves on the automated numerical analysis by inserting complete sets of synthetic observations based on models of tropical weather phenomenon. Automated plotting of observations saves time and is more accurate than the present handplotting at the Joint Typhoon Warning Center. The interactive analysis allows for input of on-scene weather information in near real-time, and produces a digital analysis that could be quickly communicated to the customers. Interactive analysis is based on the same procedures of synoptic review, adding of local data, satellite interpretation techniques for tropical systems, and careful fitting of good wind observations (while rejecting bad observations) as subjective analysis techniques currently employed at regional forecast centers. For the TS Steve example, the improved vertical wind shear calculations may have improved intensity and formation forecasting.

C. RECOMMENDATIONS

To speed the process of interactive analysis, a capability for on-screen elimination of bad observations must be developed. This capability should also include insertion of point synthetic observations in a point and click manner.

A three-dimensional version of MQI should be tested in this interactive analysis. If a three-dimensional capability could be developed, synthetic

observations of the upper-level atmosphere in the tropics produced by an interactive analysis could be included in the global model initialization. Empirical Orthogonal Functions (EOF's) could be tested as a vertical structure function to spread the influence of the large number of single-level wind observations in the tropics.

The primary limitation to automated numerical analysis in the tropics is the lack of data. The use of all available data in the tropics is necessary for the proper depiction of highly divergent tropical features. An investigation of other data sources for data compositing (e.g., water vapor winds, Special Sensor Microwave Imager (SSMI), etc) is required if an improved tropical numerical analysis is to be achieved.

More research is recommended with regard to representation of upper- and lower-level anticyclones, weak surface cyclones, and upper-level point outdrafts to ensure the best possible synthetic circulations are produced. These features should be analyzed in a three-dimensional model, but few mid-tropospheric observations are available in the tropics. Although convergent and divergent asymptotes are easily identified in satellite imagery, neither an accurate assessment of the altitude of these features nor an accurate numerical representation of these features is available.

Another possible application of interactive analysis is for mesoscale battlefield analysis. To incorporate properly an interactive analysis into the battlefield environment, numerical representations of the mesoscale circulations must be developed and new data sources found. Once these features are available, the adaptation of the MQI analysis and the interactive procedure are possible.

Prior to incorporation of this interactive analysis technique into a forecast center, an extensive redesign of the software to optimize the code would be

desirable. An efficient and user-friendly version of this interactive analysis could result in improved tropical wind analyses for operations and for scientific studies.

APPENDIX

SYNTHETIC OBSERVATION CODE DEVELOPMENT AND TESTING

A. ANALYSIS CODE DEVELOPMENT AND TESTING

The MQI technique was chosen for this interactive analysis because it is designed to draw very closely to the observations. As described by Nuss and Titley (1994), the MQI fits surfaces through all observations in such a way that values can be interpolated to any point in the field, which in this case is a 1° lat./long. grid. The degree of the surface fit to the observations is determined by specification of filtering and smoothing parameters. The user may vary the RMS difference between observations and the first-guess field. Similarly, the degree of smoothing of the observations may be varied in the analysis. Nuss and Titley demonstrate that the MQI technique has skill in the interpolation from scattered data. The version of the MQI code used here for the tropics was modified by W. Nuss.

Another desirable feature of the MQI analysis is the interactive capability for regional analysis applications. A version of the MQI code on the NPS Cray computer was converted for workstation applications. A batch file, such as in Table A-1, is the user interface for the MQI analysis. A separate batch file is created for each Date-Time-Group (DTG) and each iteration of the analysis. Most of the inputs in this batch file are set to a single value that never changes, e.g., the

Table A-1. An example of the MQI user interface Batch File.

```
/home/usr34/jeffries/thesis/nogaps/nog9308.gem  (Fields Filename)
930804/0000          (Fields DTG)
930804/1200          (Fields DTG)
NOG                  (Fields Type)
TC+                  (Grid Spacing, tc+=1°, tc=2.5°)
N                    (Satellite Overlay, y or n)
Wind                 (Analysis Type)
N                    (Output wanted, y or n)
.true.               (1st Guess Used)
.true.               (Check against 1st guess)
.false.              (Always false)
3.5                  (# standard deviation before obs rejected)
10.0                 (# of grid spaces before 1st guess used)
0.1                  (Distance minimum to accept obs)
0.01                 (Smoothing parameter)
0                    (Station plots used)
1                    (color for NCAR graphics)
1.0                  (line thickness, NCAR graphics)
2.0                  (contour interval, NCAR graphics)
.false.              (filter output obs)
4                    (size of station plot)
930804/0900          (DTG of obs data)
/home/usr34/jeffries/thesis/aireps/ar930804.mtq (Obs file)
fgge                 (Obs format)
200                  (Obs level)
Y                    (additional obs files, y or n)
930804/0600          (DTG of obs data)
/home/usr34/jeffries/thesis/satwinds/sw930804.mtq  (Obs file)
fgge                 (Obs format)
200                  (Obs level)
y                    (additional obs files, y or n)
930804/1200          (DTG of obs data)
/home/usr34/jeffries/thesis/satwinds/sw930804.mtq  (Obs file)
fgge                 (Obs format)
200                  (Obs level)
N                    (additional obs files, y or n)
N                    (additional data, y or n)
```

inputs that deal with the graphics and display. After sensitivity testing, user-specified parameters such as the RMS error or smoothing factor also are not changed. Therefore, the main inputs are the specification of composite observation files, first-guess fields, and analysis levels. This is also the method to specify the location of additional synthetic circulation or point synthetic observations for inclusion during each step of the interactive analysis approach.

1. Observation Smoothing Parameter Criterion

A series of tests was performed to determine appropriate values of the smoothing parameter and the observation versus the first-guess standard deviation criteria. The smoothing parameter in the MQI can be thought of as either a measure of the least-squares fit to the observations or a spectral low-pass filter (Nuss and Titley 1994). Analyses using smoothing parameters of 0.01, 0.005, and 0.001 (smaller numbers are associated with less smoothing so that the analysis will fit the observations more closely) were tested to determine the amount of analysis detail retained. The magnitude of the smoothing parameter also affects the length of time to obtain a solution on the workstation, so the larger the smoothing parameter, the more timely will be the analyses.

Upper-level observations from 2100 UTC 4 Aug 93 are overlaid on the MQI analyses (Figs. A1 a-c) with the three values of the smoothing parameter. The primary differences among the analyses are best highlighted by the changes in the flow pattern between 10° and 20°N, 150° and 160°E and near Mindanao. When the smoothing parameter is set to 0.01, the MQI routine did not draw to contrary-flow observations and continued the meridional flow pattern between 150° and 160° E in the first-guess field. With this relatively large smoothing parameter, the wind analysis fits the observations in the large-scale sense, but does not draw closely to individual observations in the region. Based on these observations, the

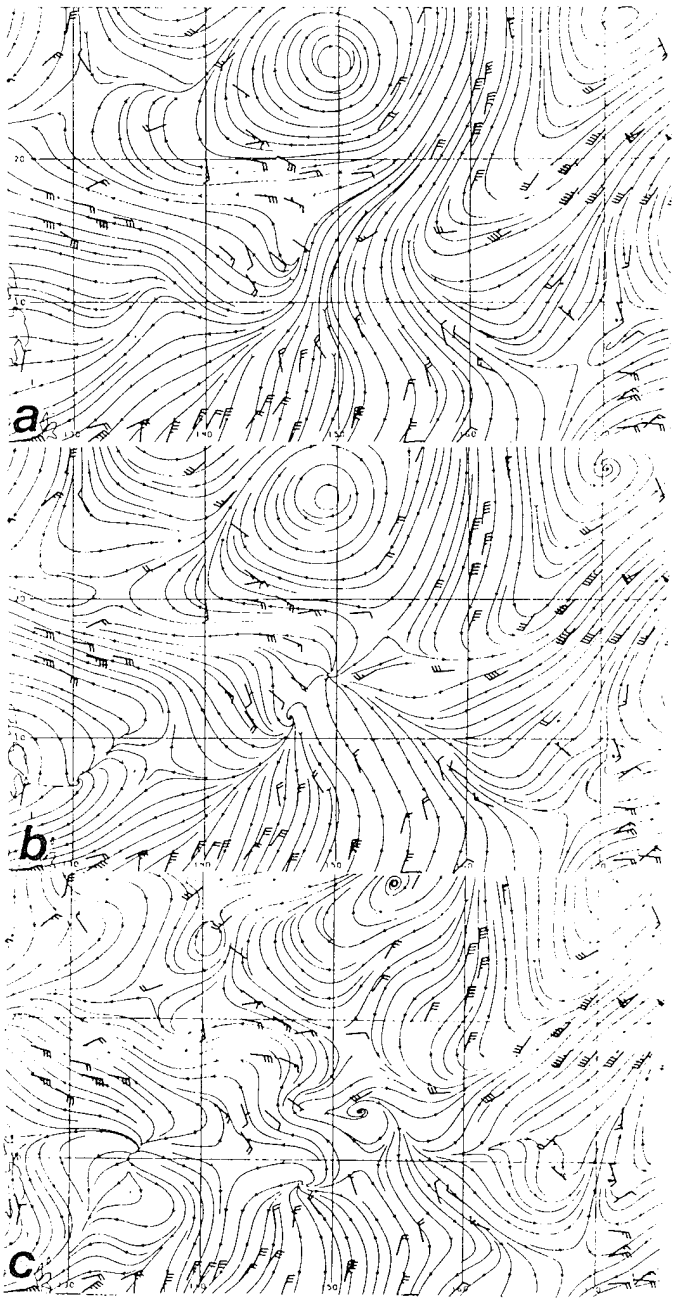

Fig. A1. 200 mb streamlines at 2100 UTC 4 Aug 93 of MQI analyses blending first-guess field and composite observations (overlaid) with the smoothing factor specified as (a) 0.01, (b) 0.005, and (c) 0.001.

flow should have turned toward both the east and west in this region to form convergent asymptotes. When the smoothing parameter was decreased to 0.005 (Fig. A1b), the flow pattern near 16°N, 152°E did turn as required because the observations were more closely fit by the MQI analysis. A further decrease in the smoothing parameter to 0.001 (Fig. A1c) resulted in the MQI analysis including a closed circulation near Mindanao, which occurred because the analysis drew to a weak diffluent wind observation. A decision to set the smoothing parameter to 0.005 was a balance between the desire that the analysis draw closely to the observations and yet not draw too closely to weak wind observations that likely have larger errors or may be unrepresentative.

2. Observation Standard Deviation Criteria

The number of standard deviations of an observation from the first-guess field is used as a gross-error check in the MQI software. This value may be adjusted by the user through the input batch file as in Table A-1. A series of sensitivity tests was completed to determine an appropriate standard value (Table A-2). The initial gross error check is a calculation of the root-mean square difference between the observations and an interpolated value from the first-guess field. This initial value becomes the standard deviation criterion for whether an observation is rejected for use in the first MQI analysis. A second gross-error check calculation is then made versus this first MQI analysis for rejection of observations in the second MQI analysis, and the cycle is repeated.

It is anticipated that the inserted synthetic observations will frequently have opposite directions and different speeds from the first-guess field. Thus, the standard deviation criterion must be set rather high to ensure that all synthetic observations will be used. Based on the desire to ensure maximum observation use, the standard deviation value was initially set to four standard deviations. However, a value of 5.0 was found to be necessary in areas of strong flow.

Table A-2 Number of observations rejected based on the gross-error check criterion expressed as the number of standard deviations from the first-guess field. A total of 483 observations were available for this test using the 0900 UTC 4 Aug 93 data set at 200 mb.

Number of Standard Deviations	Number of Rejected OBS
2.0	113
2.5	50
3.0	12
3.5	4
4.0	2
5.0	0

To improve the interactive aspect of the quality control process in the future, all observations might be included in initial analysis. Because the MQI analysis draws closely to observations (good or bad), the bad observations should appear as large anomalies. A point-and-click capability for the analyst to eliminate those bad observations in the subsequent analyses should be developed.

The results for a value of 5.0 in Table A-2 imply every one of the observations is good (or at least reasonable). The advocates of the optimum interpolation technique will object to such a loose criterion, which here turns out to be no criterion. Philosophical differences between an interactive versus an automated analysis are the justification, because the interactive analyst will have the ultimate decision to reject an observation. In an automated analysis, a more conservative approach must be taken because no further review takes place. Not only do bad observations degrade the analysis, but the error may be perpetuated in the short-term forecast that is the first-guess field for the next analysis. A

procedure for overriding a bad observation by insertion of point synthetic observations is described in Chapter V.

B. CIRCULATION CODE DEVELOPMENT

The development of the synthetic observation code was a joint effort of CDR L.E. Carr, III and LT R. A. Jeffries. CDR Carr developed the initial tropical cyclone wind field code and LT Jeffries modified and adapted this code to allow for interactive input. Additional code was developed to create synthetic observations for TUTT cells, point outdrafts, weak surface cyclones, monsoon gyres, and both upper- and lower-level anticyclones.

The synthetic circulation code creates synthetic observations on a 1° lat./long. grid over the area from 0° to 40°N, 100° to 180°E. The circulations can be described as either a total wind flow (circulation plus mean environmental winds), or as only the eddy circulation. These synthetic observations are included in the MQI analyses as dropwindsonde observations using the FGGE format.

1. Tropical Cyclone

The tropical cyclone is represented with an equation based on the conservation of angular momentum (Carr and Elsberry 1994). At low-levels the angular momentum is assumed to be partially conserved as a parcel moves radially inward from a radius of zero winds, R_o. At upper-levels, angular momentum is assumed to be precisely conserved as a parcel moves radially outward from the radius of maximum winds, r_{max}. Using code originally developed by CDR L.E. Carr, III in terms of the equations (3), (4), (5), and (6) in Chapter III, the tangential and radial wind components are calculated on the 1° lat./long. grid with an observation cut-off radius (r_{cut}) specified by the analyst. This original code was modified by LT R.A. Jeffries to allow for user specification of the lat./long., maximum wind, radius of circulation, current motion vector, and wind observation cutoff radius.

This value of r_{cut} is necessary to allow for the smooth blend of the synthetic observations and the adjacent real observations in this analysis procedure. If the synthetic circulation produced by this code is allowed to become too large, it could conflict with the real observations (AIREPS, SATWINDS, and soundings). For example, a tropical cyclone outdraft circulation created by this code may introduce a 10 kt wind in close proximity of an opposing 10 kt wind in the composite data. In this situation, the two values would cancel. In the atmosphere, the 10 knot composite wind consists of both the perturbation and the background environmental flow. Thus, re-entry of a synthetic wind observation to describe the outdraft circulation would result in a poorly specified analysis. Based on this scenario, the r_{cut} value will normally be specified so the synthetic observations do not overpower the real observations.

Once the synthetic observations are calculated, they are converted to the format of FGGE dropwindsonde observations. In addition to this data file for input into the MQI analysis, another file is created in GEMPAK format so the synthetic observations can easily be displayed.

Examples of lower- and upper-level tropical cyclone circulations from the synthetic circulation code are shown in Figs. A2a and A2b respectively. Whereas the low-level flow is cyclonic throughout, the upper-level flow is cyclonic near the center and becomes anticyclonic at larger radii.

A sensitivity test of the user-specified input R_o is given in Fig. A3a-c for the 200 mb MQI analysis at 2100 UTC 4 Aug 93 in which the value of Ro is varied in 200 km increments starting at 1000 km and decreasing to 600 km. In this test, the cutoff radius (r_{cut}) is fixed at 200 km, which results in the inclusion

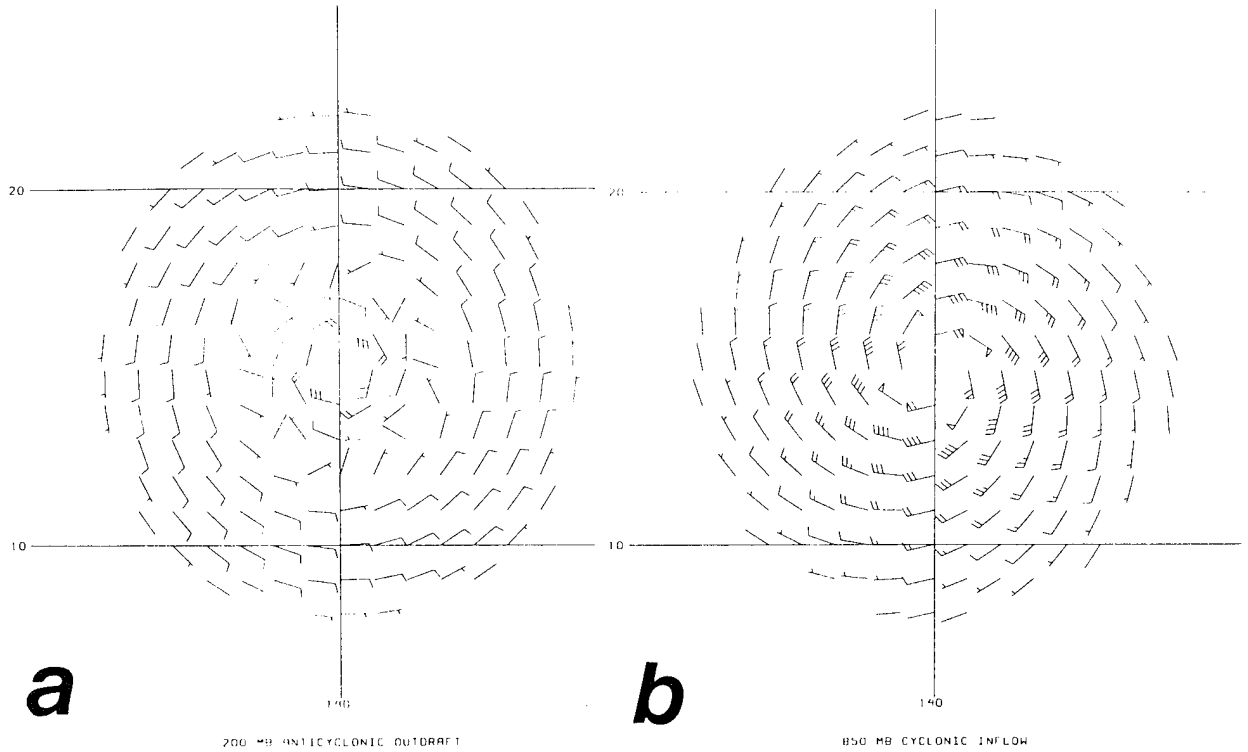

Fig. A2. Tropical cyclone (a) upper- and (b) lower-level wind fields created using the algorithm described by Carr and Elsberry (1994) with V_{max} = 80 kt, R_o = 800 km, f_o = 15°N, and r_{cut} = 800 km.

of nine observations to describe the upper-level outflow pattern. As shown by Carr and Elsberry (1994), decreasing the radius of the circulation R_o for the same V_{max} results in a smaller radius of maximum winds and a weaker upper-level circulation. The weaker circulation arises in part from the coarse 1° by 1° grid not being able to resolve the smaller inner cyclonic circulation. These tests illustrate that the upper-level circulation is sensitive to the outer circulation radius value specified. This value will normally vary between 500 km for a small cyclone to 1000 km or more for a large cyclone.

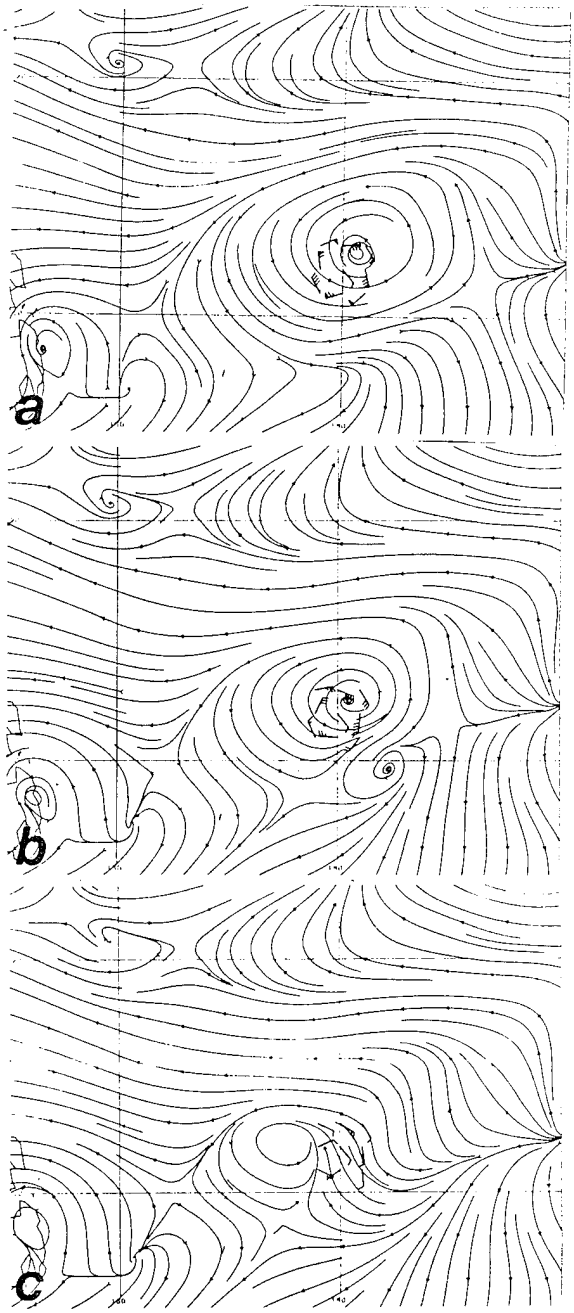

Fig. A3. 200 mb streamline analyses at 2100 UTC 4 Aug 93 blending first-guess fields, composite, and synthetic observations. The synthetic tropical cyclone observations are based on an R_o of (a) 1000 km, (b), 800 km, and (c) 600 km.

To test the effects of changing r_{cut} from 150 km to 500 km, the storm intensity was fixed at 80 kt, and R_o was fixed at 800 km. As shown in Fig. A4a-d, the numbers of synthetic observations are 5, 9, 18, and 58, respectively. In general, a larger r_{cut} is specified in an area without observations. In areas where numerous real observations are close to the synthetic circulation, a minimum number of synthetic observations should be used so they may blend smoothly with the surrounding flow. Since a constant smoothing is specified in the MQI for the entire domain, a synthetic circulation that is too large (e.g., Fig. A4d) will overpower or be overpowered by the observations, depending on which flow is stronger. In essence, the MQI routine will not draw closely to a cluster of observations that conflict with the large-scale MQI analysis that fits the surrounding observations. The observations that are ignored are a function of data density and it is not always obvious which ones will be ignored. A significant decrease in the smoothing parameter will force the MQI scheme to draw to these dense observations. However, this will result in problems in other areas of the analysis where the MQI draws to weak, unrepresentative observations. In contrast, a smaller group of synthetic observations will typically not be ignored (e.g., Fig. A4b).

2. TUTT Cells

The original code for the TUTT cell synthetic observations was developed by CDR L. E. Carr, III for illustrating the effects of translation speed with TUTT cell vortex structure. The equations for this illustration are shown in Chapter III. The adaptation for the interactive system allows the analyst to place a TUTT cell circulation with a specified V_{max} and r_{max} at any location. As in the tropical cyclone example above, the radial cutoff (r_{cut}) is specified for smooth blending of the synthetic circulation with the available observations. The TUTT circulation reduces to zero at twice the radius of maximum winds.

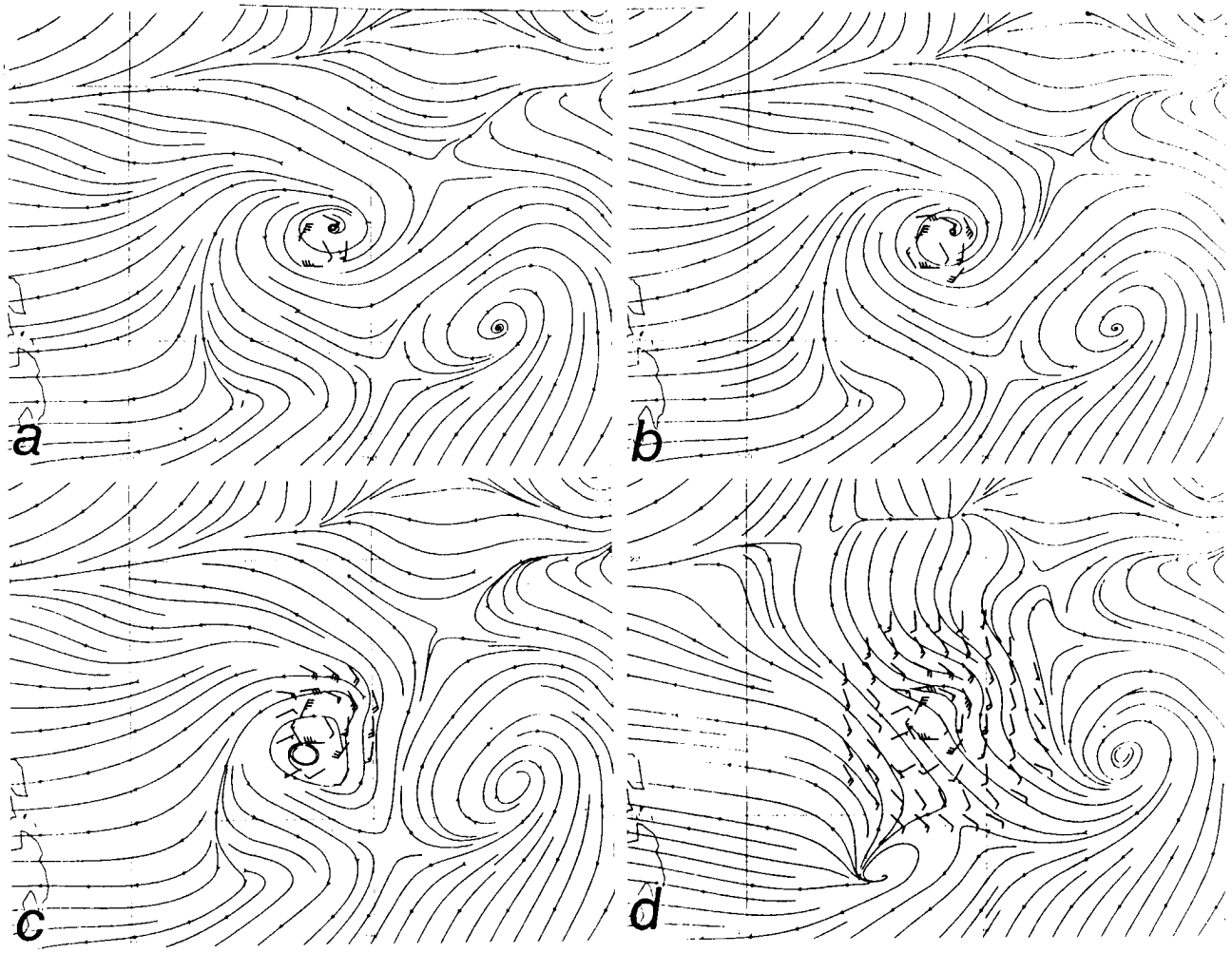

Fig. A4. 200 mb streamlines from 2100 UTC 4 Aug 93 MQI analyses with synthetic and composite observations overlaid. The r_{cut} is varied from (a) 150 km, (b) 200 km, (c) 300 km, and (d) 500 km.

The 200 mb wind fields before and after the introduction of synthetic TUTT circulation observations near 28°N, 174°E are shown in Figs. 32a and 32c (Chapter VI). The synthetic observations introduced to describe the TUTT plus the background environmental flow are highlighted in Fig. 32c. A r_{cut} value of 150 km was used, which resulted in a zero wind at the center and four surrounding observations. During sensitivity testing, it was determined that a weaker circulation than might be inferred from the surrounding winds should be used for TUTT cells, otherwise blending of the synthetic observations and the background winds will result in a too strong circulation. However, this does not present a major difficulty because the interactive nature of the analysis allows a weaker circulation to be entered when necessary so that the total flow of environment plus the TUTT circulation blends smoothly with adjacent observations.

3. Point Outdrafts

As indicated in Chapter III, Lander (personal communication, 1990) has described the point outdraft as the resulting horizontal flow as strong convection impinges on the tropopause. To develop synthetic observation software to describe a point outdraft, the tropical cyclone circulation was adapted with V_{max} set equal to zero. The analyst is required to specify a radial wind (U_{rad}), a radius of maximum radial wind (r_{max}), and a wind cutoff radius (r_{cut}). These user-specified inputs are determined based on a review of the observations in the vicinity of the point outdraft and the intensity of the convective outflow inferred from the satellite imagery.

The 200 mb wind fields before and after the inclusion of synthetic observations of the point outdraft near 11°N, 150 °E that was associated with pre-Steve are shown in Figs. 15a and 15c (Chapter VI) respectively. The synthetic circulation used in Fig. 15c was developed using U_{rad} = 15 m s^{-1}, r_{max} = 100 km, and r_{cut} = 150 km, which results in five observations. Additional testing was

accomplished to verify the impact of diurnal fluctuations in the convection. The radial wind speed was set to 15 m s^{-1} and a larger cutoff radius (200 km) of wind observations was used to describe the point outdrafts at the time of diurnal maximum convection, and a smaller cutoff radius (150 km) was used for the time of diurnal minimum, which resulted in nine and five observations, respectively. Based on this limited sensitivity test, the desired depiction of a larger point outdraft at diurnal maximum and a smaller outdraft at dirunal minimum is achieved using these r_{cut} changes. However, a more extensive test should be conducted to verify the generality of these values in other cases.

4. Weak Surface Cyclones and Monsoon Gyres

Weak, low-level cyclonic circulations in the tropics are often evident in areas of organized convection in the high resolution satellite imagery, but are not represented in the automated analysis because of limited observations. Additionally, broad areas of cyclonic turning associated with monsoon gyres are often observed. It is important for the tropical analyst/forecaster to maintain continuity of these circulation features because they can develop into tropical cyclones. This interactive procedure allows two methods to describe these features. The analyst can elect to use either the tropical cyclone vortex or a modified version of the TUTT code.

When the tropical cyclone code is used, the analyst must specify the maximum cyclone circulation radius (R_o), the maximum winds (V_{max}), and the observation cutoff radius (r_{cut}). Wind analyses before and after the inclusion of synthetic wind observations to describe the low-level circulation center near 10.3°N, 153.5°E associated with pre-TS Steve are shown in Figs. 19a and 19c (Chapter VI), respectively. To develop the circulation for pre-TS Steve in Fig. 19c, a value of R_o = 500 km, V_{max} = 25 kt, motion vector of 295° at 8 kt, and a r_{cut} = 150 km was used, which resulted in five observations. After some testing, it

was determined that a limited number of synthetic observations should be entered to describe properly a weak circulation. For most of the weak low-level circulations in the test sample, five observations circulation were sufficient for inclusion in the MQI analyses.

When R_o is difficult to estimate, an alternate method for specifying weak low-level circulations is the TUTT circulation code. This allows the analyst to specify a maximum wind at a radius from the center and allows for the weakening of the winds with radius toward the center. Low-level wind field before and after the introduction of synthetic observations for a weak low-level circulation near 12.5°N, 123°E developed with the monsoon gyre algorithm are shown in Figs. 13a and 13b (Chapter VI). As shown in Fig. 13b, a limited number of observations is all that is necessary to insert these weak low-level cyclones.

5. Upper- and Lower-level Anticyclones

During the testing of the interactive analysis, it was occasionally necessary to re-position or enter a missing anticyclone in either the upper- or lower-level analysis. These circulations are often in regions of few or no observations, such as the eastern portion of the western North Pacific or in regions of dense cirrus near tropical cyclones.

As a first trial for this study, a simple modification of reversing the sign of the V component in equations (1) and (2) (see Chapter III) for the TUTT circulation code was tested. The analysis before and after the introduction of synthetic circulation observations for an upper-level anticyclone near 27°N, 141°E are shown in Figs. 27a and 27b (Chapter VI), respectively. This example highlights the rapid placement of an anticyclone feature in the interactive analysis using the modified TUTT code. Because this approach has had only limited testing, further testing is recommended for other scenarios.

LIST OF REFERENCES

Baker, N. L., 1992: Quality control for the Navy atmospheric database. *Wea. Forecasting*, **7**, 250-261.

Carr, L. E., III, and R. A. Jeffries, 1993: Synoptic analysis program, Appendix A. of "Tropical Cyclone Motion (TCM-93) Field Experiment Summary" (Harr, et. al.).Tech Report NPS-MR-93-004, Naval Postgraduate School, Monterey, CA 93943, 95-117.

Carr, L. E., III, and R. L. Elsberry, 1994: Systematic approach to tropical cyclone track forecasting. Part I. Approach overview and description of meteorological basis. Tech. Rep. NPS-MR-94-002, Naval Postgraduate School, Monterey, CA 93943, 273 pp.

Chen, G. T., and L. F. Chou, 1994: An investigation of cold vortices in the upper troposphere over the western North Pacific during the warm season. *Mon. Wea. Rev.*,**122,** 1436-1448.

DeMaria, M., J.J Baik, and J. Kaplan, 1993: Upper-level eddy angular momentum fluxes and tropical cyclone intensity change. *J. Atmos. Sci.*, **50**, 1133-1148.

Doswell, C.A. 1986: The human element in weather forecasting. *National Weather Digest,* **2**, 6-18.

Doswell, C. A., 1992: Forecaster workstation design: Concepts and issues. *Wea. Forecasting,* **7**, 398-407.

Doswell, C.A., L. R. Lemon, and R. A. Maddox, 1981: Forecaster training-A review and analysis. *Bull. Amer. Meteor. Soc.*, **62**, 983-988.

Goerss, J.S., and P.A. Phoebus, 1992: The Navy's operational atmospheric analysis. *Wea. Forecasting*, **7**, 232-249.

Gray, W. M., 1968: Global view of the origin of tropical disturbances and storms. *Mon. Wea. Rev.*, **96**, 669-700.

Haltiner, G.J., and R.T. Williams, 1980: *Numerical prediction and dynamic meteorology*. John Wiley and Sons, New York, 477 pp.

Harr, P.A., R.L. Elsberry, E.A. Ritchie, H.E. Willoughby, M.A. Boothe, L.E. Carr, R.A. Jeffries, 1993: Tropical Cyclone Motion (TCM-93) field experiment summary. Tech. Rep. NPS-MR-93-004, Naval Postgraduate School, Monterey, CA, 120 pp.

Nelson, C. A., and W. T. Aldinger, 1992: An overview of Fleet Numerical Oceanography Center operations and products. *Wea. Forecasting*, **7**, 204-219.

JTWC, 1993: Annual Tropical Cyclone Report, NAVOCEANCOMCEN/JTWC, FPO San Francisco 96630-5000, 269 pp.

Lander, M. A., 1994: Description of a monsoon gyre and its effects on the tropical cyclones in the western North Pacific during August 1991. *Wea. Forecasting*, **9**, 640-654.

Nuss, W. A., and D. W. Titley, 1994: Use of multiquadric interpolation for meteorological objective analysis. *Mon. Wea. Rev.*, **122**, 1611-1631.

Rao, P. K., S. J. Holmes, R. K. Anderson, J. S. Wilson, and P. E. Lehr, 1990: Weather satellites: Systems, data, and environmental applications. Amer. Meteor. Soc., Boston MA 02108, 503 pp.

Smith, D. K., 1994: Tropical cyclone development and intensification under moderate to strong vertical wind shear. Masters thesis, Naval Postgraduate School, Monterey, CA, 104 pp.

Zehr, R. M., 1992: Tropical cyclogenesis in the western North Pacific. NOAA Tech. Rep. NESDIS 61, U.S. Dept. Commerce, Washington, DC, 181 pp.

INITIAL DISTRIBUTION LIST

		No. Copies
1.	Defense Technical Information Center Cameron Station Alexandria VA 22304-6145	2
2.	Librarian Code 52 Naval Postgraduate School 411 Dyer Rd Rm 104 Monterey CA 93943-5101	2
3.	Oceanography Department Code OC/BO Naval Postgraduate School 833 Dyer Rd Rm 331 Monterey CA 93943-5122	1
4.	Meteorology Department Code MR/HY Naval Postgraduate School 589 Dyer Rd Rm 254 Monterey CA 93943-5114	1
5.	Dr. R. L. Elsberry Code MR/Es Naval Postgraduate School 589 Dyer Rd Rm 254 Monterey CA 93943-5114	2
6.	CDR L. E. Carr III Code MR/Cr Naval Postgraduate School 589 Dyer Rd Rm 254 Monterey CA 93943-5114	1

7.	LT Richard A. Jeffries RR1 Meriden, KS 66512	2
8.	Commanding Officer Fleet Numerical Meteorology and Oceanography Center 7 Grace Hopper Ave Stop 4 Monterey CA 93943-0120	1
9.	Chief of Naval Research 800 N. Quincy Street Arlington VA 22217	1
10.	Commanding Officer Naval Pacific Meteorology and Oceanography Center COMNAVMARIANAS Box 12 FPO AP 96540-0051	1
11.	Air Weather Service Technical Library Scott AFB, IL 62225-5008	1
12.	Dr. P. A. Harr Code MR/Hr Naval Postgraduate School 589 Dyer Rd Rm 254 Monterey CA 93943-5114	1
13.	Dr. Wendell Nuss Code MR/Nu Naval Postgraduate School 589 Dyer Rd Rm 254 Monterey CA 93943-5114	1
14.	J. W. Raby Army Research Laboratory Attn: AMSRL-BE-E White Sands Missile Range NM 88002-5501	1

15. Tsgt Ron Sinnard 1
Tropical and Far East Regions
HQ AWS/XOTS
102 W. Losey St, Rm 105
Scott AFB IL 62225-5206